Bρ-defined Isochronous Mass Spectrometry and Mass Measurements of Short-lived Nuclides at CSRe-Lanzhou

1. Principle of *B*ρ-defined IMS
2. Velocity determination with two TOF detectors
3. Realization of *B*ρ-defined IMS
4. New masses from the *B*ρ-defined IMS
5. Summary

Yu-Hu Zhang (张玉虎)

Institute of Modern Physics, Chinese Academy of Sciences
Lanzhou 730000, China

1. Principle of $B\rho$-defined IMS

Conventional IMS $(\gamma = \gamma_t)$

$$\frac{\Delta T}{T} = \frac{1}{\gamma^2}\frac{\Delta(m/q)}{m/q} + \left(\frac{1}{\gamma_t^2} - \frac{1}{\gamma^2}\right)\frac{\Delta(B\rho)}{B\rho}$$

$$\gamma_t^{-2} = \frac{dC/C}{d(B\rho)/(B\rho)}$$

γ_t : machine parameter determined by beam optics

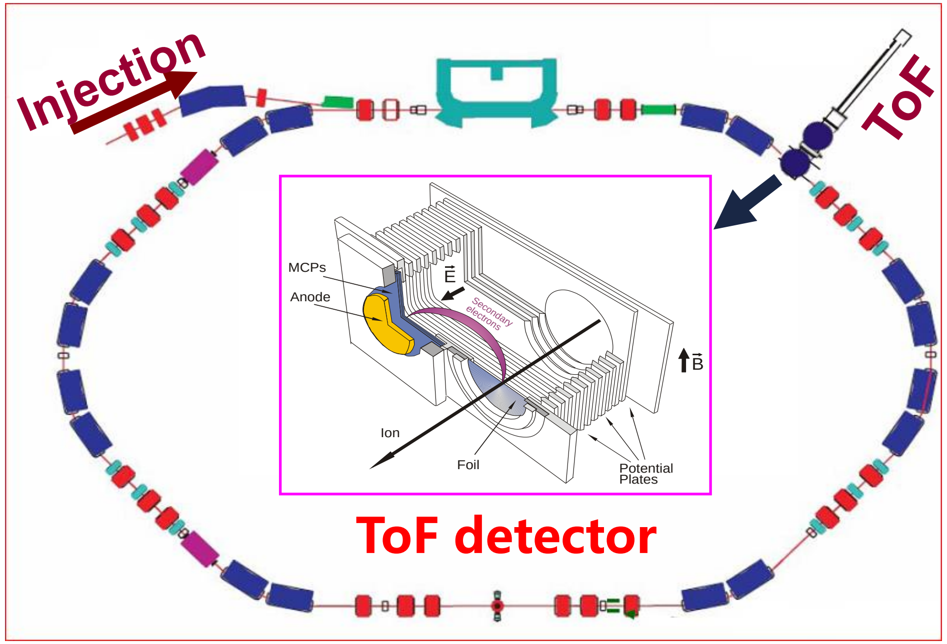

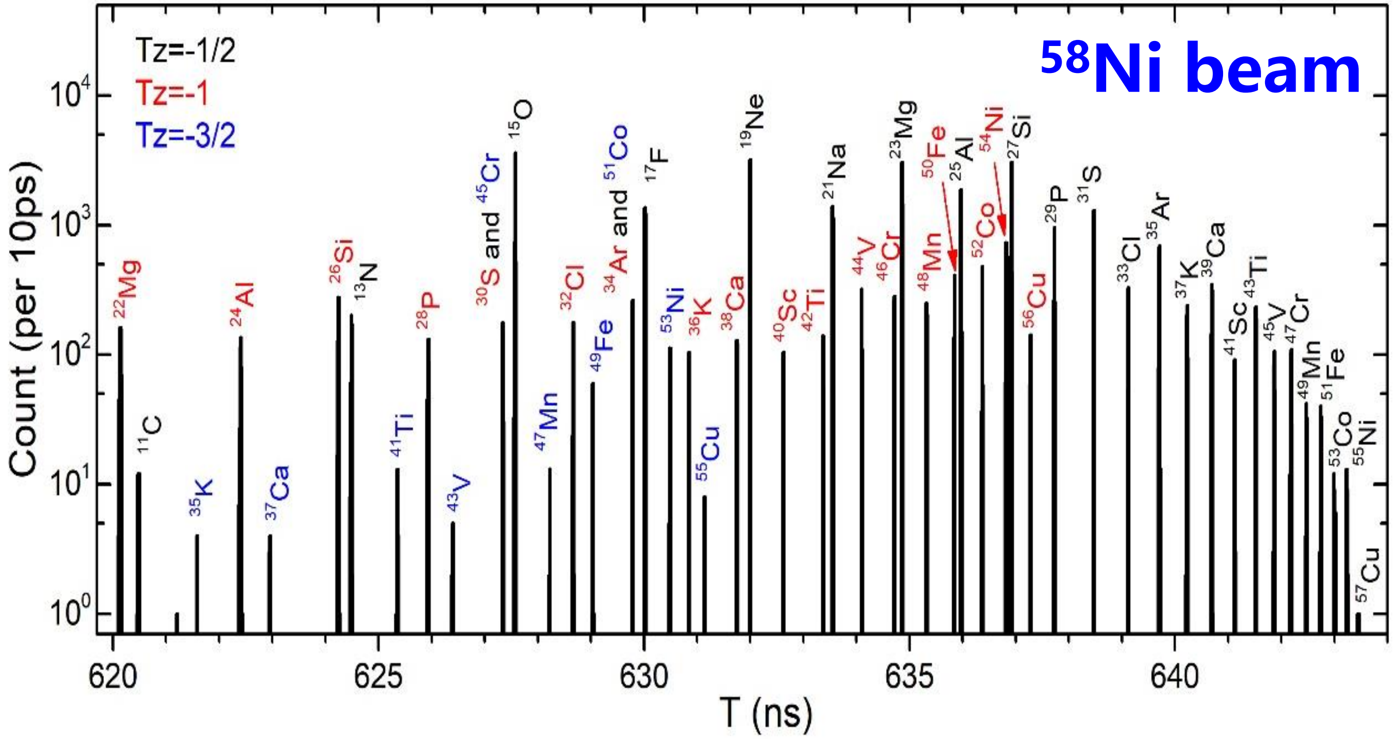

1. Principle of $B\rho$-defined IMS

Limitation of conventional IMS

^{58}Ni beam

1) Phase slip factor: $\frac{\delta T}{T} = \left(\frac{1}{\gamma_t^2} - \frac{1}{\gamma^2}\right) \cdot \frac{\delta(B\rho)}{B\rho}$

2) Orbit-dependent γ_t
3) Asymmetric momentum distribution of stored ions
4) Energy losses of stored ions

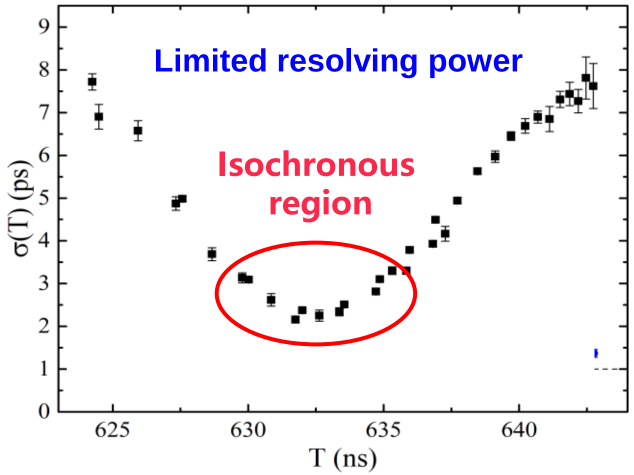

Bρ acceptance

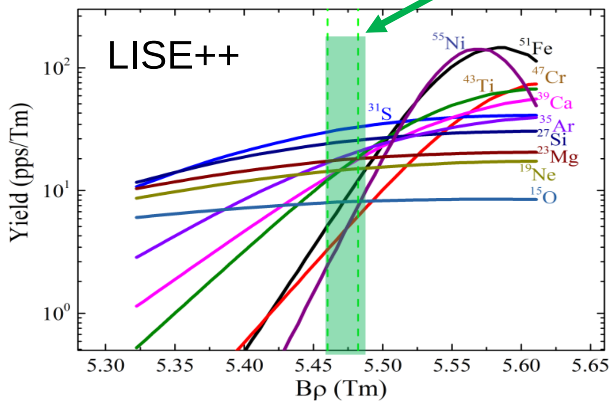

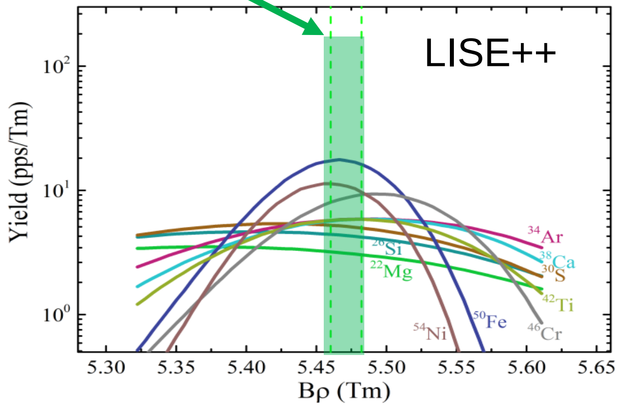

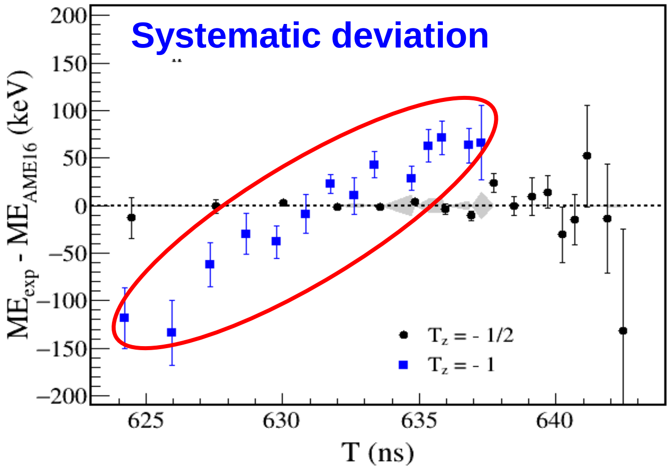

1. Principle of $B\rho$-defined IMS

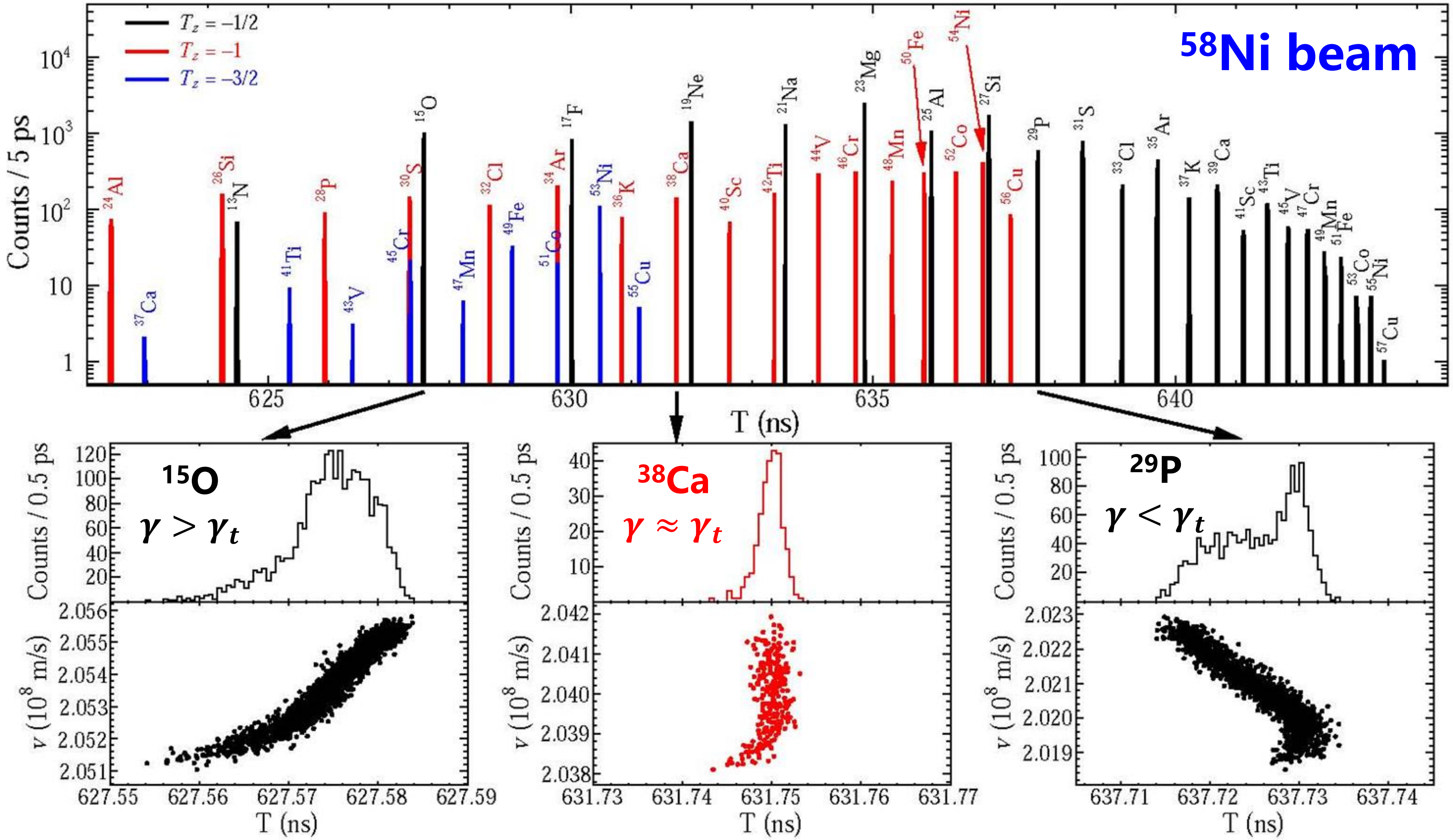

1. Principle of $B\rho$-defined IMS

From $\left\{T, v, \frac{m}{q}\right\}, \quad \rightarrow \; B\rho, C$

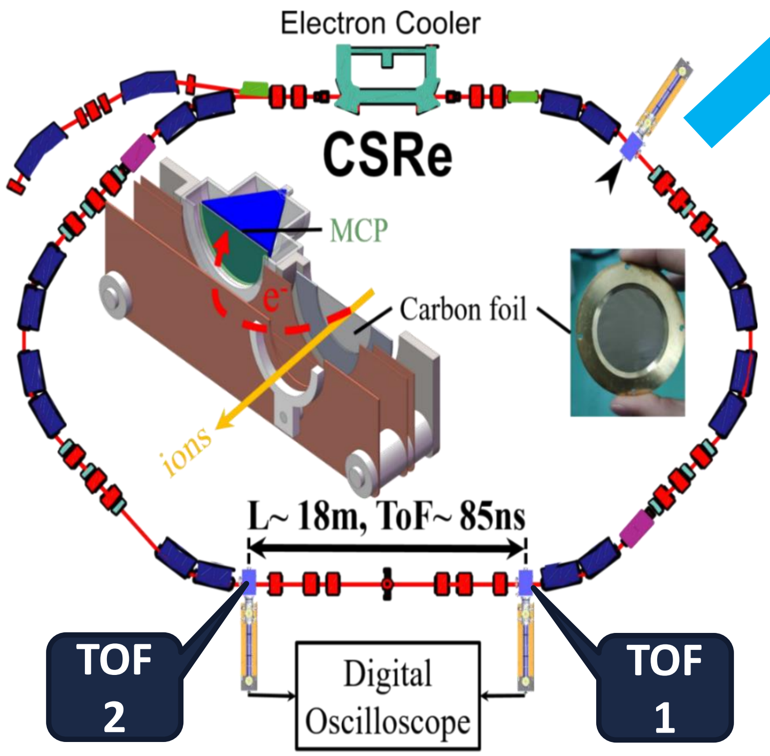

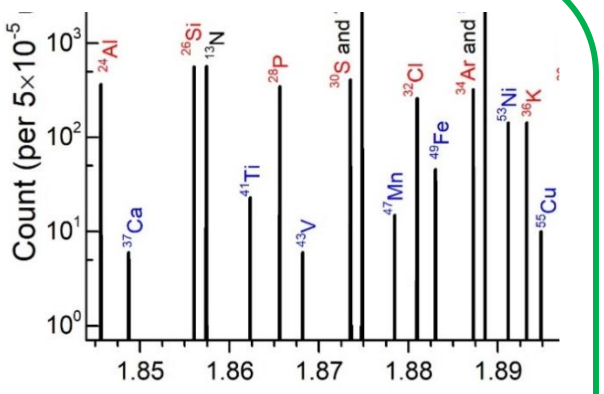

$$\frac{m}{q} = B\rho\sqrt{\left(\frac{1}{v}\right)^2 - \left(\frac{1}{v_c}\right)^2}$$

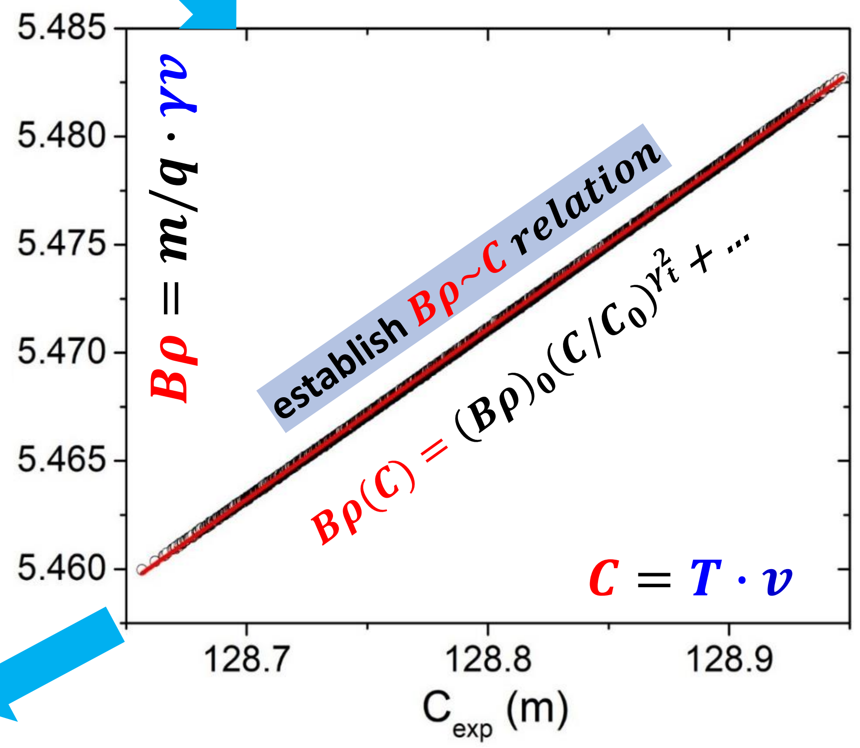

1. Principle of $B\rho$-defined IMS

Accuracy of velocity determination is of top importance

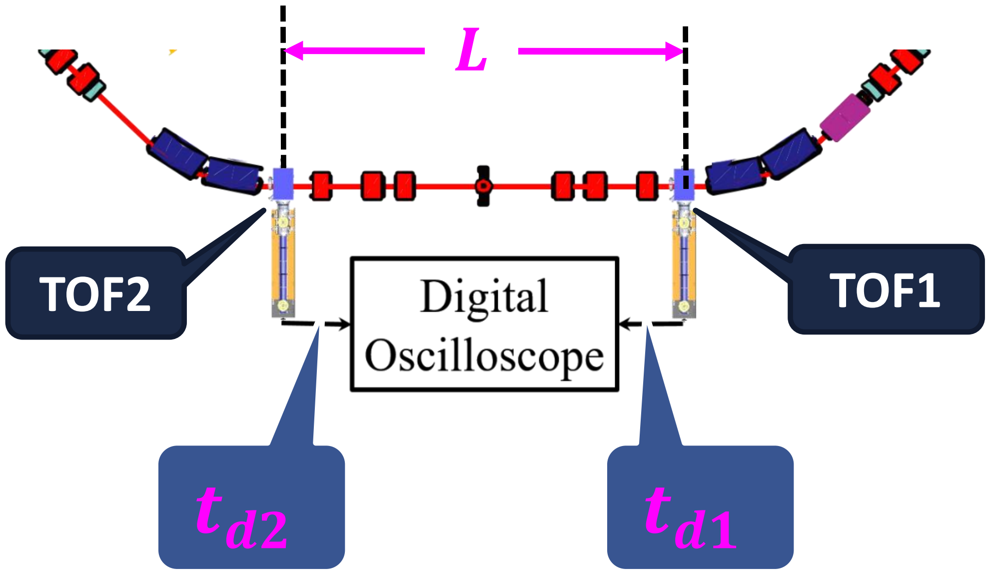

$$v = \frac{L}{\Delta t_{ion}} = \frac{L}{\Delta t_{exp} - \Delta t_d}$$

$L = 18034(1.3)$ mm

$\Delta t_d = 99(4)\ ps$

Effects of velocity uncertainties

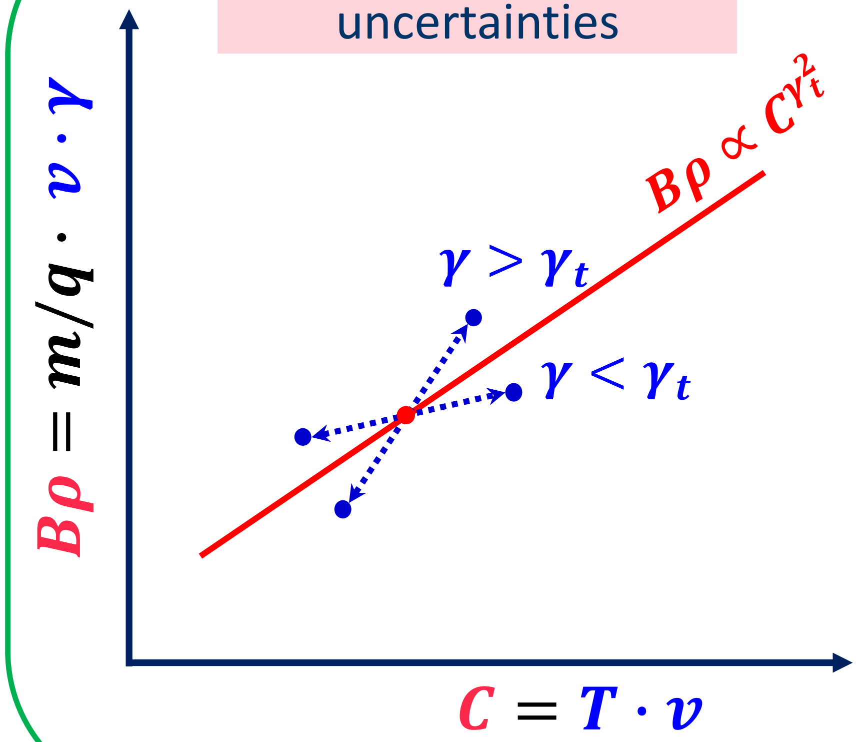

1. Principle of $B\rho$-defined IMS

Accuracy of velocity determination is of top importance

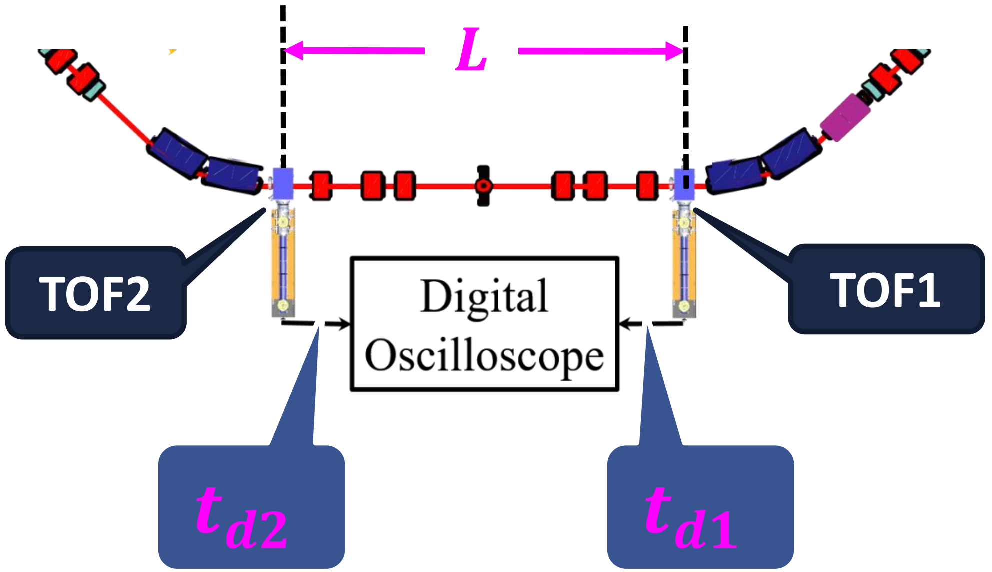

$$v = \frac{L}{\Delta t_{ion}} = \frac{L}{\Delta t_{exp} - \Delta t_d}$$

$L = 18034(1.3)$ mm

$\Delta t_d = 99(4)\ ps$

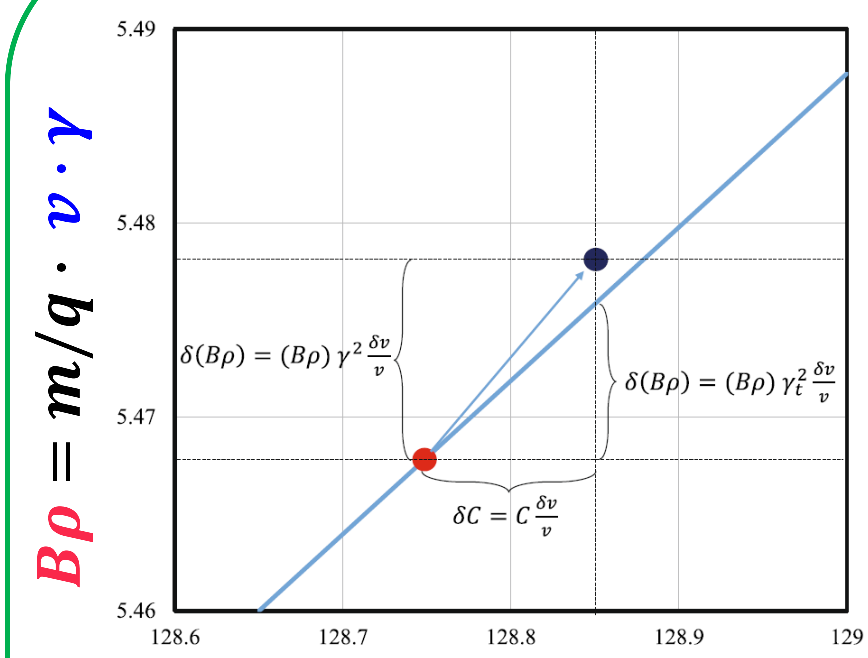

$C = T \cdot v$

1. Principle of $B\rho$-defined IMS

Accuracy of velocity determination is of top importance

$\sigma(T_i) = 0\,ps$

$\frac{\sigma(v_i)}{v_i} =$ 1.0×10^{-4} | 1.0×10^{-5} | 1.0×10^{-6}

$\frac{\sigma(\gamma_t)}{\gamma_t} =$

1.0×10^{-3}

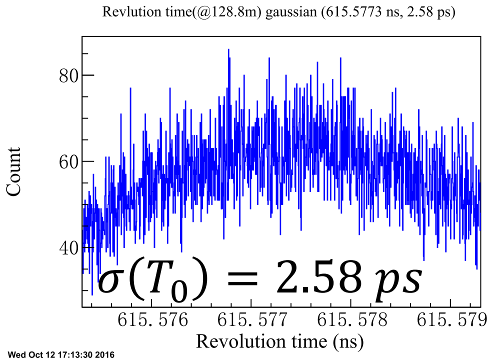

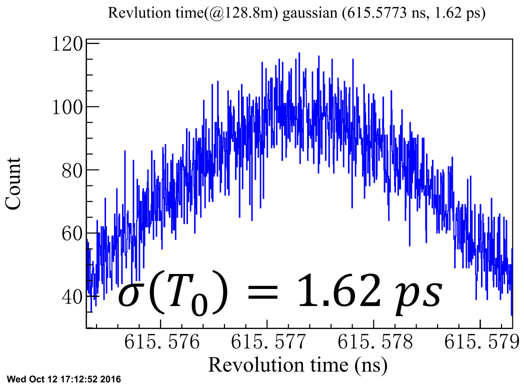

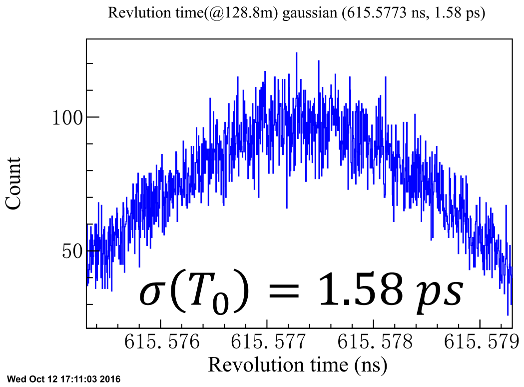

1.0×10^{-4}

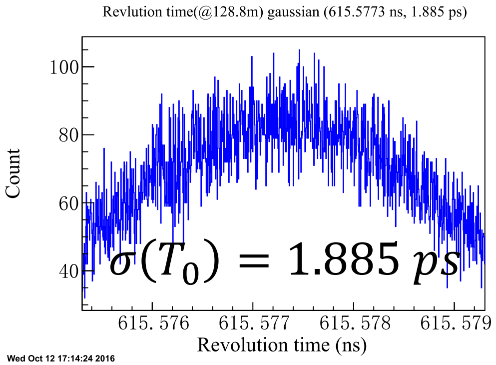

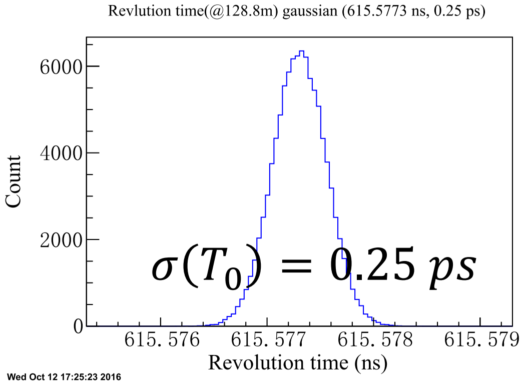

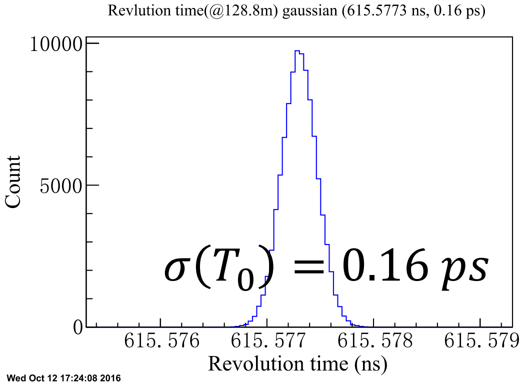

2. Velocity determination with two TOF detectors

Δt_{exp} determinations using coincidence time stamps

$$v = \frac{L}{\Delta t_{exp} - \Delta t_d}$$

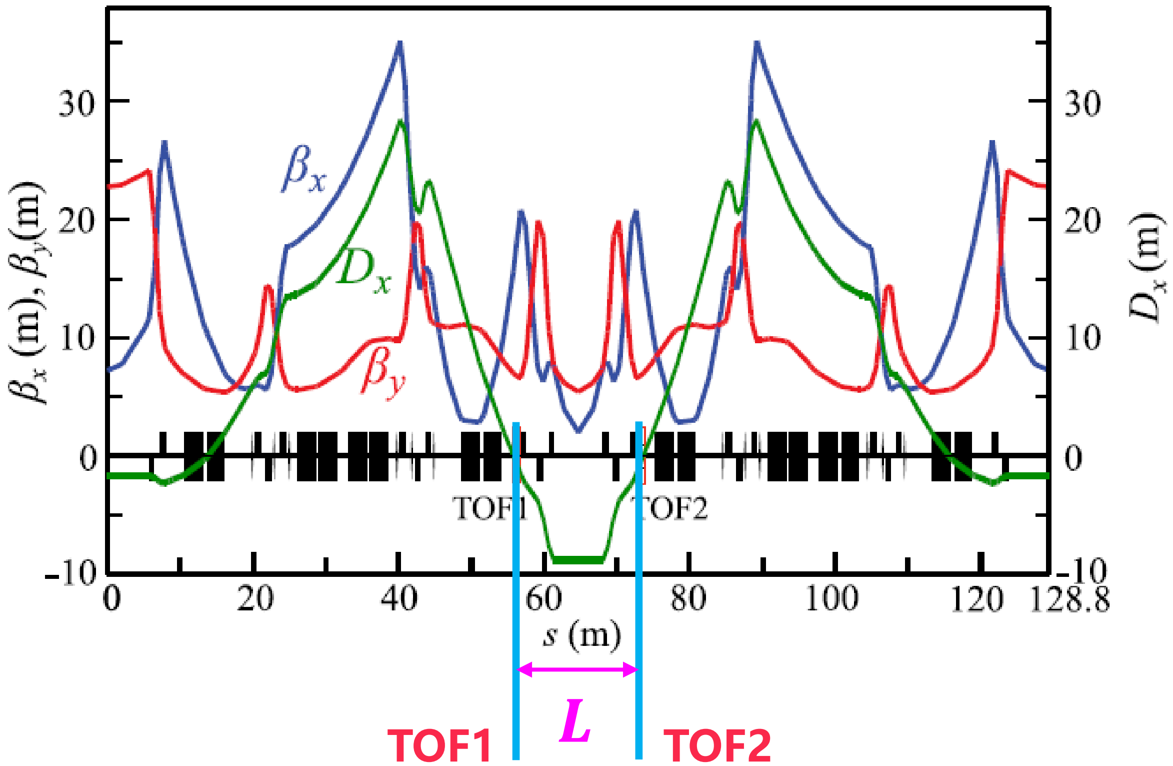

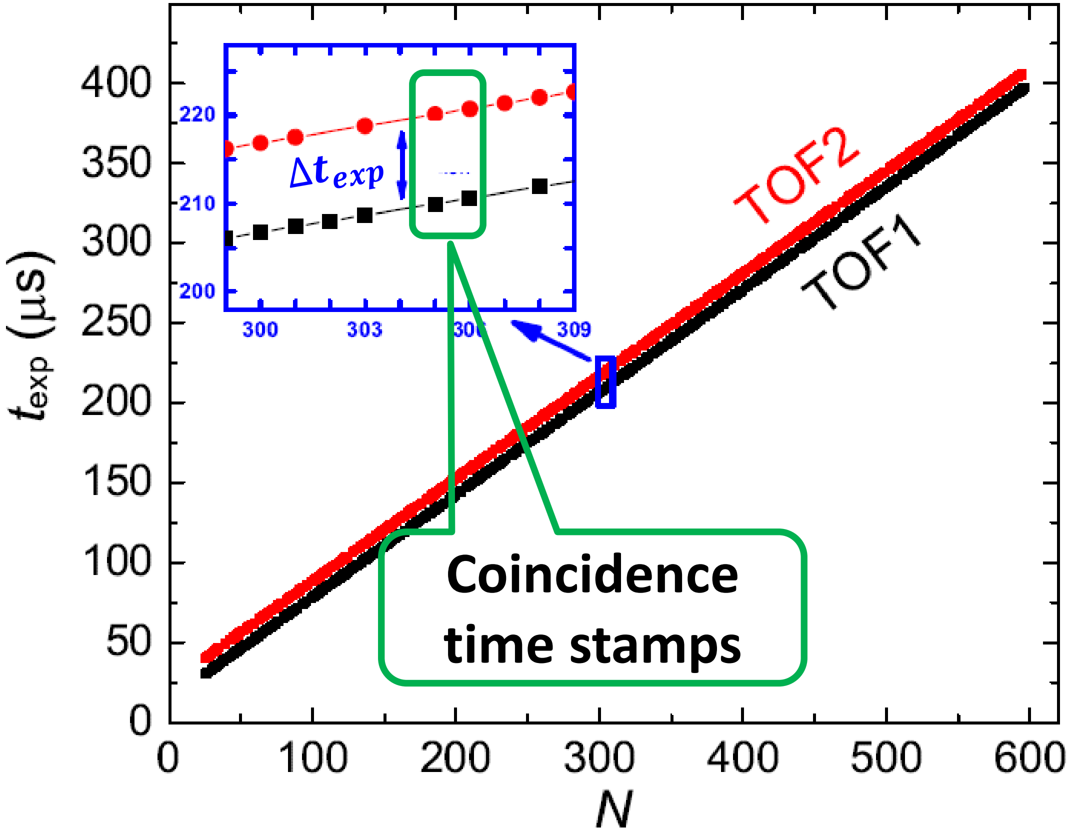

2. Velocity determination with two TOF detectors

Δt_{exp} determinations using coincidence time stamps

$$v = \frac{L}{\Delta t_{exp} - \Delta t_d}$$

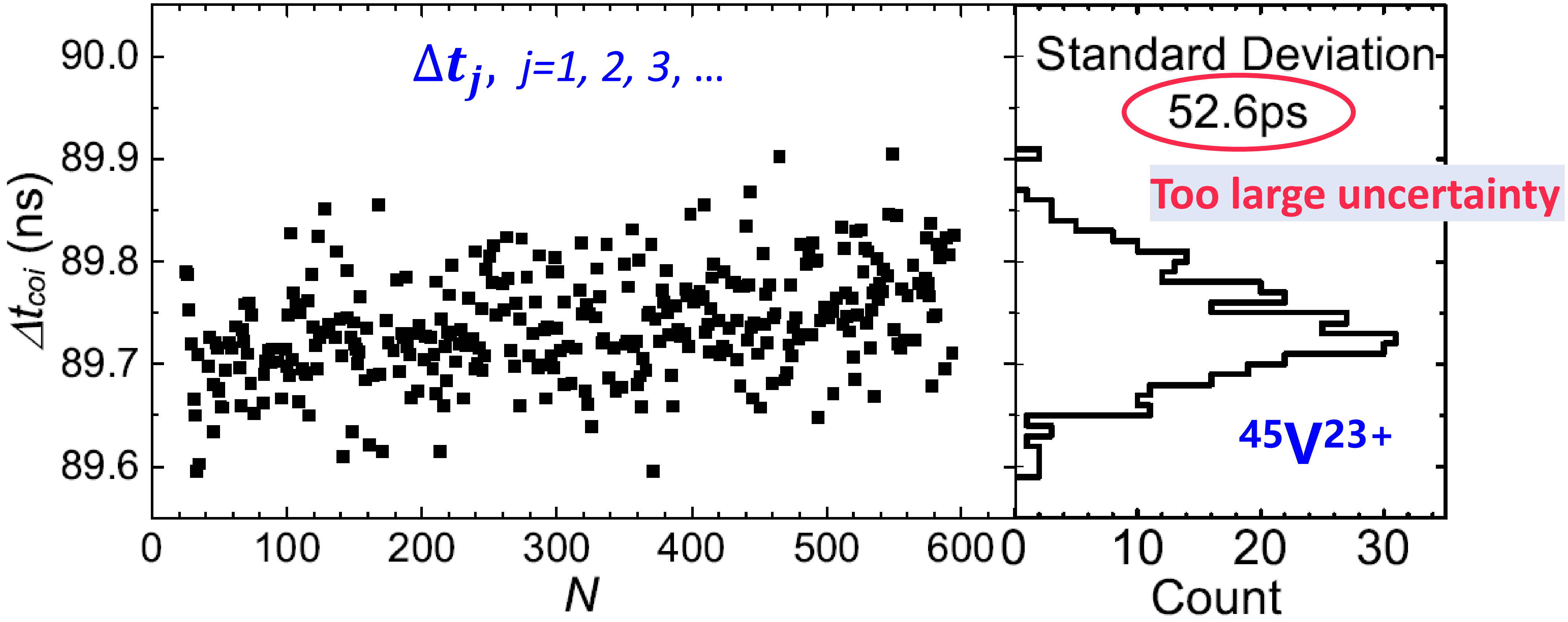

2. Velocity determination with two TOF detectors

Δt_{exp} determinations using polynomial fit to all time stamps

$$\Delta t_{exp}(N) = \Delta t_{fit}(N) = t_{fit}^{TOF2}(N) - t_{fit}^{TOF1}(N)$$

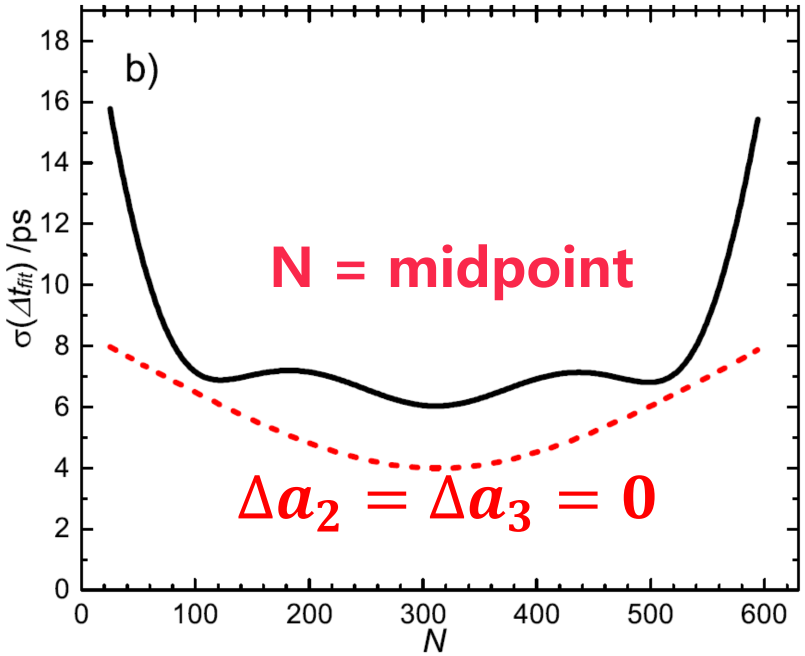

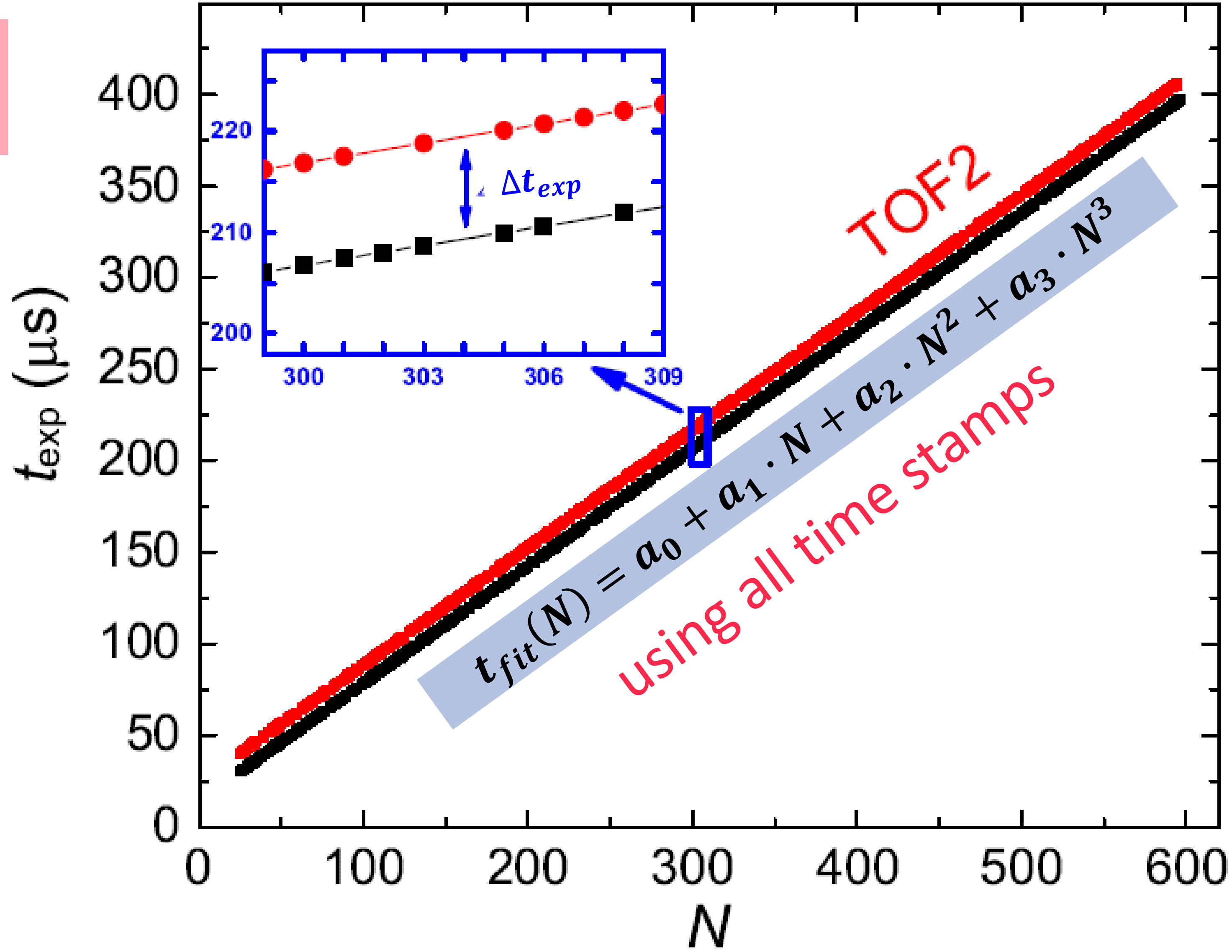

2. Velocity determination with two TOF detectors

σ_{TOF} are too large and asymmetric

Fit residuals

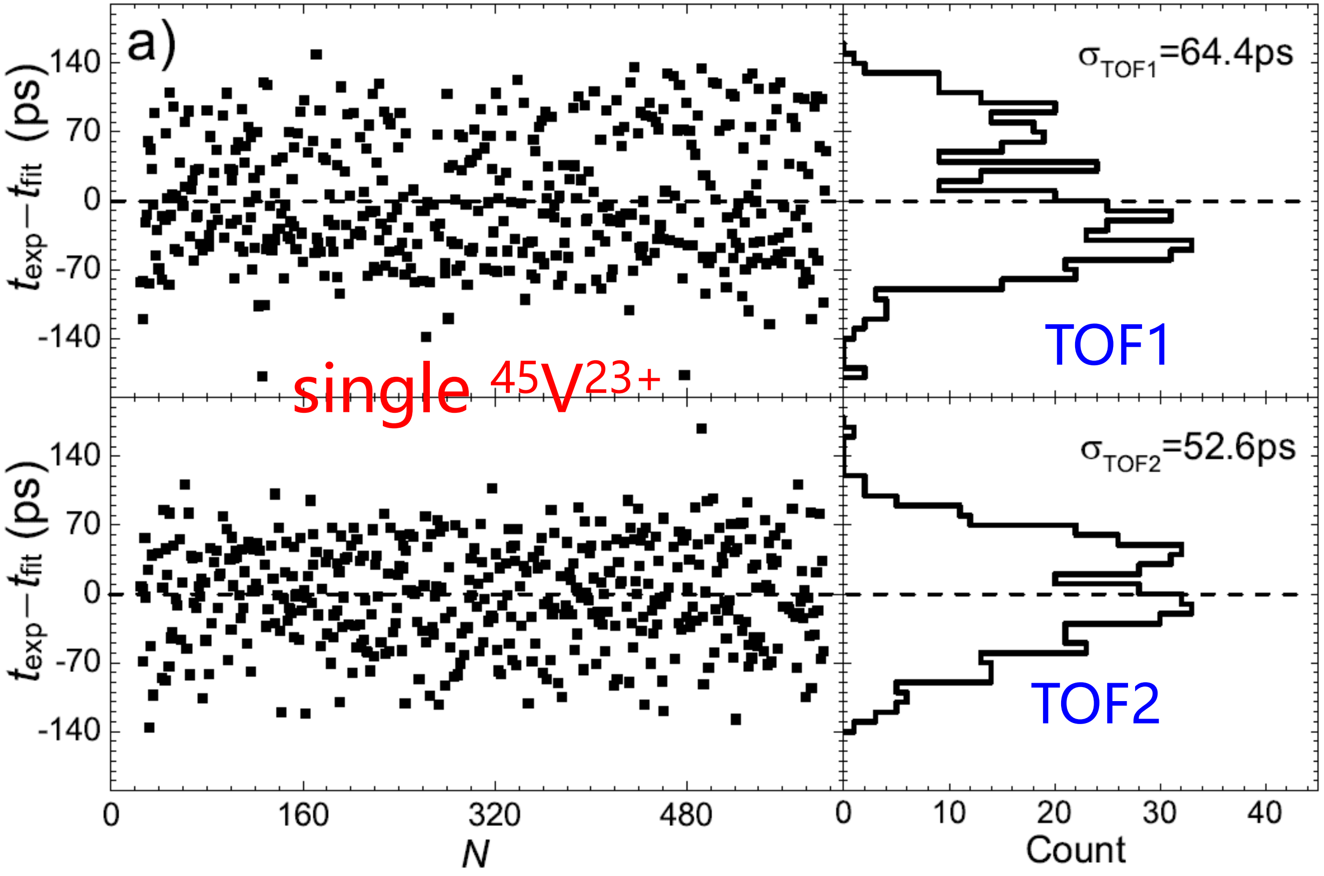

σ_{TOF1} is correlated with σ_{TOF1}

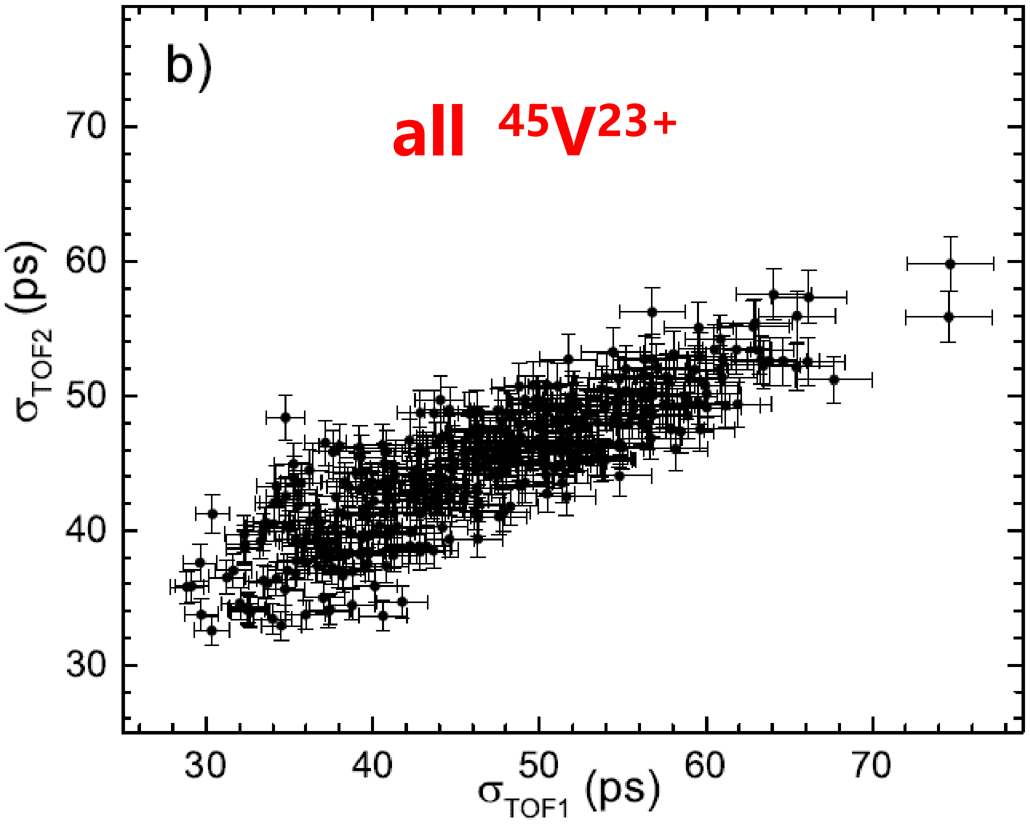

2. Velocity determination with two TOF detectors

$$P(f) = \frac{1}{n_s}\left\{\left[\sum_j^{n_s} X_{N_j} \cdot cos(2\pi f \cdot N_j)\right]^2 + \left[\sum_j^{n_s} X_{N_j} \cdot sin(2\pi f \cdot N_j)\right]^2\right\}$$

Fit residuals

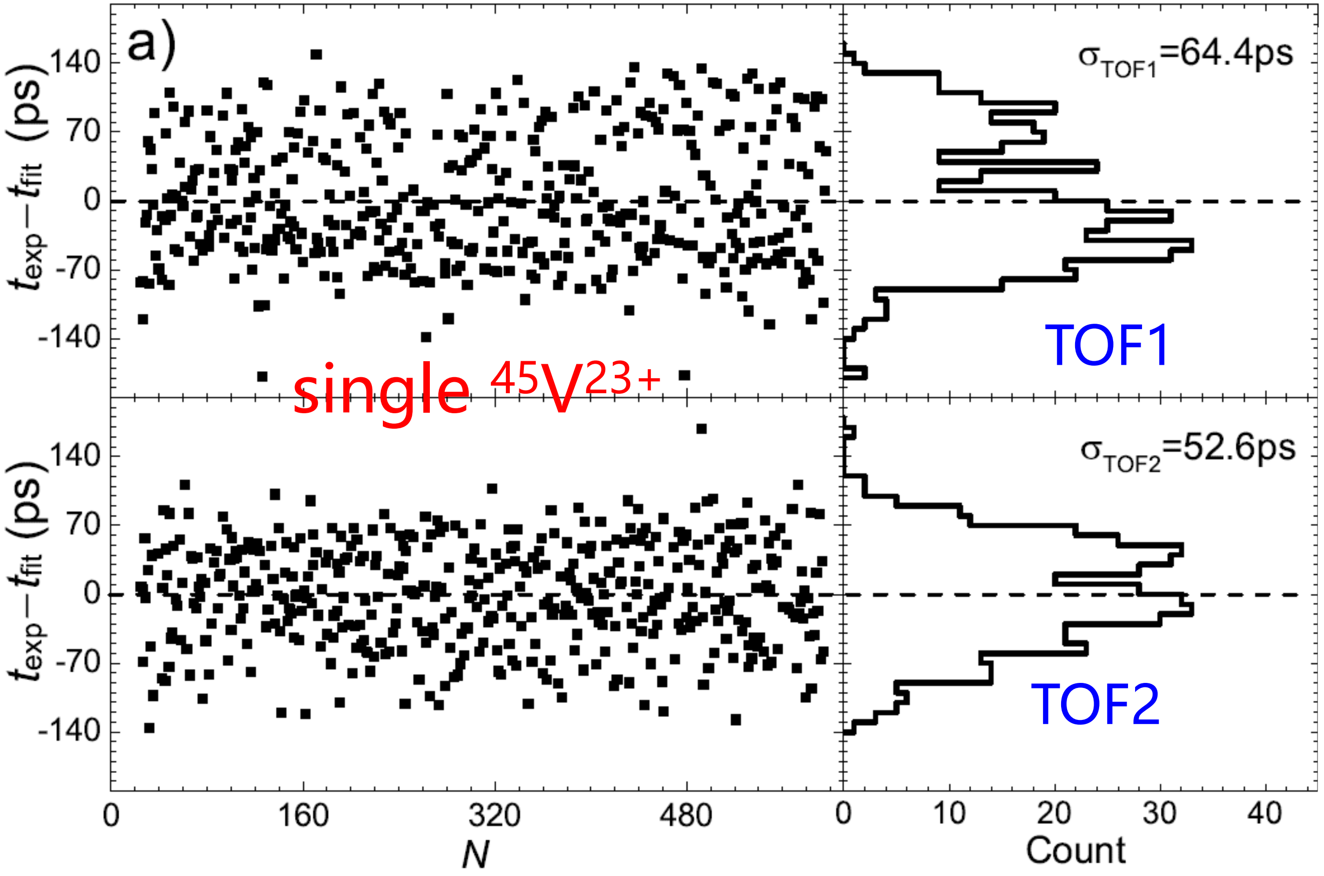

Discrete Fourrier Transform

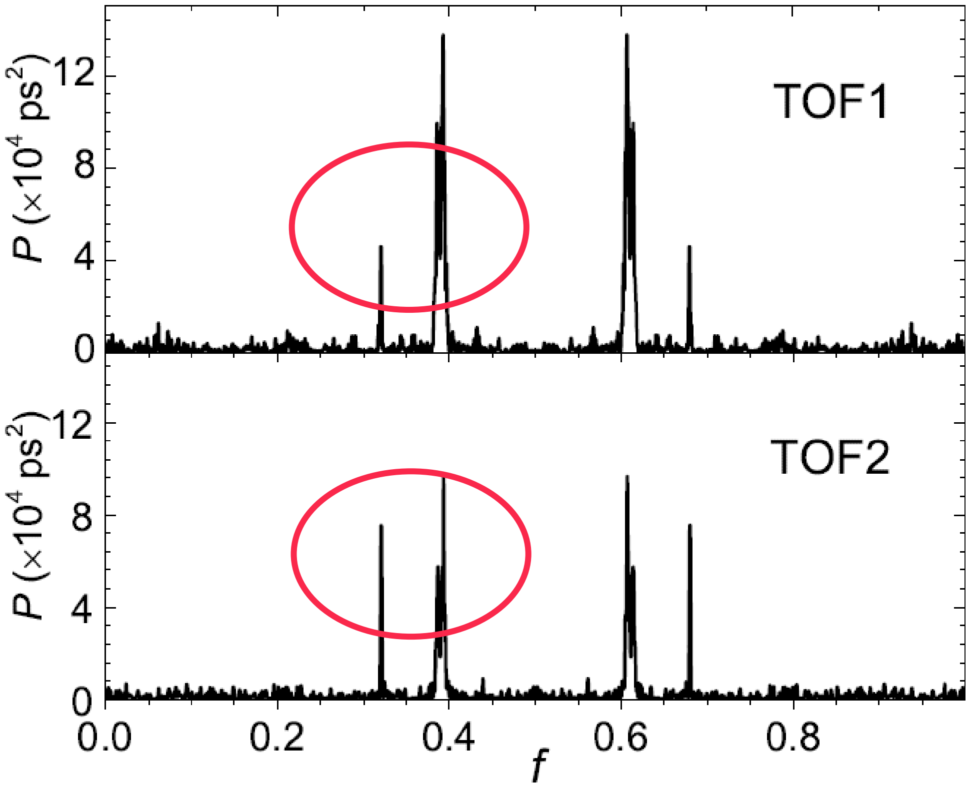

Two peaks at same f

2. Velocity determination with two TOF detectors

$$P(f)=\frac{1}{n_s}\left\{\left[\sum_j^{n_s} X_{N_j}\cdot cos(2\pi f\cdot N_j)\right]^2+\left[\sum_j^{n_s} X_{N_j}\cdot sin(2\pi f\cdot N_j)\right]^2\right\}$$

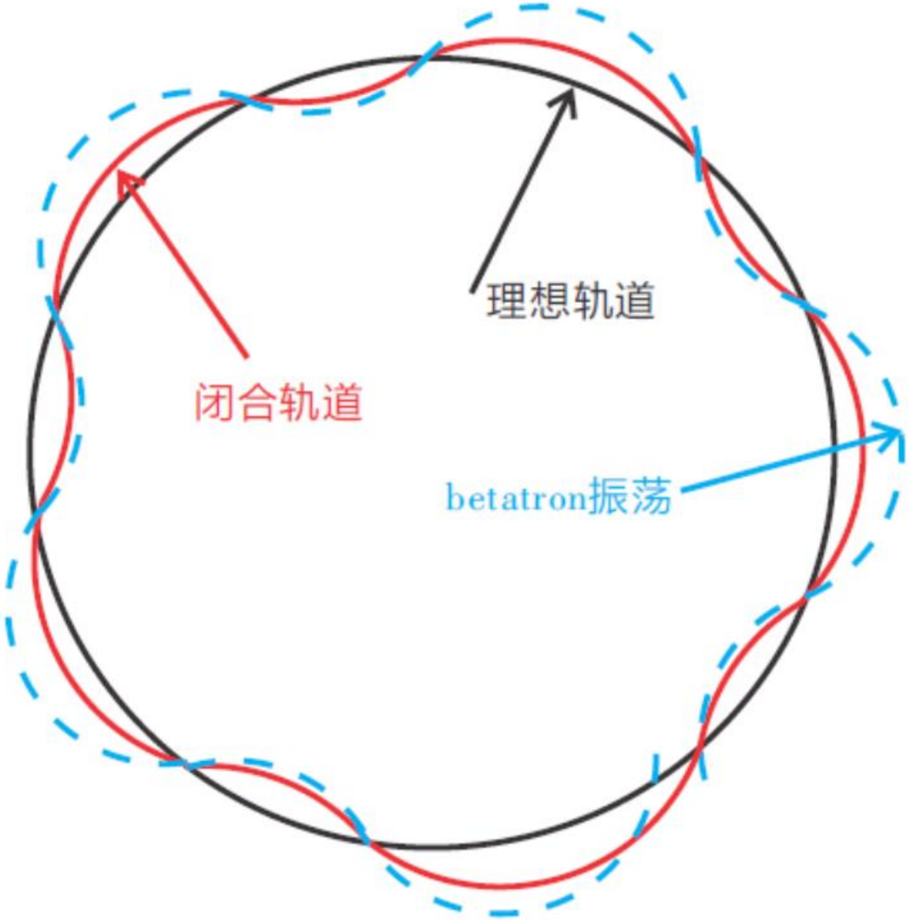

Discrete Fourrier Transform

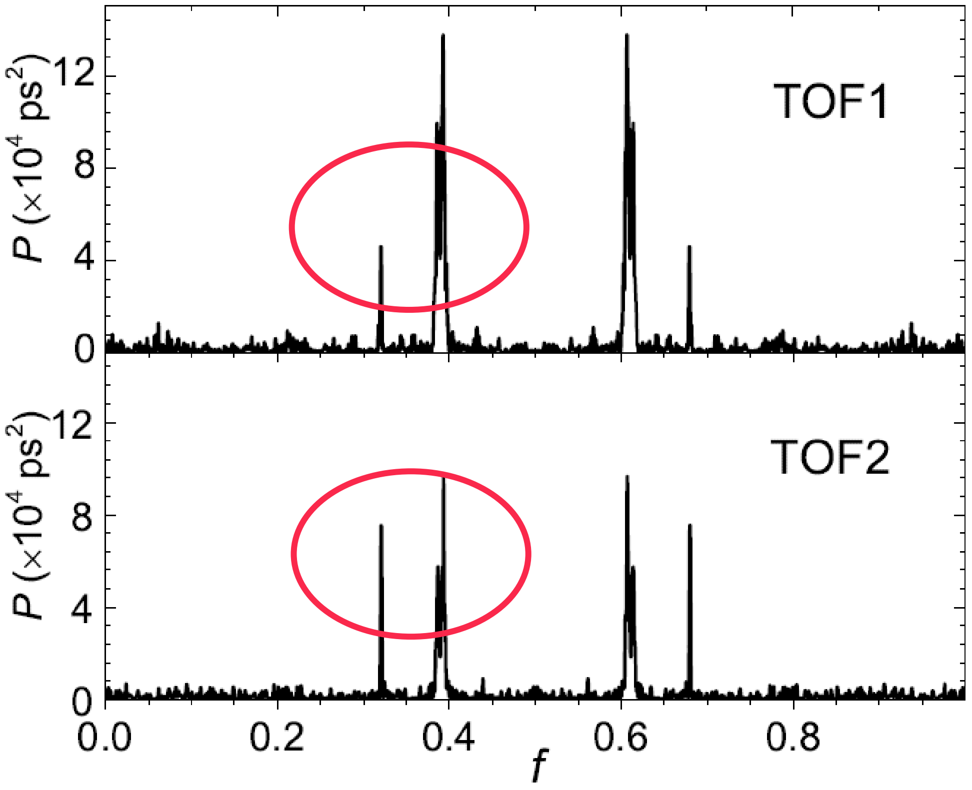

Two peaks at same f

2. Velocity determination with two TOF detectors

Δt_{exp} determinations considering betatron oscillation of stored ions

$$t_{fit}(N) = \sum_{i=0}^{i=3} a_i \cdot N^i$$
$$+A_x \cdot sin[2\pi(Q_{x0}N + Q_{x1}N^2) + \varphi_x]$$
$$+ A_y \cdot sin[2\pi(Q_{y0}N + Q_{y1}N^2) + \varphi_y]$$

- **The polynomial function describes ion motion with a mean orbital length**
- **The sine-like terms describe the periodic time fluctuations due to betatron oscillations.**

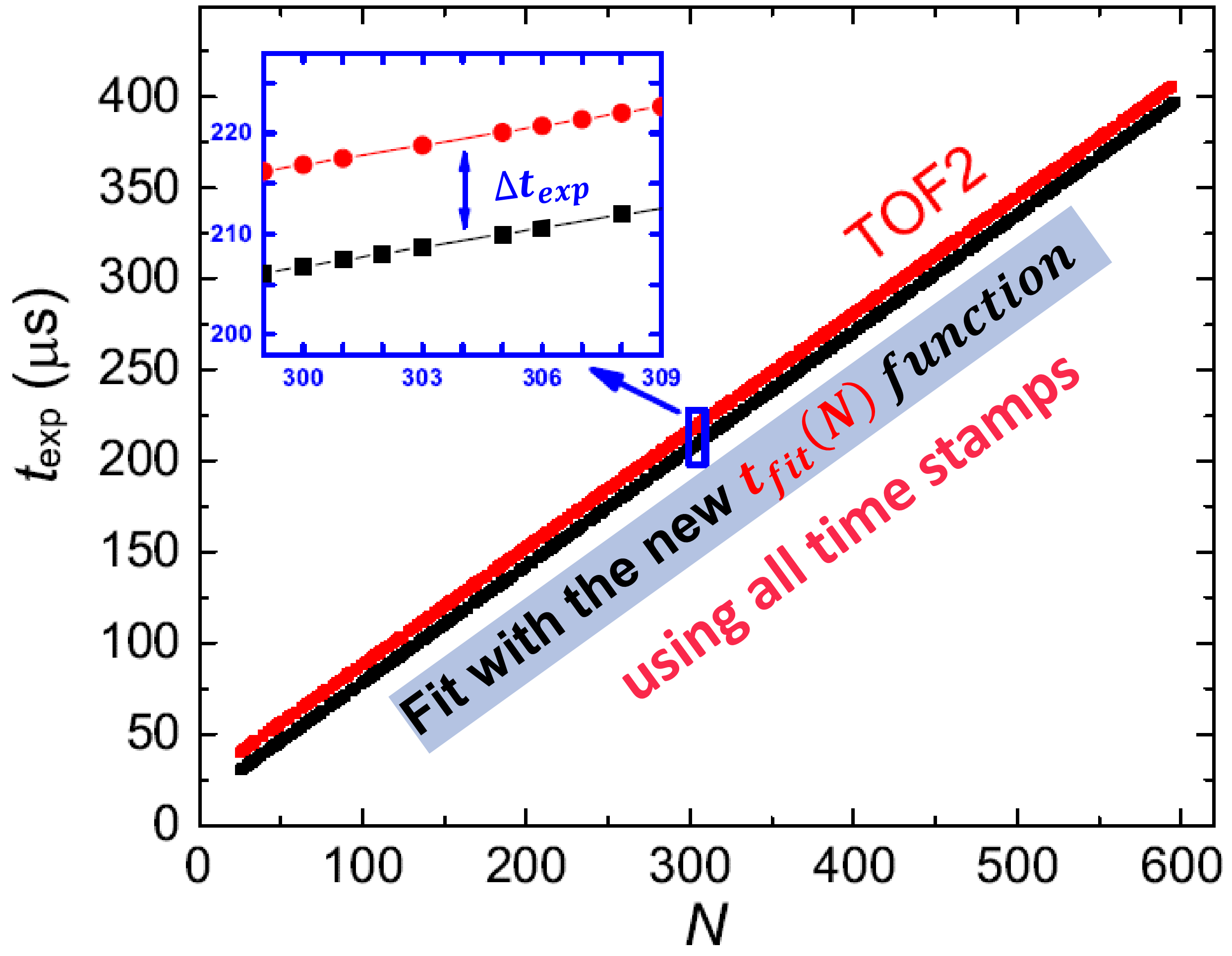

2. Velocity determination with two TOF detectors

Δt_{exp} determinations considering betatron oscillation of stored ions

$$t_{fit}(N) = \sum_{i=0}^{i=3} a_i \cdot N^i$$
$$+A_x \cdot sin\left[2\pi\left(Q_{x0}N + Q_{x1}N^2\right) + \varphi_x\right]$$
$$+ A_y \cdot sin\left[2\pi\left(Q_{y0}N + Q_{y1}N^2\right) + \varphi_y\right]$$

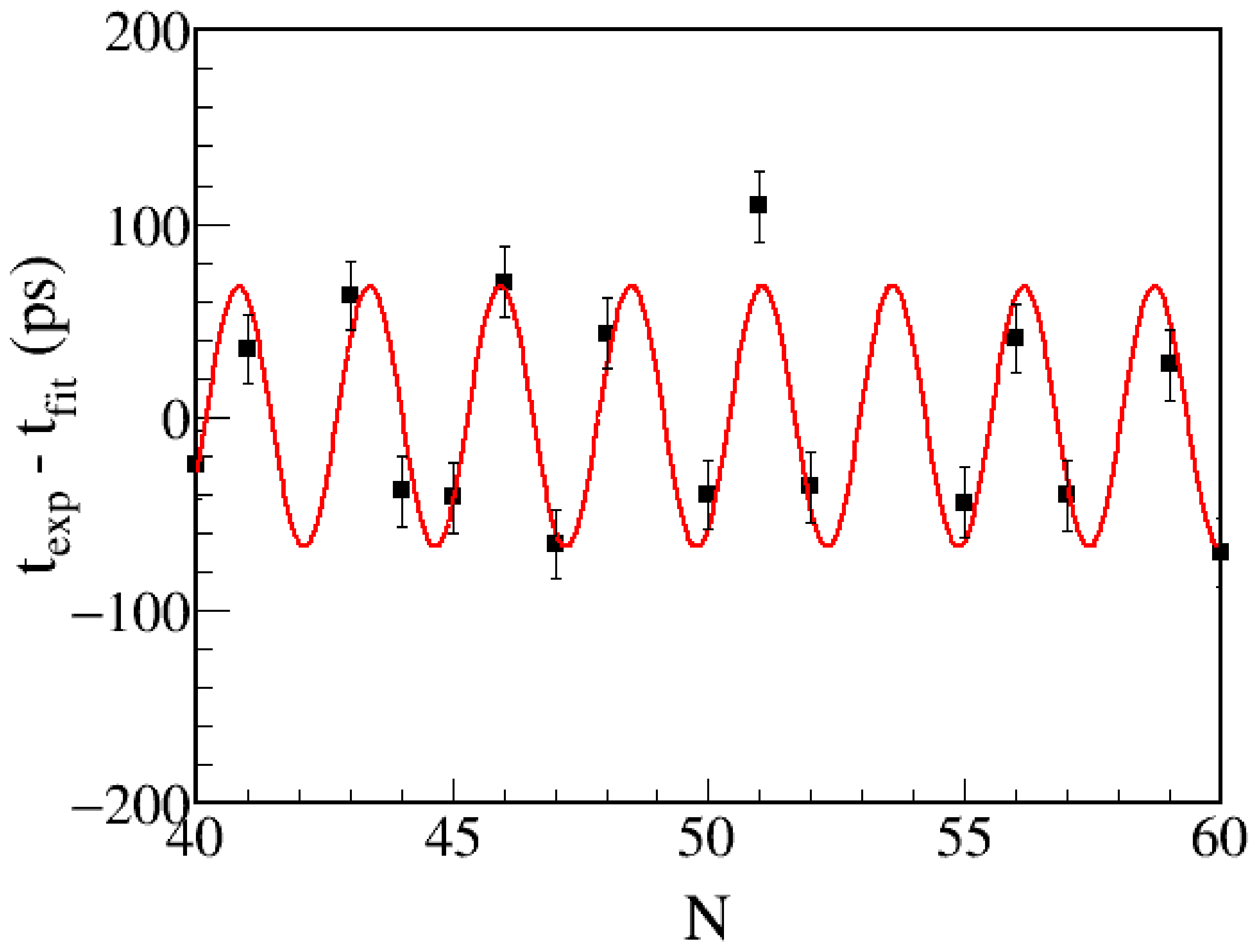

- The polynomial function describes ion motion with a mean orbital length
- The sine-like terms describe the periodic time fluctuations due to betatron oscillations.

2. Velocity determination with two TOF detectors

$$t_{fit}(N) = \sum_{i=0}^{3} a_i \cdot N^i + A_x \sin[2\pi(Q_{x0}N + Q_{x1}N^2) + \varphi_x] + A_y \sin[2\pi(Q_{y0}N + Q_{y1}N^2) + \varphi_y]$$

Fit residuals

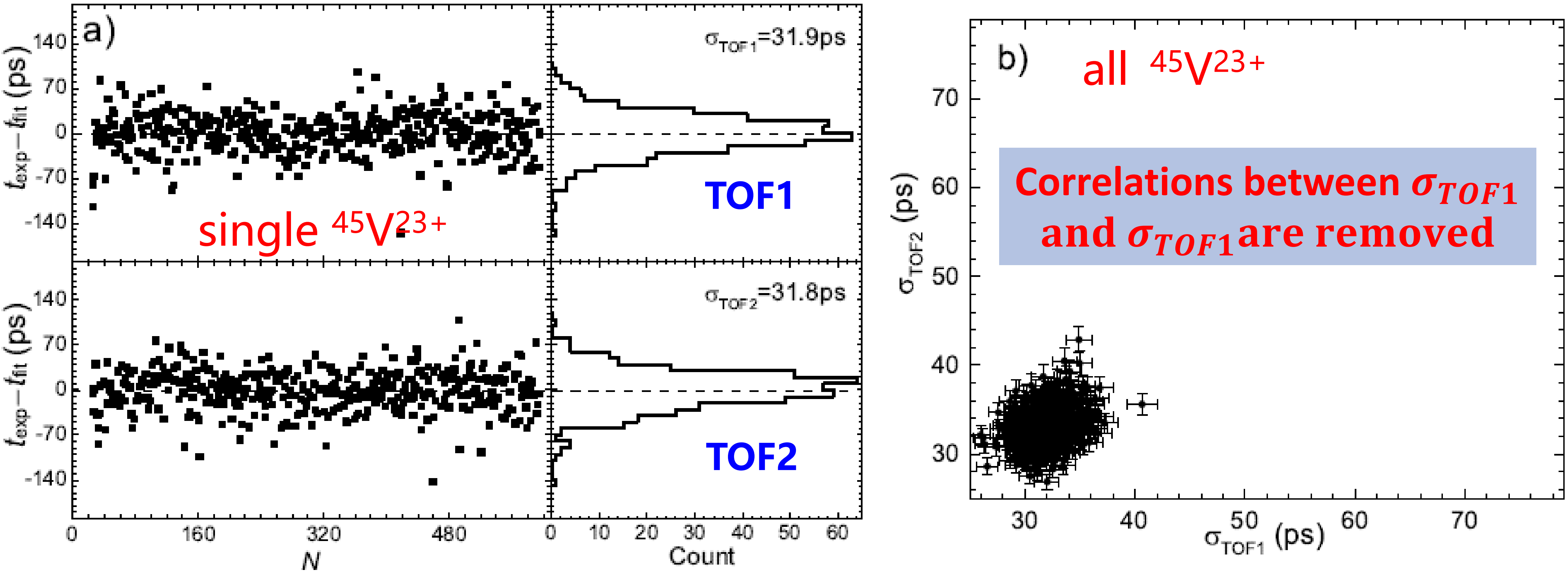

Correlations between σ_{TOF1} and σ_{TOF1} are removed

2. Velocity determination with two TOF detectors

$$\Delta t_{exp}(N) = \sum_{i=0}^{i=3} \Delta a_i \cdot N^i$$

$$\overline{\sigma(\Delta t_{exp})} = (2.0\sim6.4)\ ps,$$
$$relative: (2.2\sim7.2) \times 10^{-5}$$

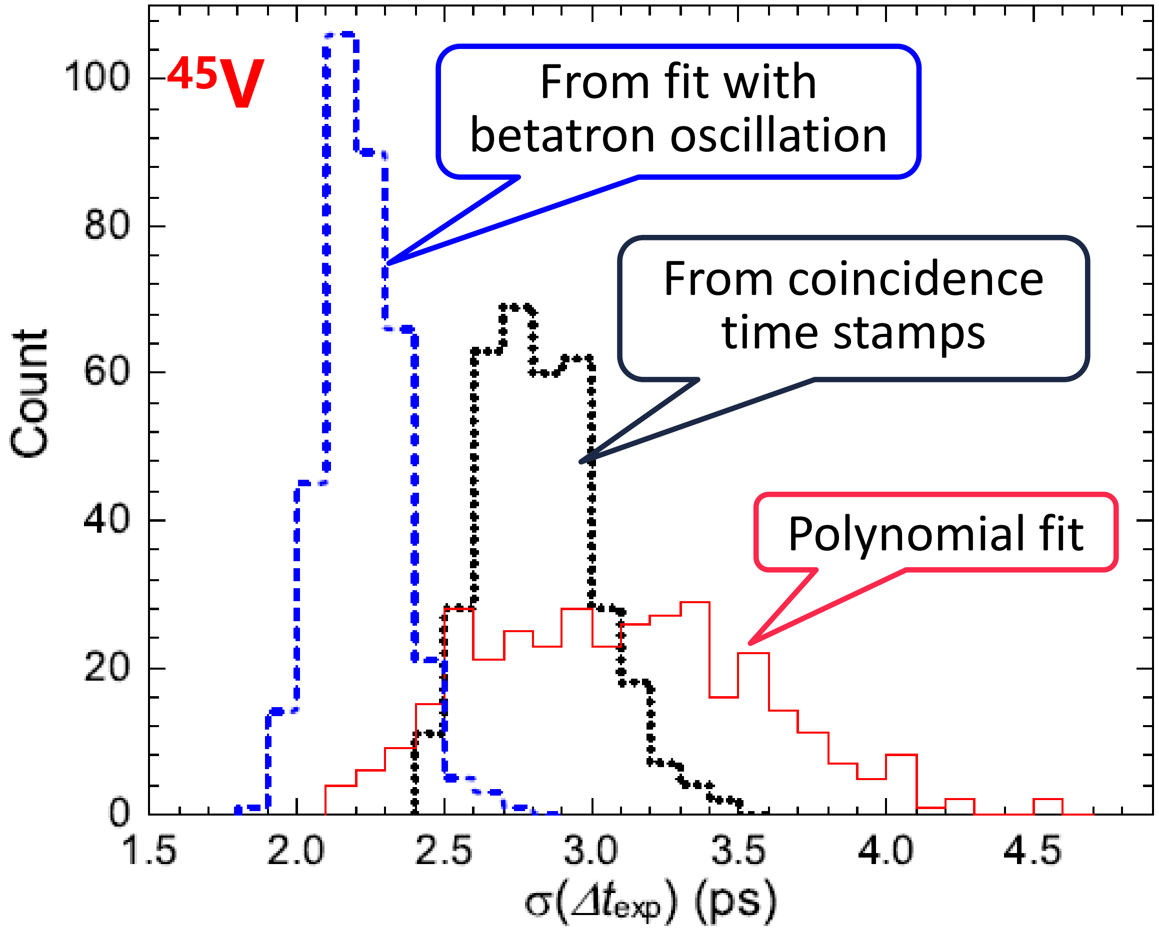

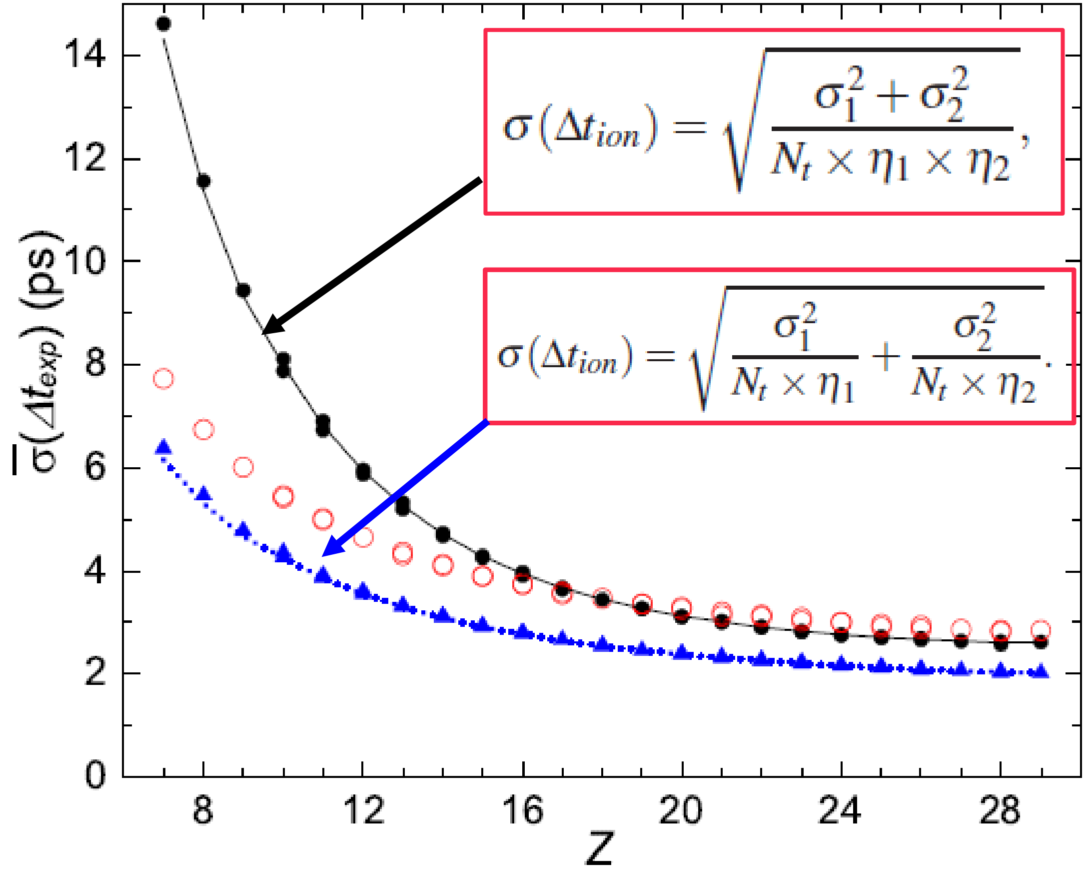

2. Velocity determination with two TOF detectors

$$\Delta t_{exp}(N) = \sum_{i=0}^{i=3} \Delta a_i \cdot N^i$$

$$v = \frac{L}{\Delta t_{exp} - \Delta t_d}$$

$L = 18034(1.3)$ mm

$\Delta t_d = 99(4)\ ps$

Using FL-266nm-Pico laser

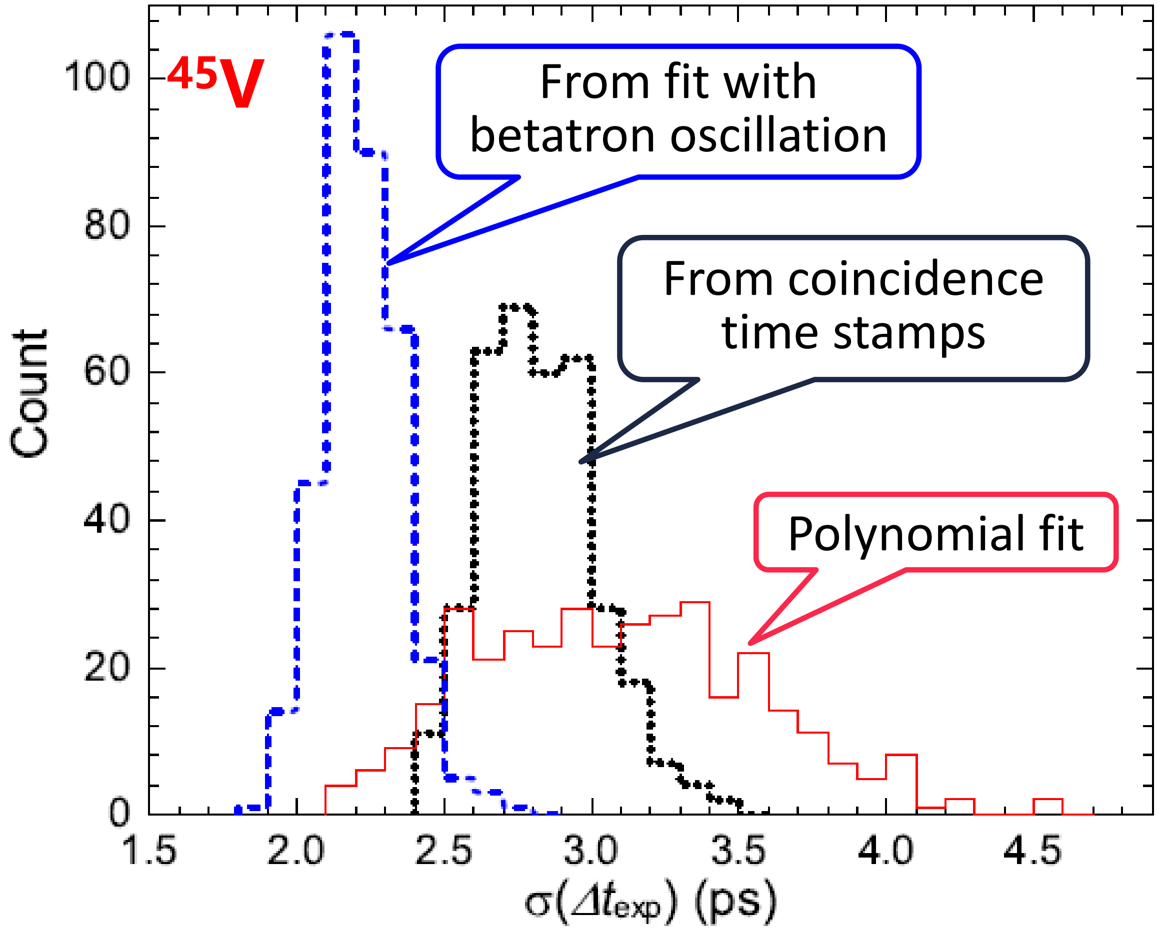

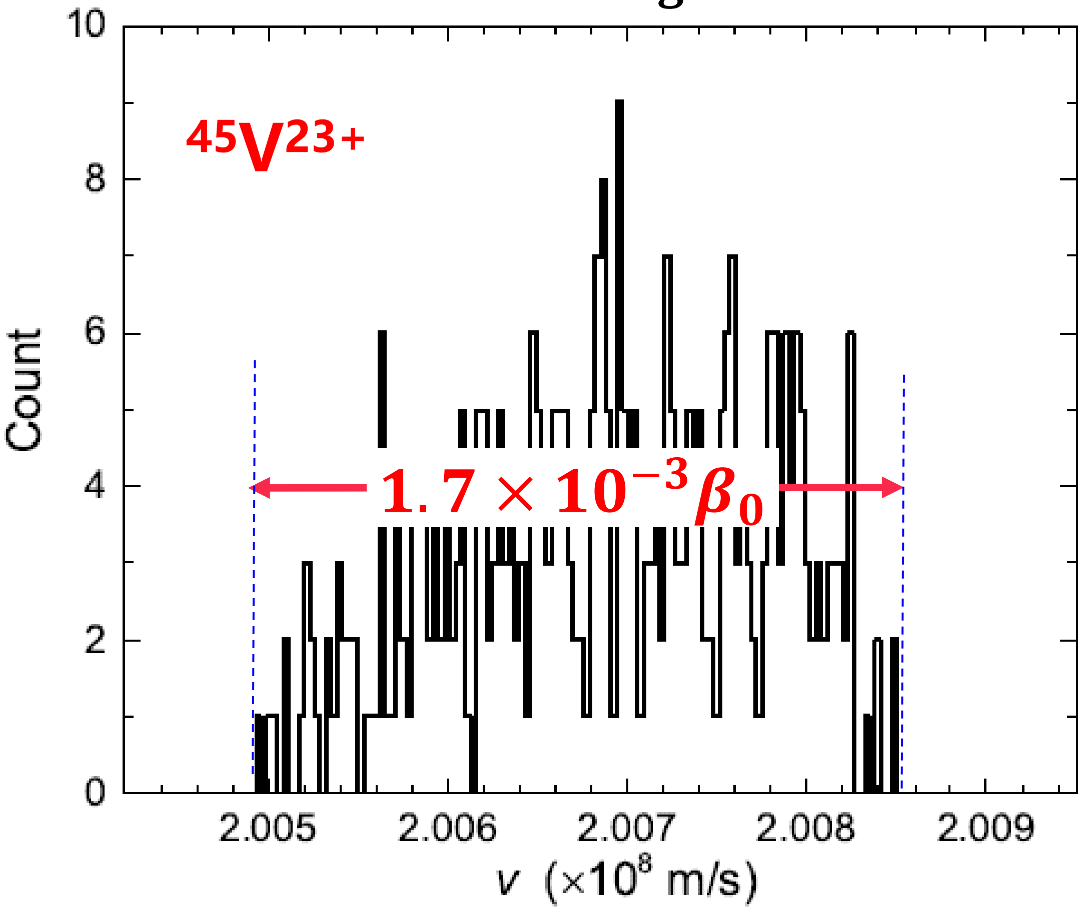

2. Velocity determination with two TOF detectors

PHYSICAL REVIEW ACCELERATORS AND BEAMS **24**, 042802 (2021)

Editors' Suggestion

In-ring velocity measurement for isochronous mass spectrometry

X. Zhou,[1,2] M. Zhang,[1,2] M. Wang,[1,2,*] Y. H. Zhang,[1,2,†] Y. J. Yuan,[1,2,‡] X. L. Yan,[1,§] X. H. Zhou,[1,2] H. S. Xu,[1,2] X. C. Chen,[1] Y. M. Xing,[1] R. J. Chen,[1,3] X. Xu,[4,1] P. Shuai,[1] C. Y. Fu,[1] Q. Zeng,[1,5] M. Z. Sun,[1] H. F. Li,[1,2] Q. Wang,[1,2] T. Bao,[1] M. Si,[1,2,6] H. Y. Deng,[1,2] M. Z. Liu,[1,2] T. Liao,[1,2] J. Y. Shi,[1,2] Y. N. Song,[1,2] J. C. Yang,[1] W. W. Ge,[1] Yu. A. Litvinov,[1,3] S. A. Litvinov,[1,3] R. S. Sidhu,[3] T. Yamaguchi,[7] S. Omika,[7] K. Wakayama,[7] S. Suzuki,[1,8] and T. Moriguchi[8]

[1]*CAS Key Laboratory of High Precision Nuclear Spectroscopy, Institute of Modern Physics, Chinese Academy of Sciences, Lanzhou 730000, China*

[2]*School of Nuclear Science and Technology, University of Chinese Academy of Sciences, Beijing 100049, China*

[3]*GSI Helmholtzzentrum für Schwerionenforschung, Planckstraße 1, 64291 Darmstadt, Germany*

[4]*School of Physics, Xi'an Jiaotong University, Xi'an 710049, China*

[5]*School of Nuclear Science and Engineering, East China University of Technology, Nanchang 330013, China*

[6]*Université Paris-Saclay, CNRS/IN2P3, IJCLab, F-91405 Orsay, France*

[7]*Department of Physics, Saitama University, Saitama 338-8570, Japan*

[8]*Institute of Physics, University of Tsukuba, Ibaraki 305-8571, Japan*

3. Realization of $B\rho$-defined IMS

Logic of mass determinations

Measurements

T_i, v_i
$(i = 1, 2, \ldots N)$

Construct

$$(B\rho)^i = \frac{m}{q} \cdot (\gamma v)_i$$

$$C_i = v_i \cdot T_i$$

$B\rho \sim C$ line using known m/q

Outputs

$$\frac{m}{q} = B\rho \sqrt{\left(\frac{1}{v}\right)^2 - \left(\frac{1}{v_c}\right)^2}$$

new $(m/q)^i$ using $(B\rho)^i_{fit}$

T spectrum T^i_{fix} @ C_{fix}

$$T^i_{fix} = C_{fix} \sqrt{\frac{1}{(B\rho)^2_{fix}} \left[\left(\frac{m}{q}\right)^i_{exp}\right]^2 + \left(\frac{1}{v_c}\right)^2}$$

3. Realization of $B\rho$-defined IMS

$$B\rho = f(C) = (B\rho)_0 \cdot \left(\frac{C}{C_0}\right)^K + a_1 \cdot e^{-a_2 \cdot (C - C_0)}$$

^{58}Ni beam

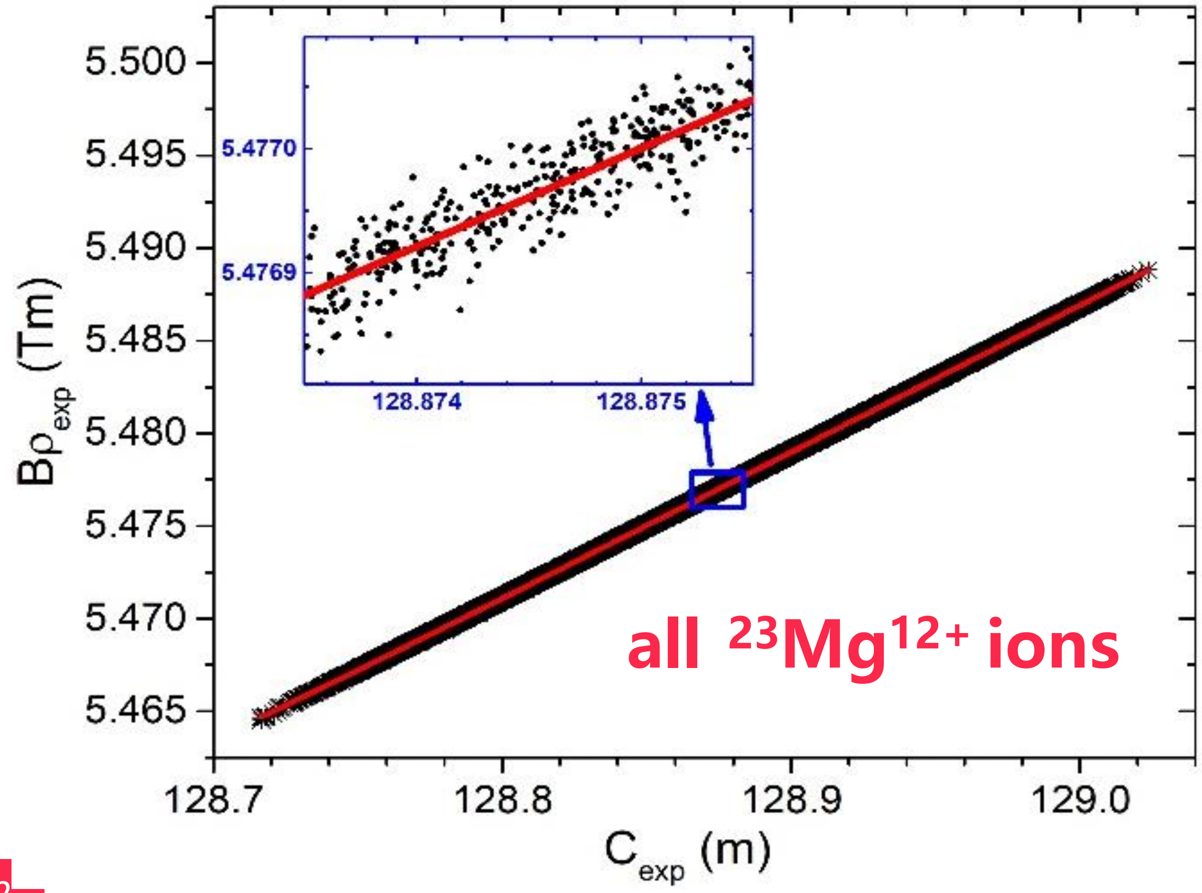

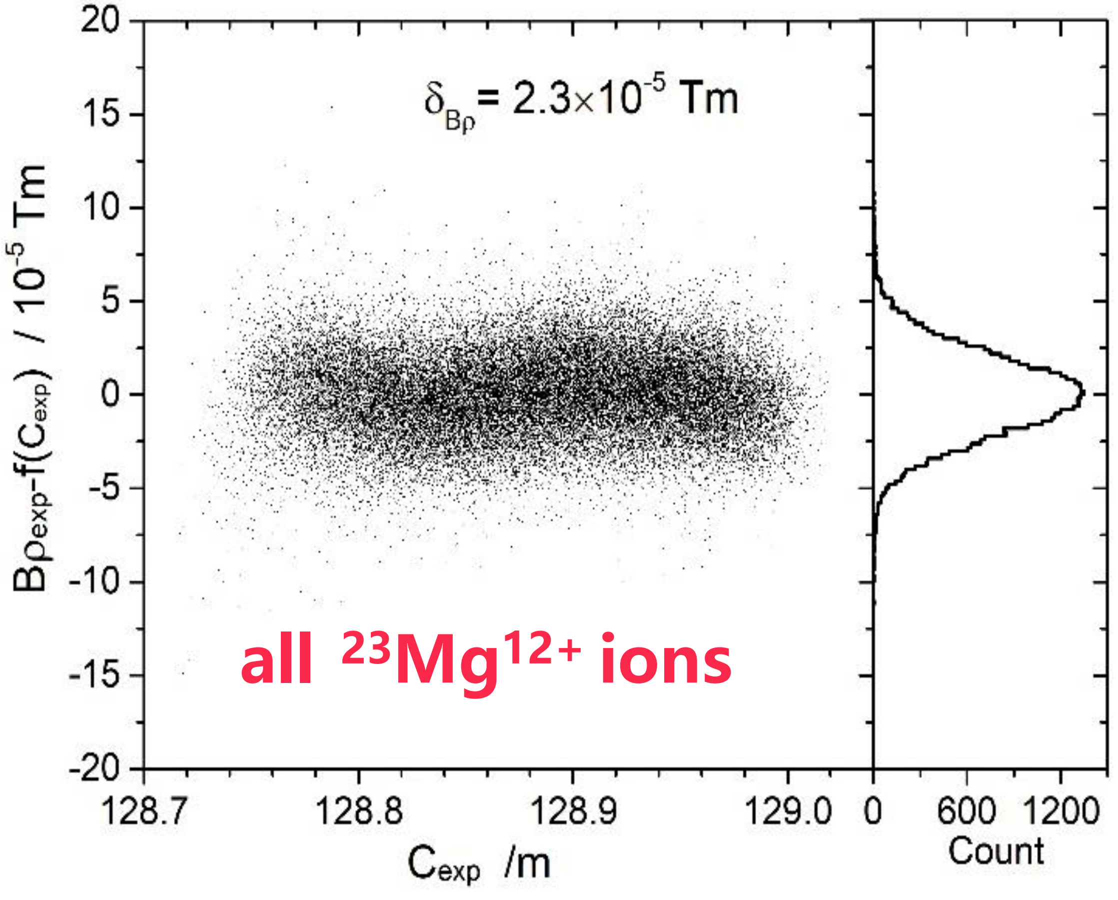

3. Realization of $B\rho$-defined IMS

$$\left(\frac{m}{q}\right)^i_{exp} = \frac{f(C^i_{exp})}{(\gamma v)^i_{exp}},\ i = 1, 2, 3 \ldots.$$

$$v = \frac{L}{\Delta t_{exp} - \Delta t_d}$$

$L = 18034(1.3)$ mm

$\Delta t_d = 99(4)\ ps$

Using FL-266nm-Pico laser

$\frac{m}{q}$ spectrum

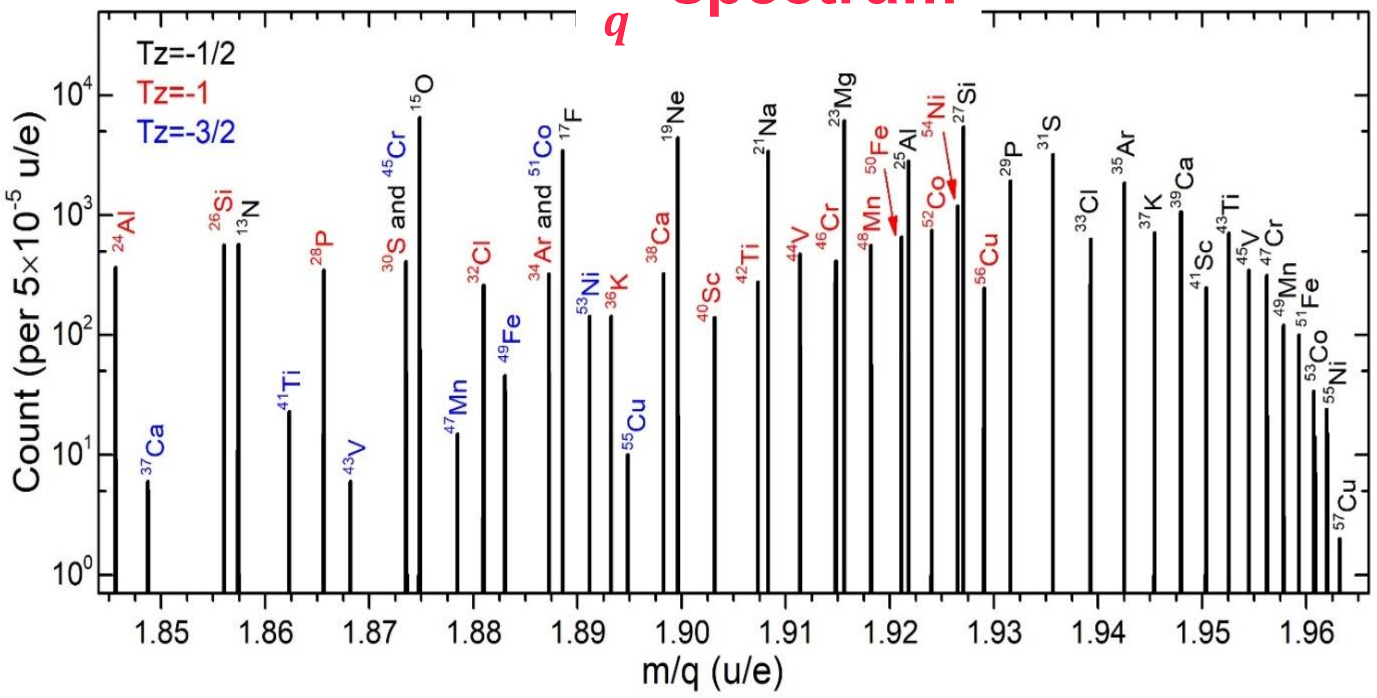

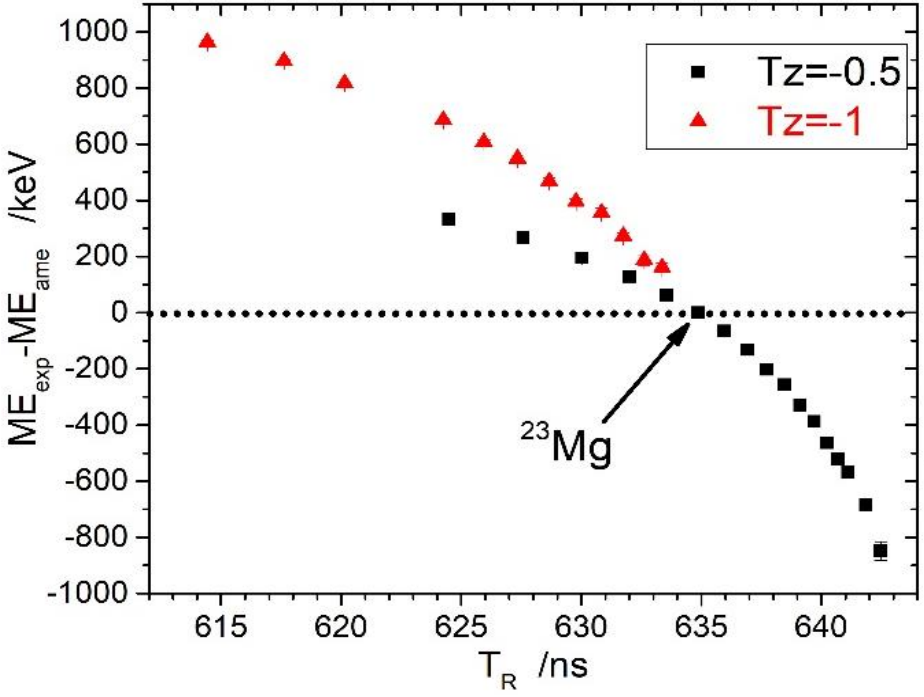

Systematic errors are due to biased L and Δt_d in the velocity determination

3. Realization of $B\rho$-defined IMS

L and Δt_d determinations

$$v = \frac{L}{\Delta t_{exp} - \Delta t_d}$$

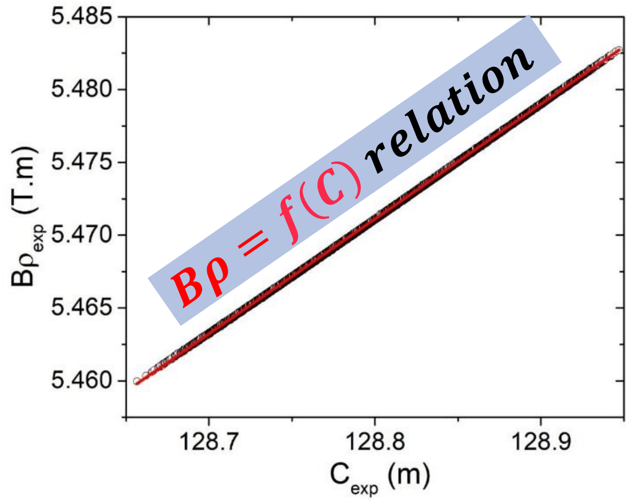

- Calibration with known-mass nuclei in order to find the correct L and Δt_d

- Procedure:
  Minimize the χ^2 by varying L and Δt_d

$$\chi^2 = \frac{1}{N_c} \cdot \sum_i \frac{\left(ME^i_{exp} - ME^i_{AME}\right)^2}{\sigma\left(ME^i_{exp}\right)^2}$$

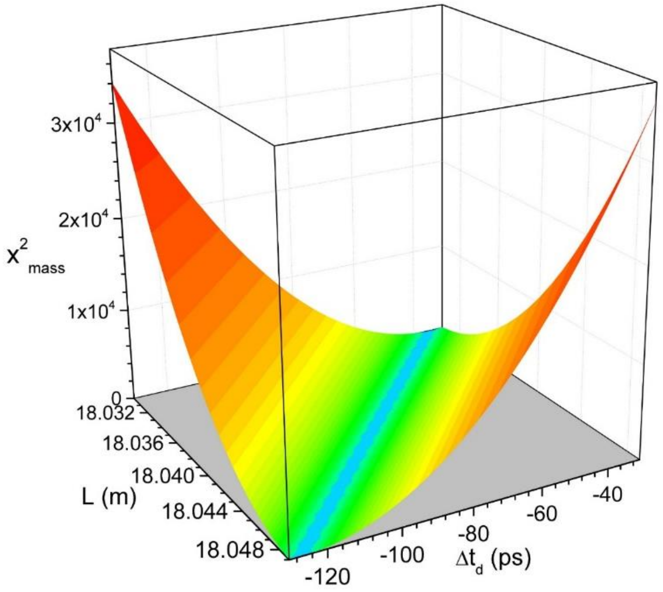

3. Realization of $B\rho$-defined IMS

L and Δt_d determinations

$$v = \frac{L}{\Delta t_{exp} - \Delta t_d}$$

- Calibration with known-mass nuclei in order to find the correct L and Δt_d

- Procedure:
  Minimize the χ^2 by varyng L and Δt_d

$$\chi^2 = \frac{1}{N_c} \cdot \sum_i \frac{\left(ME_{exp}^i - ME_{AME}^i\right)^2}{\sigma\left(ME_{exp}^i\right)^2}$$

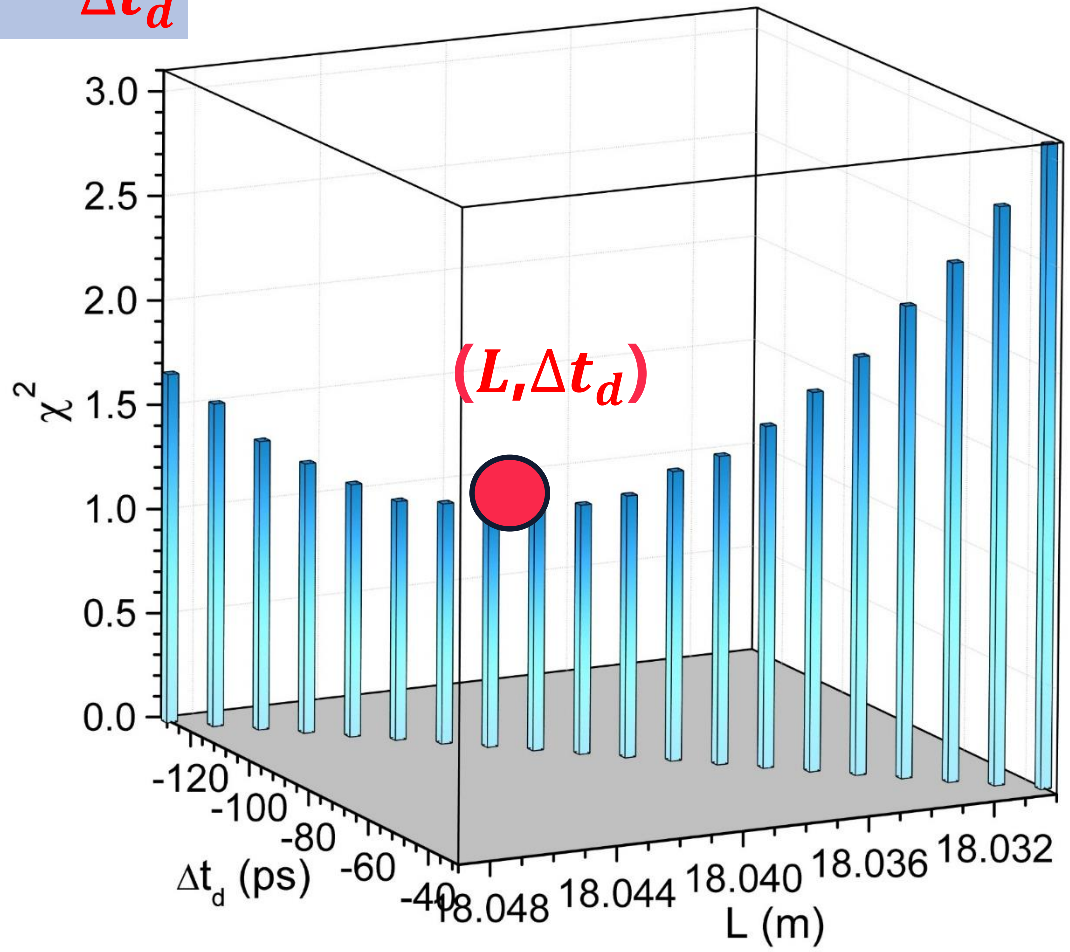

3. Realization of $B\rho$-defined IMS

Using the new L and Δt_d values:

$L = 18037$ mm
$\Delta t_d = 101.6\ ps$

- Re-recalculate the $\{(B\rho)^i_{exp}, C^i_{exp}\}$ data using known-mass nuclei.
- Fit the $\{(B\rho)^i_{exp}, C^i_{exp}\}$ data using

$$f(C) = (B\rho)_0 \cdot \left(\frac{C}{C_0}\right)^K + a_1 \cdot exp[-a_2 \cdot (C - C_0)]$$

- Individual m/q determinations via

$$(m/q)^i_{exp} = \frac{f(C^i_{exp})}{(\gamma v)^i_{exp}}, \qquad i = 1, 2, 3, \ldots N_t$$

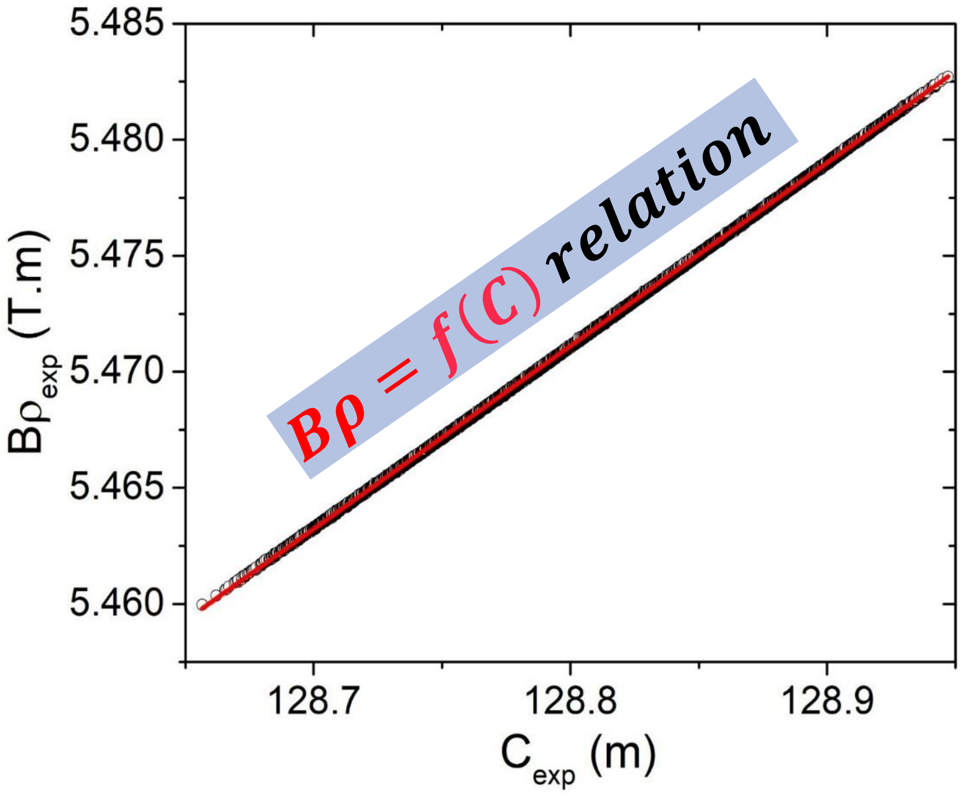

3. Realization of $B\rho$-defined IMS

Error estimation

$$\gamma_t{}^2 = \frac{d(B\rho)/(B\rho)}{dC/C} = \frac{C}{f(C)} \cdot \frac{df(C)}{dC}$$

$$\sigma_{B\rho}(\gamma, \gamma_t) = b_0 + b_1 \cdot (\gamma^2 - \gamma_t^2) + b_2 \cdot (\gamma^2 - \gamma_t^2)^2$$

$$\frac{\sigma[(m/q)^i_{exp}]}{(m/q)^i_{exp}} = \frac{\sigma_{B\rho}(\gamma^i_{exp}, \gamma^i_t)}{f(C^i_{exp})}, i = 1, 2, 3 \dots N_t.$$

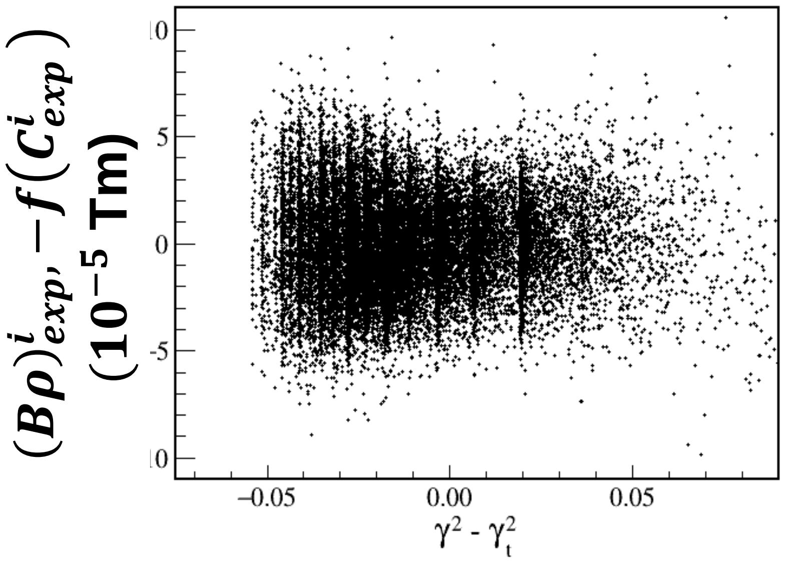

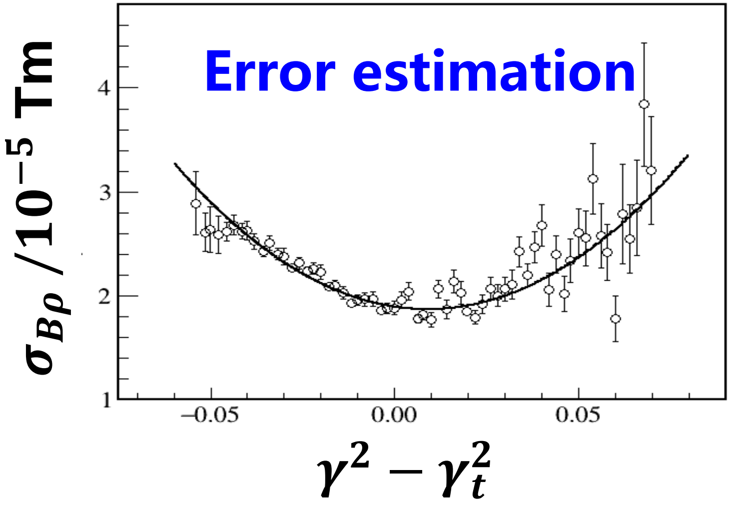

3. Realization of $B\rho$-defined IMS

Masses and uncertainties

$$(m/q)^i_{exp} = \frac{f(C^i_{exp})}{(\gamma v)^i_{exp}}, \qquad i = 1, 2, 3, \dots N_t$$

$$\frac{\sigma[(m/q)^i_{exp}]}{(m/q)^i_{exp}} = \frac{\sigma_{B\rho}(\gamma^i_{exp}, \gamma^i_t)}{f(C^i_{exp})}, i = 1, 2, 3 \dots N_t.$$

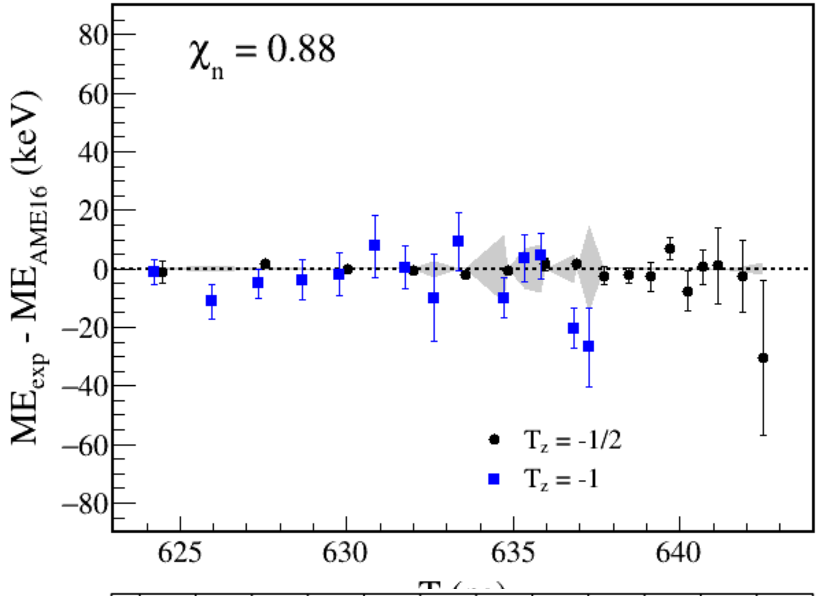

$\frac{m}{q}$ spectrum

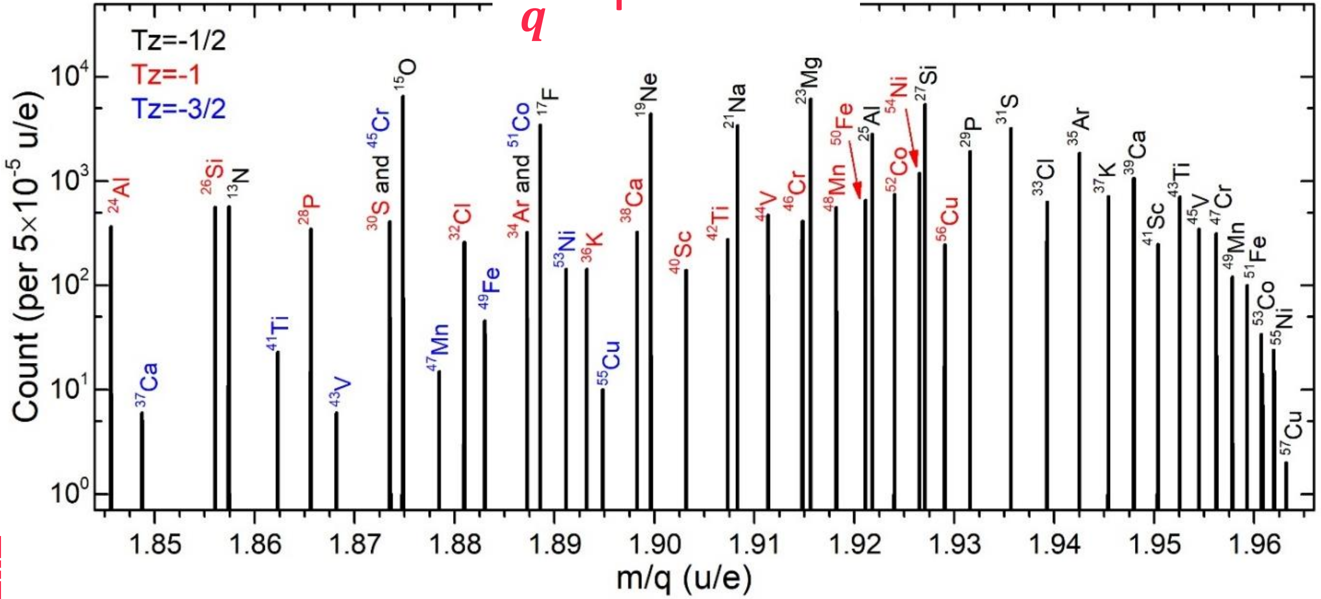

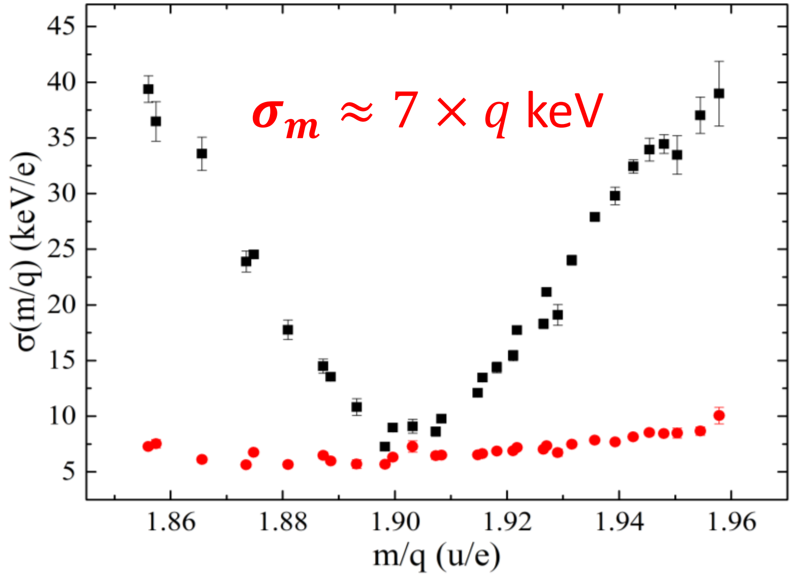

3. Realization of $B\rho$-defined IMS

Masses and uncertainties

$$(m/q)^i_{exp} = \frac{f(C^i_{exp})}{(\gamma v)^i_{exp}}, \qquad i = 1, 2, 3, \ldots N_t$$

$$\frac{\sigma[(m/q)^i_{exp}]}{(m/q)^i_{exp}} = \frac{\sigma_{B\rho}(\gamma^i_{exp}, \gamma^i_t)}{f(C^i_{exp})}, i = 1, 2, 3 \ldots N_t.$$

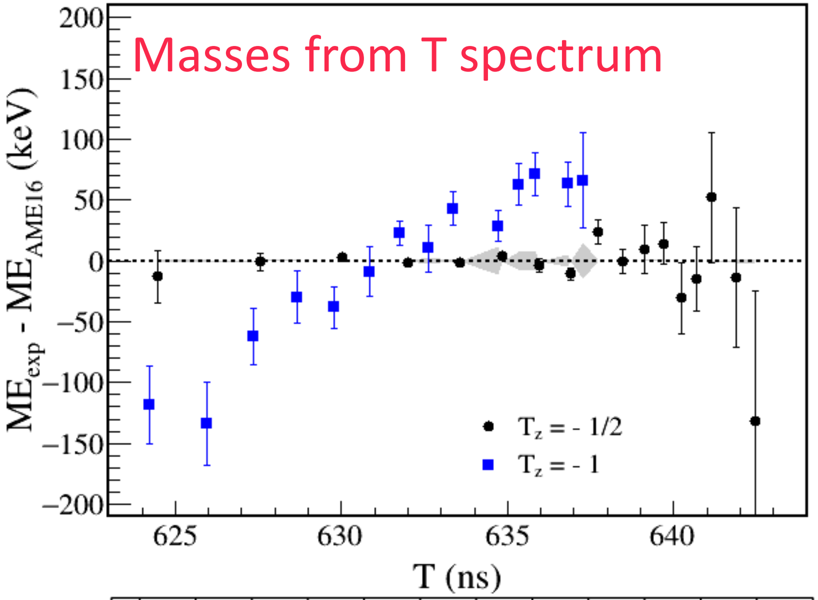

$\frac{m}{q}$ spectrum

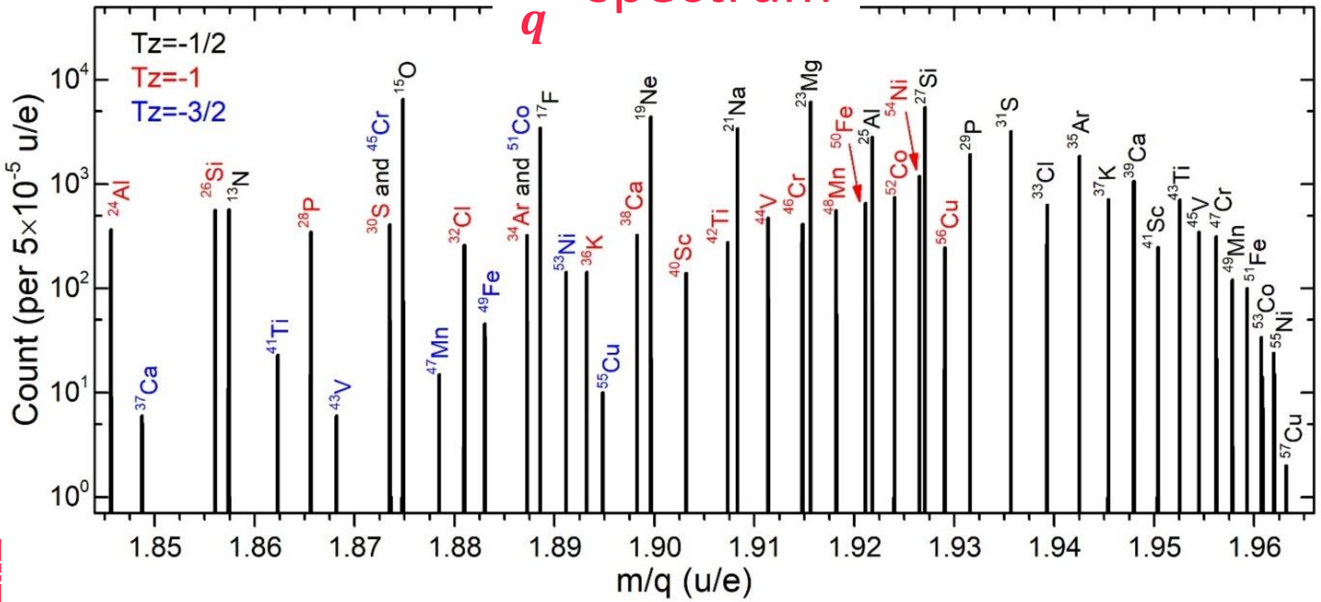

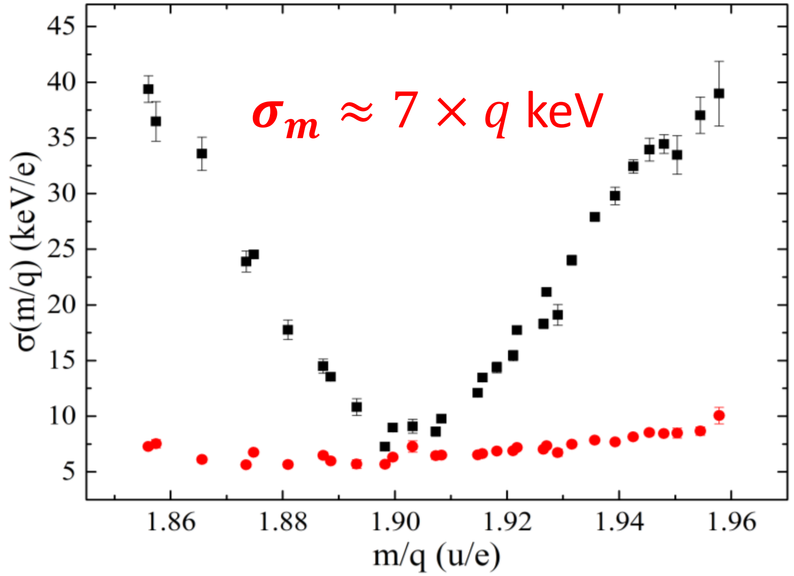

3. Realization of $B\rho$-defined IMS

Mass resolving powers are significantly improved after field drift correction for all nuclides in the large *m/q*-range of $\Delta(m/q) \approx 0.10\ ue^{-1}$

$\frac{m}{q}$ spectrum

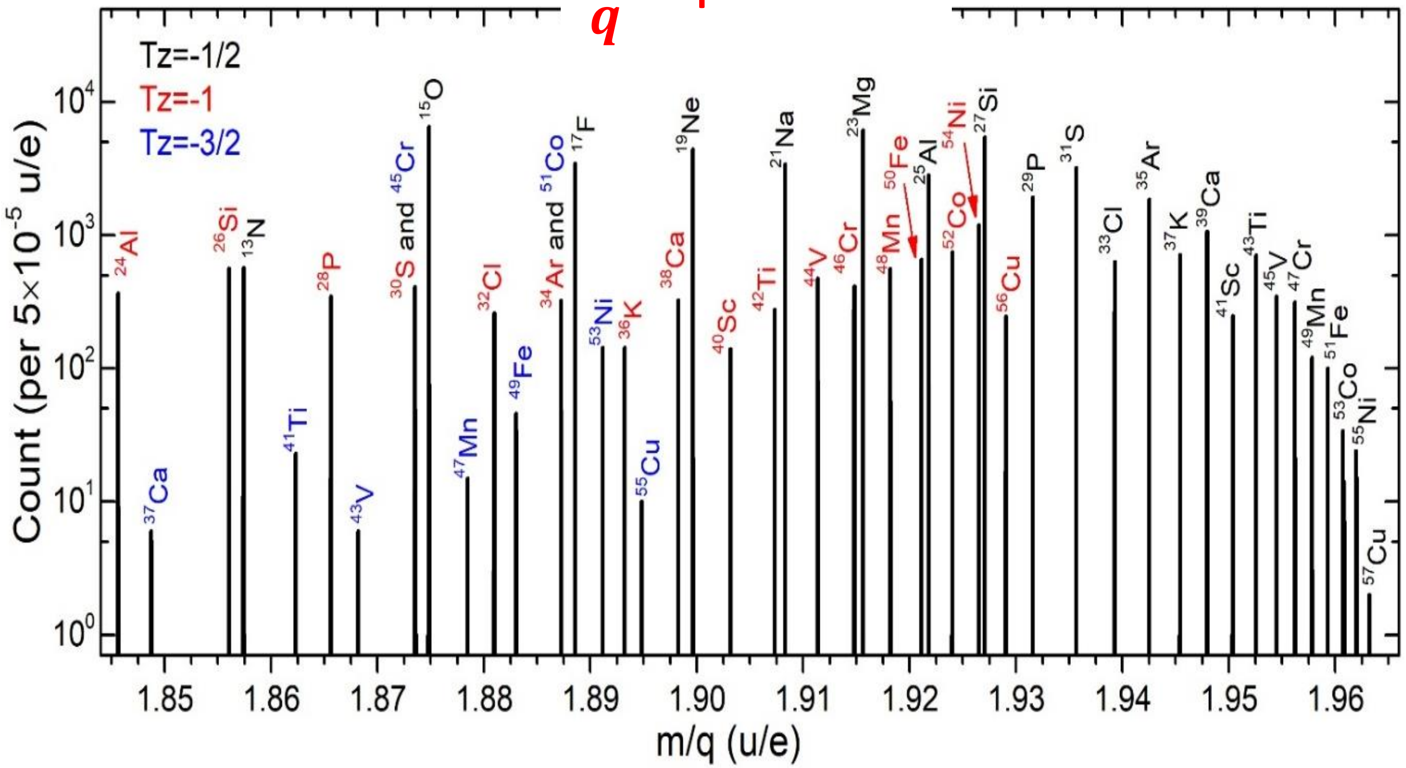

^{58}Ni beam

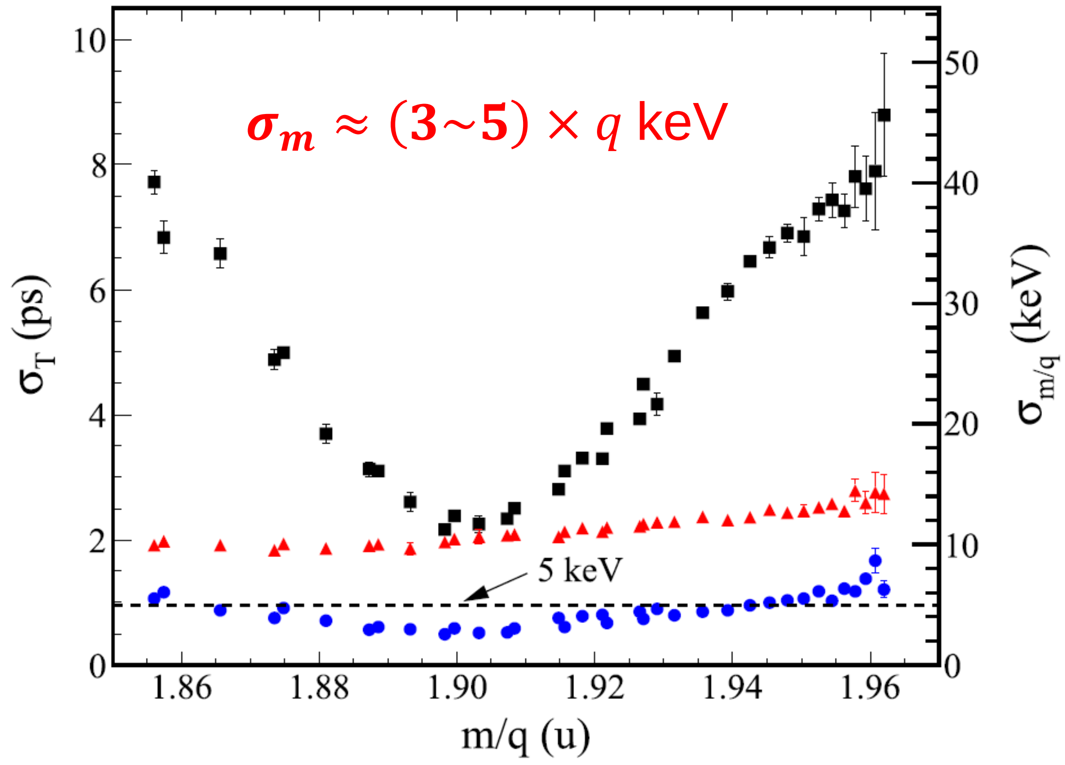

3. Realization of $B\rho$-defined IMS

$$T_{fix}^{i} = C_{fix} \cdot \sqrt{\frac{1}{(B\rho)_{fix}^{2}} \cdot \left[\left(\frac{m}{q}\right)_{exp}^{i}\right]^{2} + \left(\frac{1}{v_c}\right)^{2}}, \qquad i = 1, 2, 3 \ \ldots$$

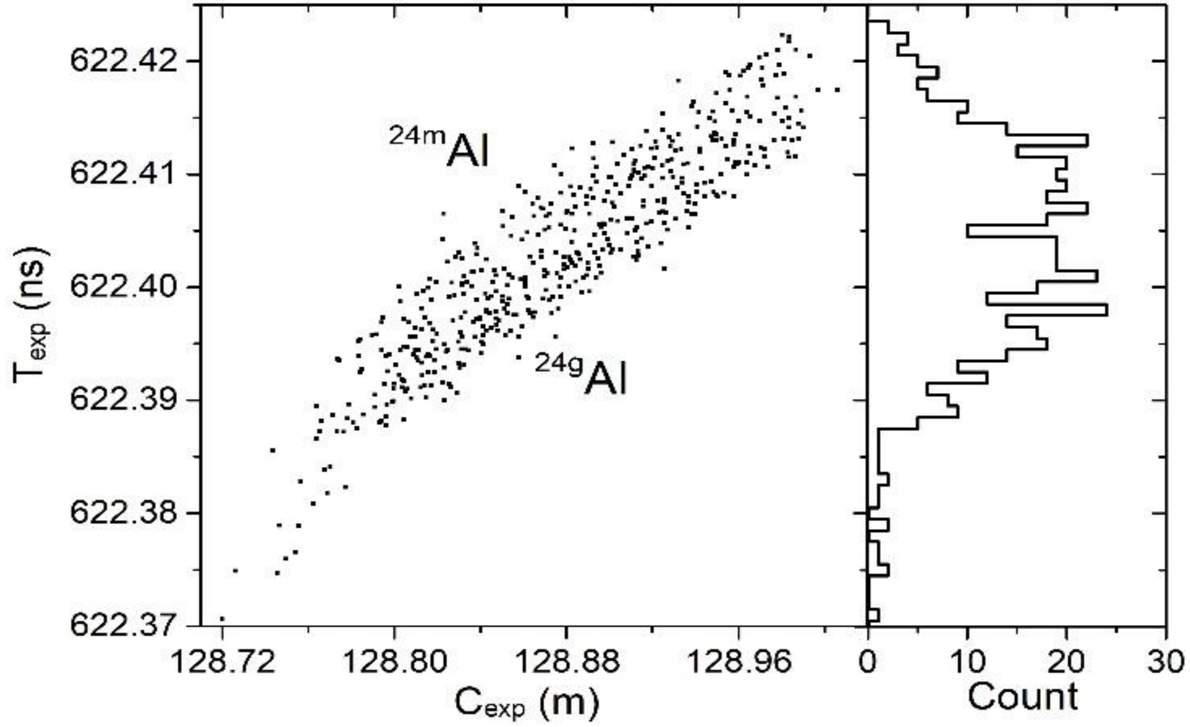

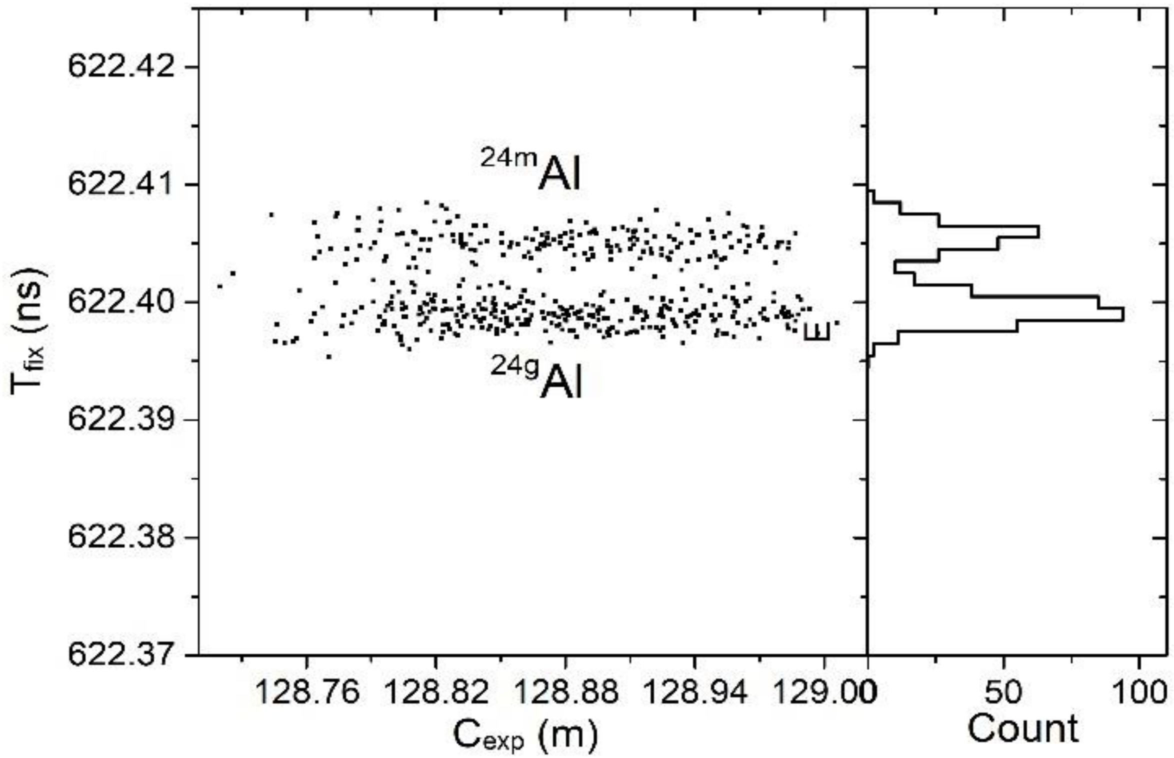

3. Realization of *B*ρ-defined IMS

Asymmatric *T* and *v* distributions

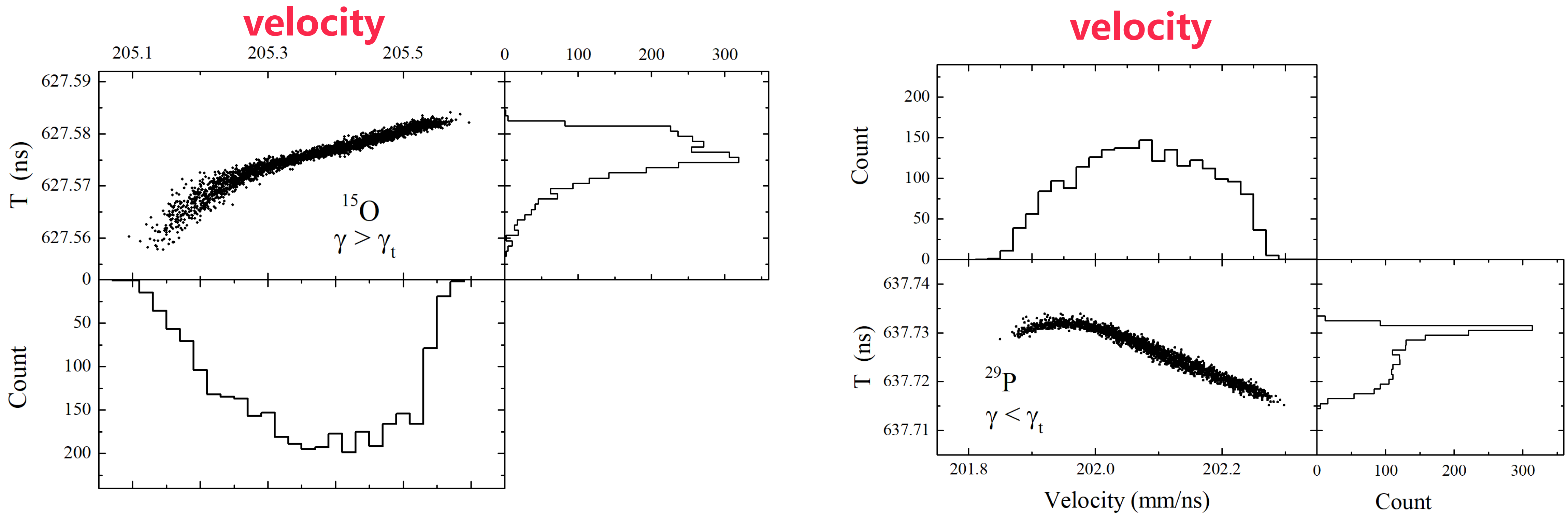

3. Realization of $B\rho$-defined IMS

All ions

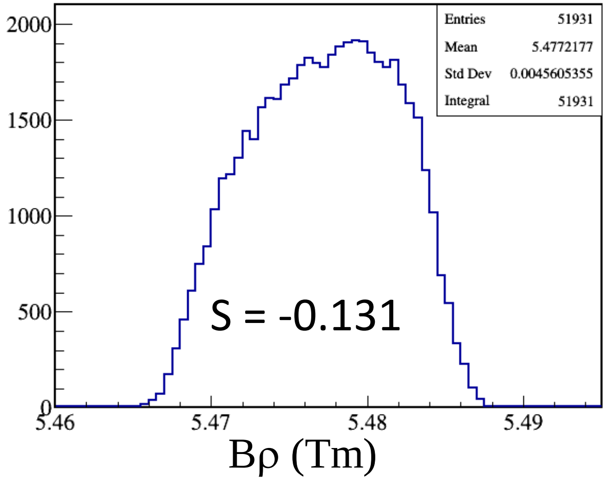

$T_z = -1/2$

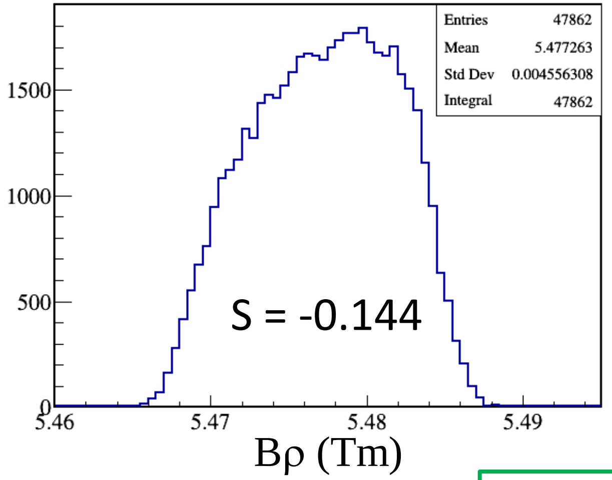

$T_z = -1$

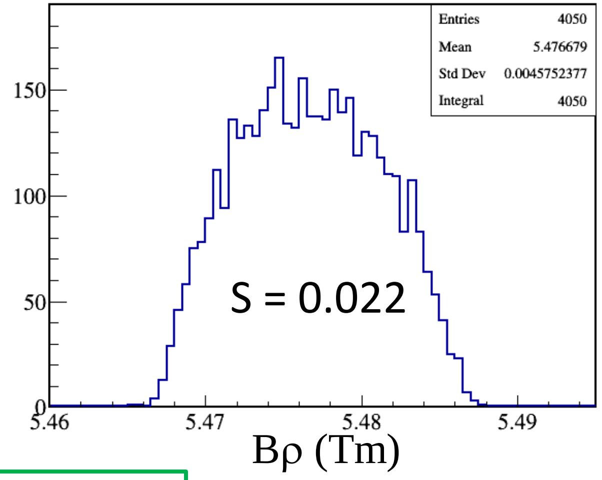

偏度（Skewness）

$$S = \left(\frac{1}{n}\sum_{i=1}^{n}(x_i - \bar{x})^3\right)/\sigma^3$$

$\bar{x}$是平均值，σ是标准差

LISE++计算

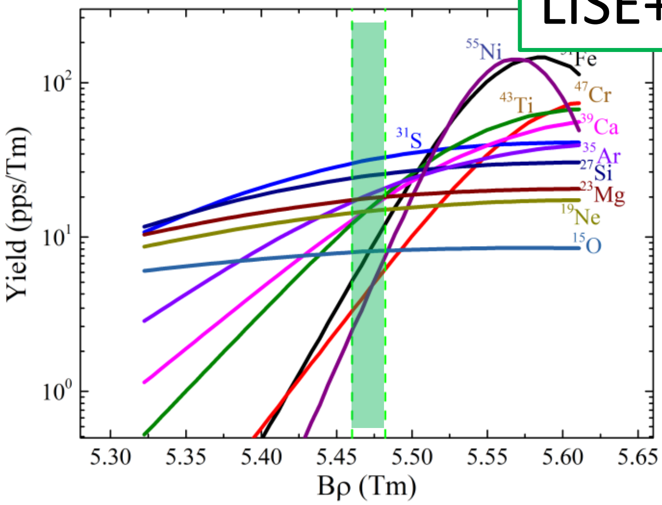

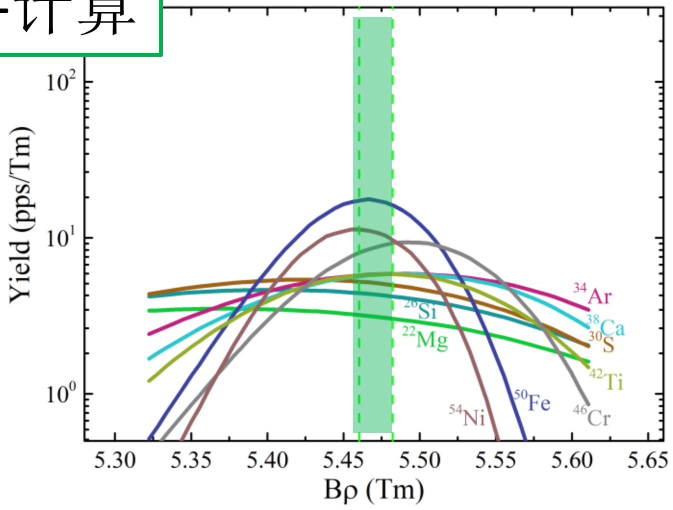

3. Realization of $B\rho$-defined IMS

All ions **$T_z = -1/2$** **$T_z = -1$**

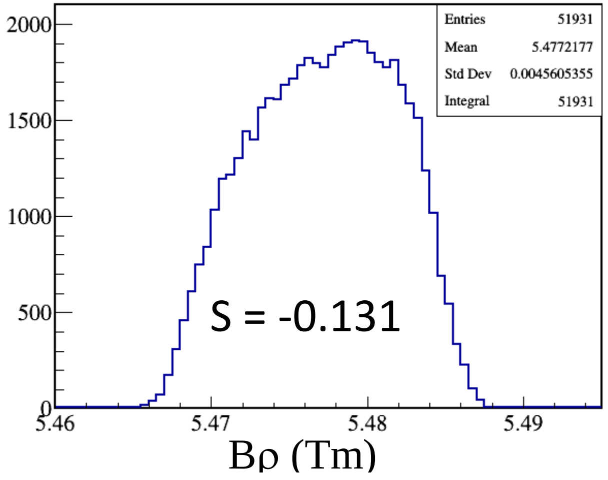

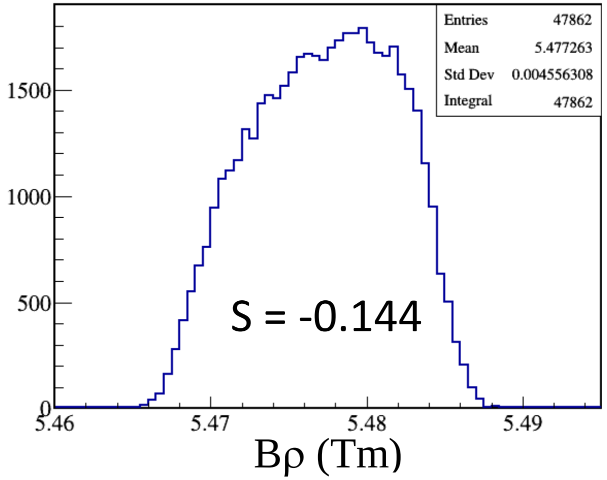

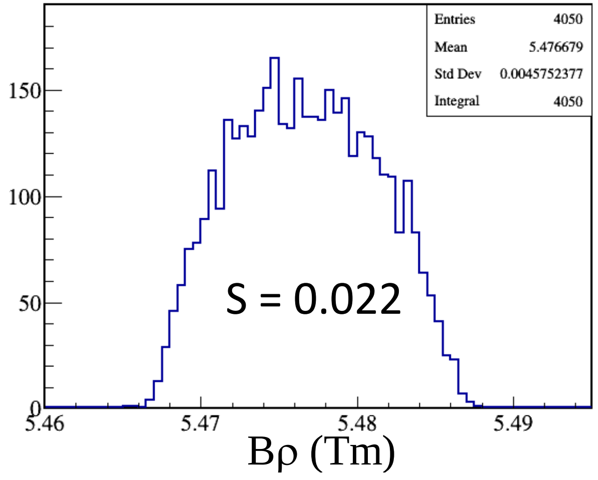

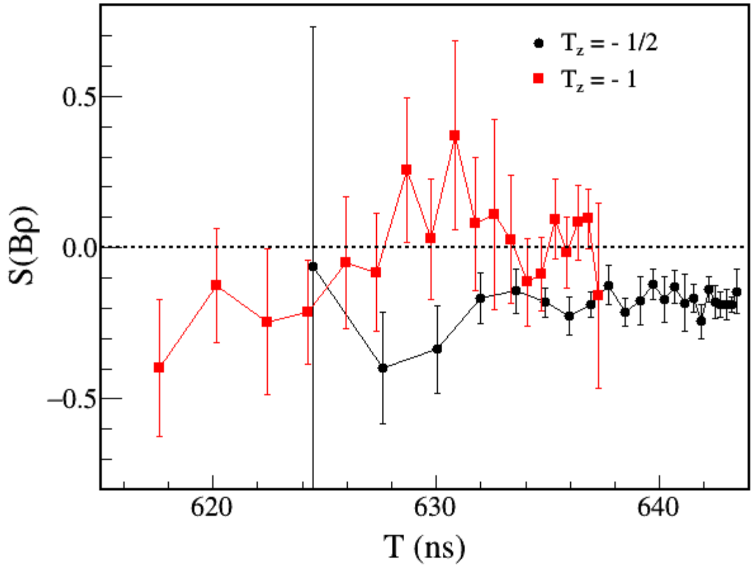

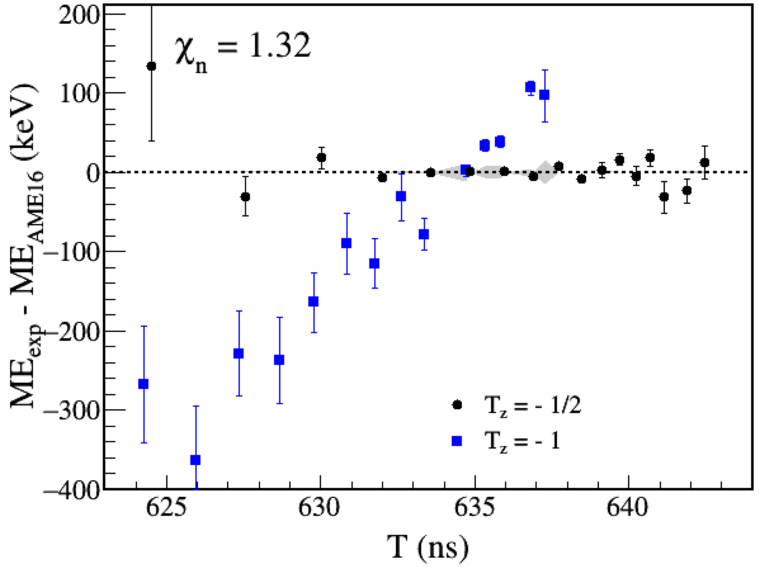

Obtained from T spectrum

轨道长度区间 (128.70, 129.05)m, 动量接受 0.4%

3. Realization of $B\rho$-defined IMS

All ions $\qquad T_z = -1/2 \qquad T_z = -1$

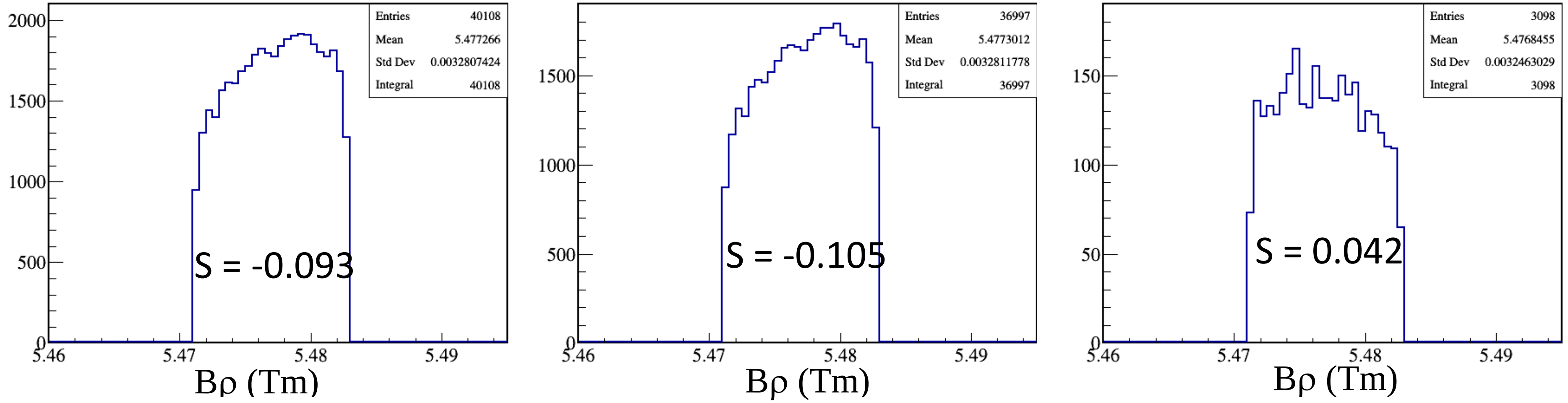

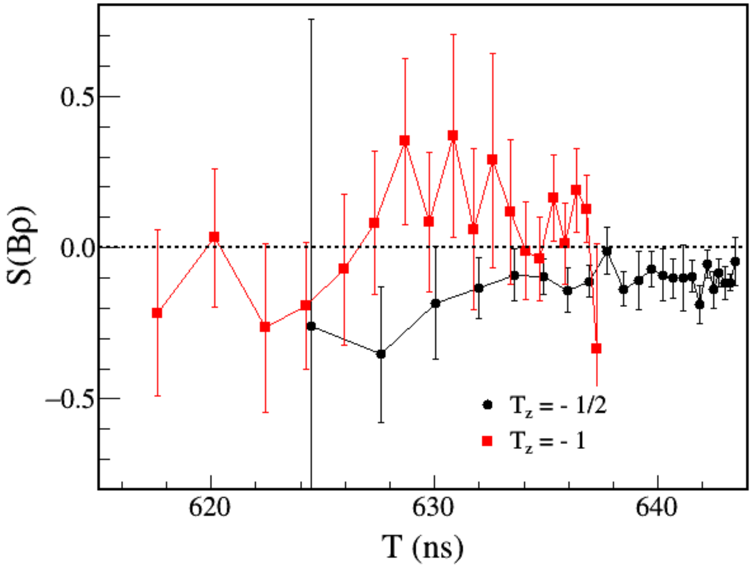

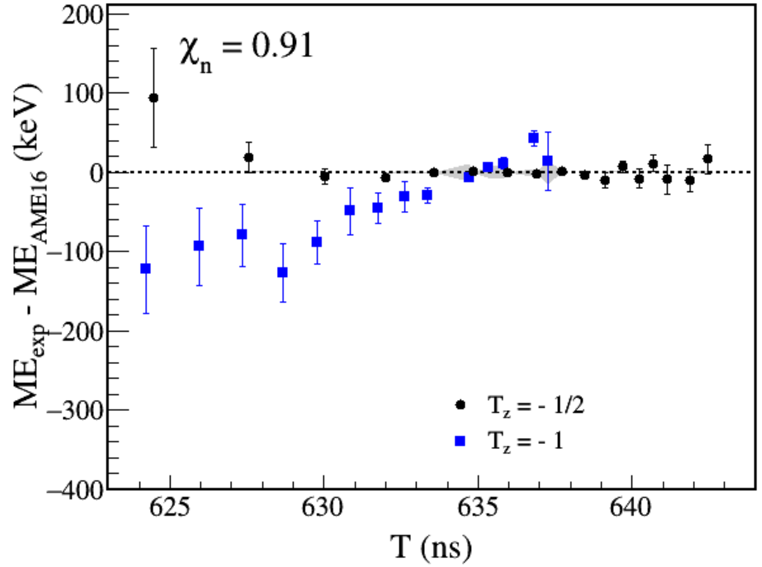

Obtained from T spectrum

轨道长度区间 (128.80, 128.95)m, 动量接受度 0.2%

3. Realization of $B\rho$-defined IMS

所有离子　　$T_z = -1/2$　　$T_z = -1$

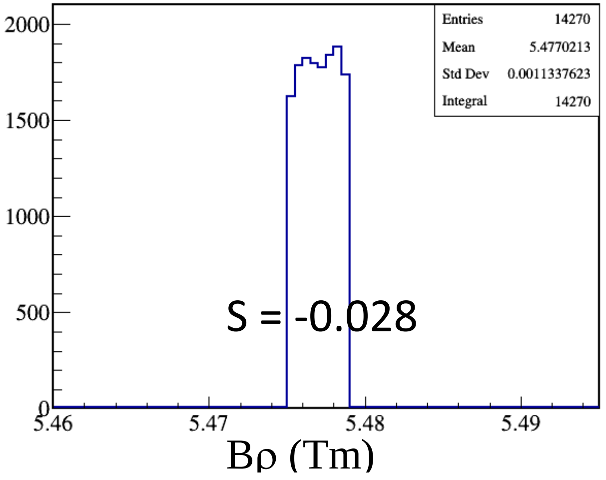

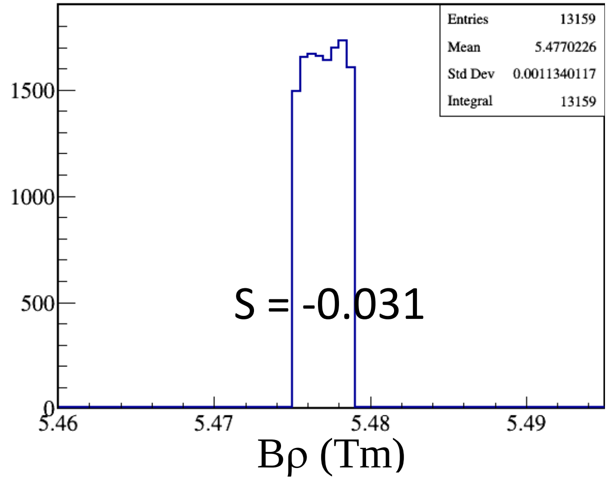

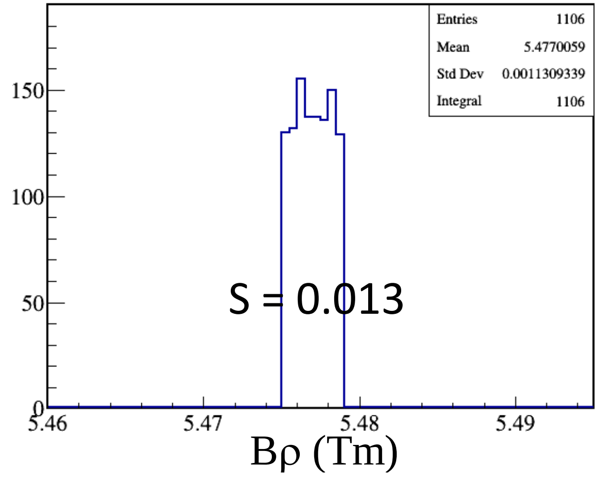

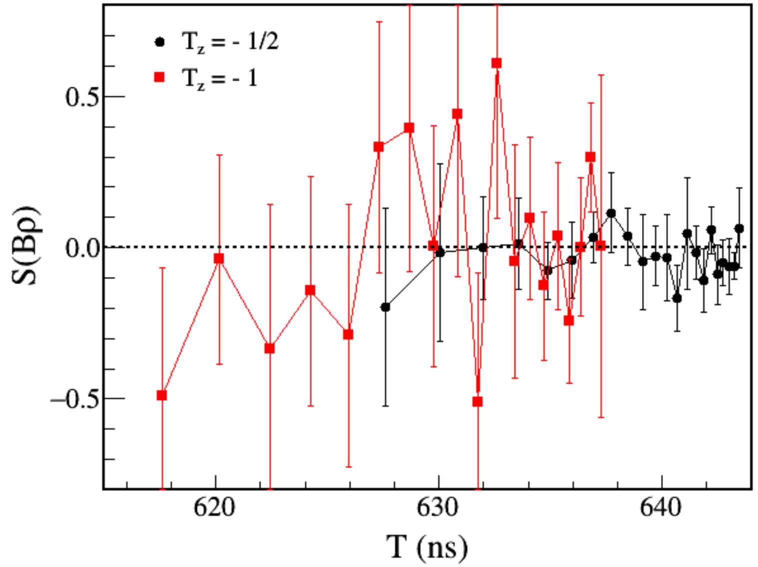

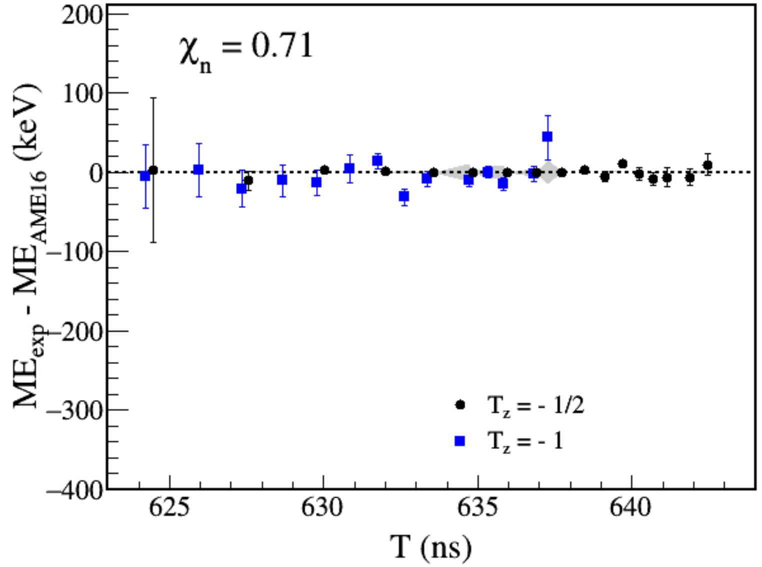

Obtained from T spectrum

轨道长度区间 (128.85, 128.90)m, 动量接受度 0.08%

3. Realization of $B\rho$-defined IMS

Single TOF

Double TOF

Without Field correction

With Field correction

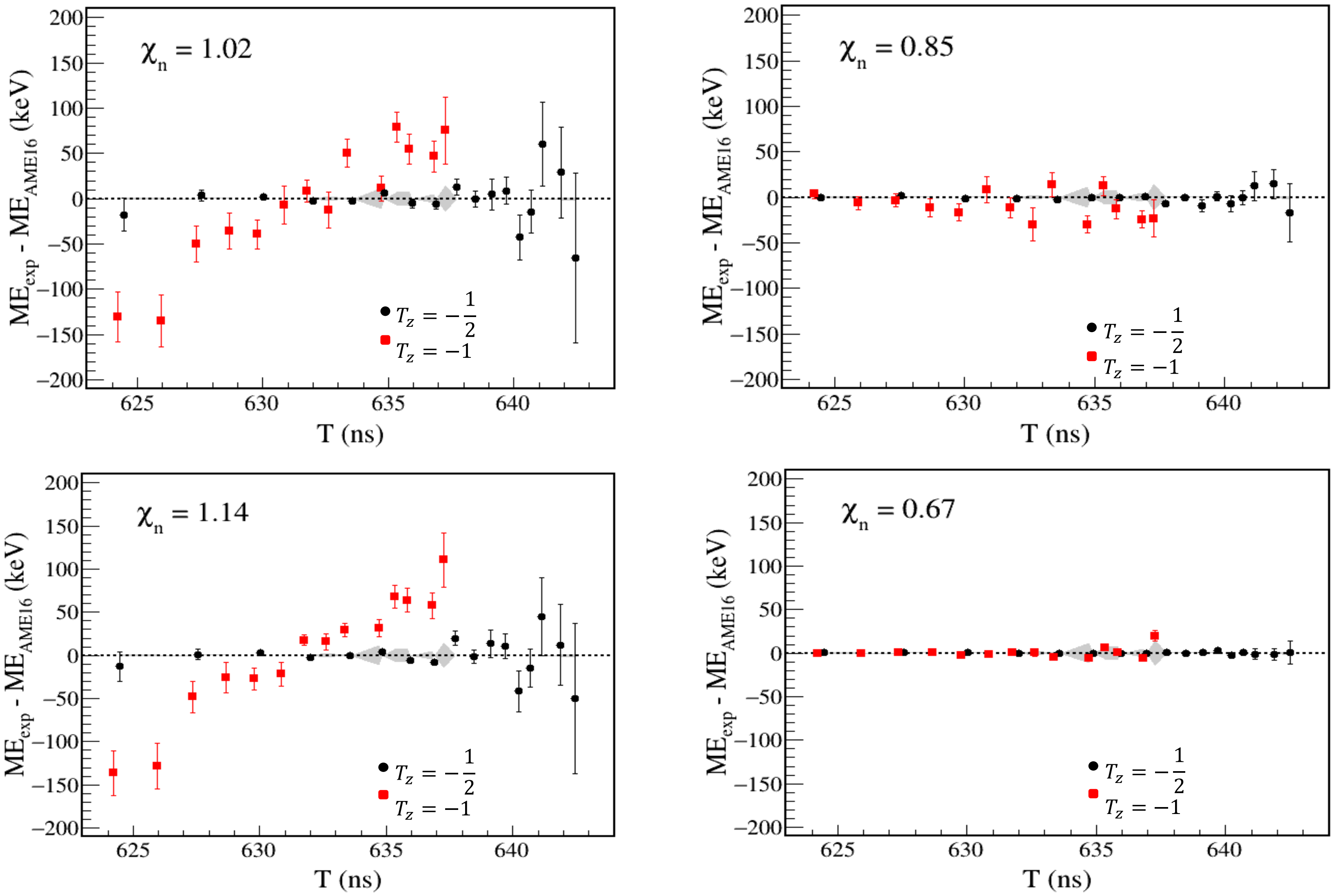

3. Realization of *B*ρ-defined IMS

Hyperfine Interact 173: 49-54 (2006

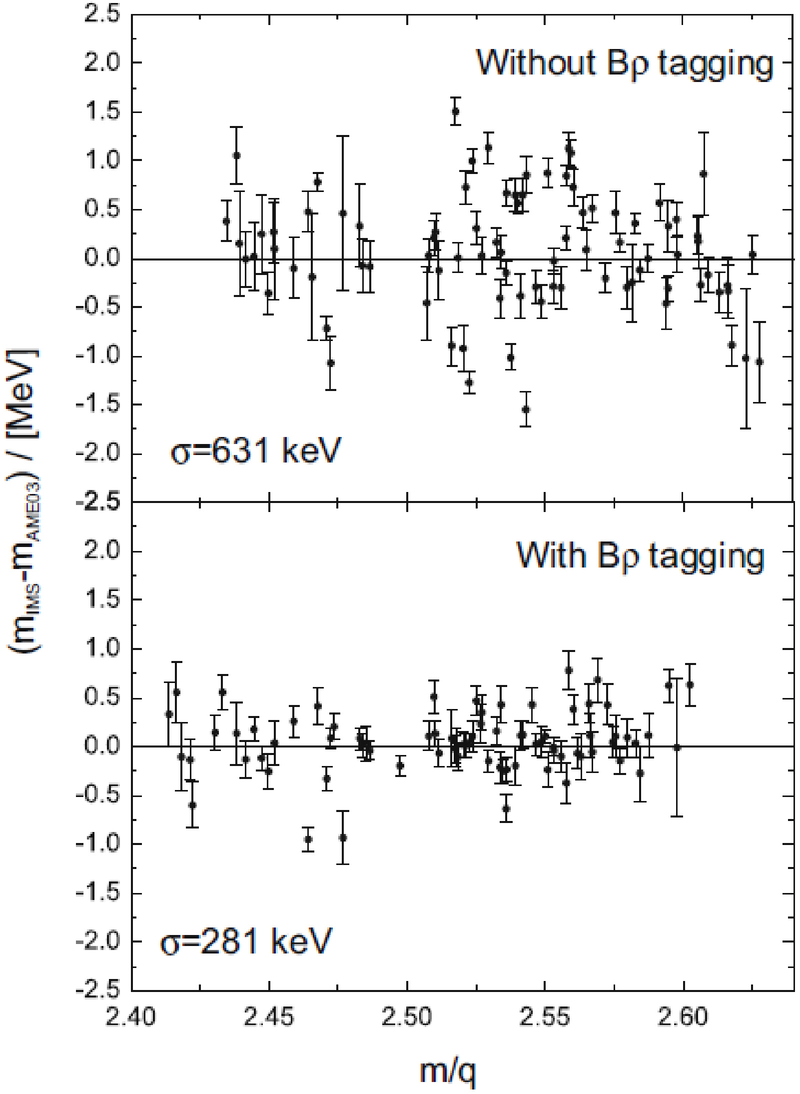

Eur. Phys. J. A52, 138 (2016)

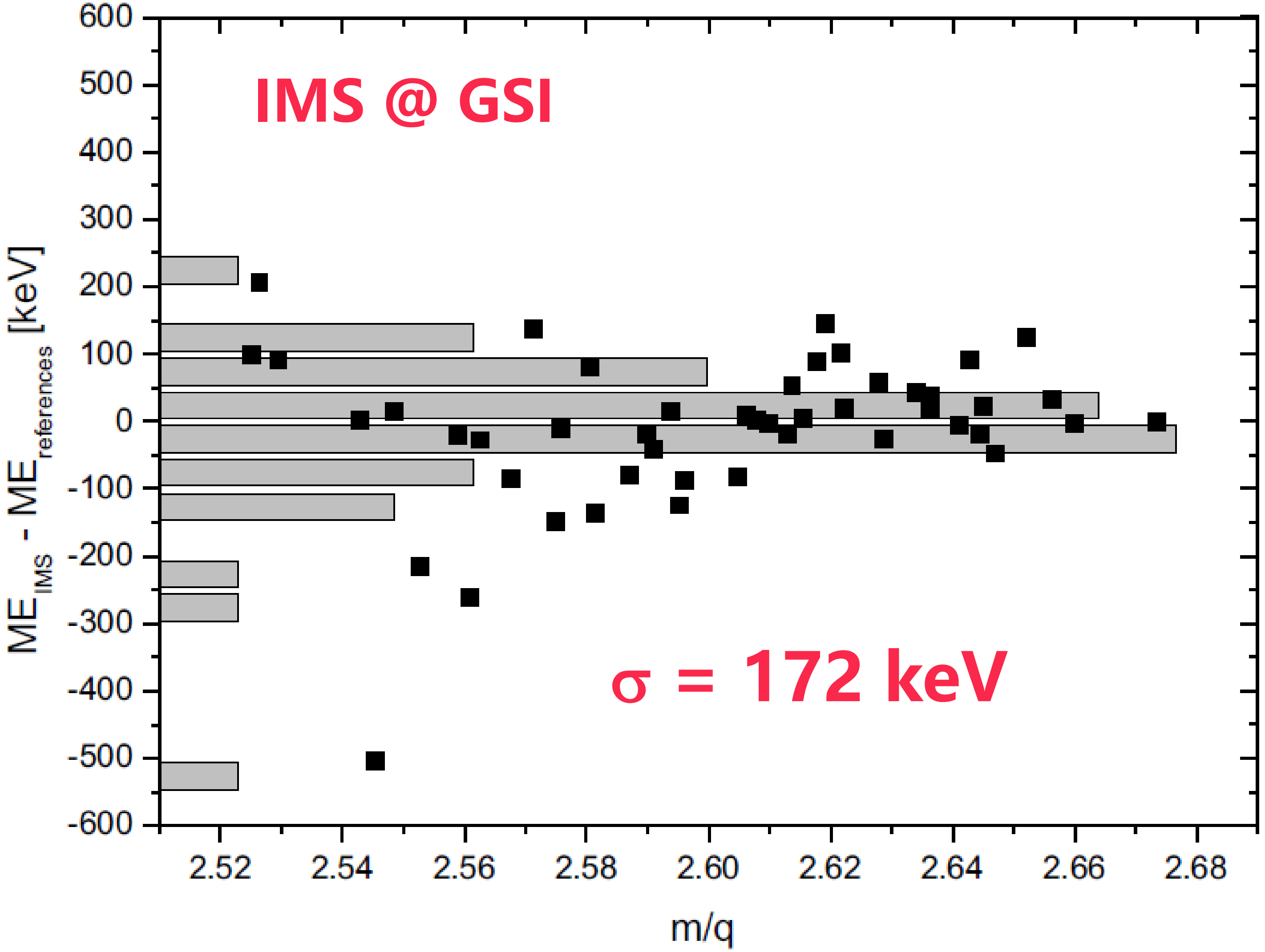

3. Realization of $B\rho$-defined IMS

Re-determined masses of $T_Z = -1$ nuclei

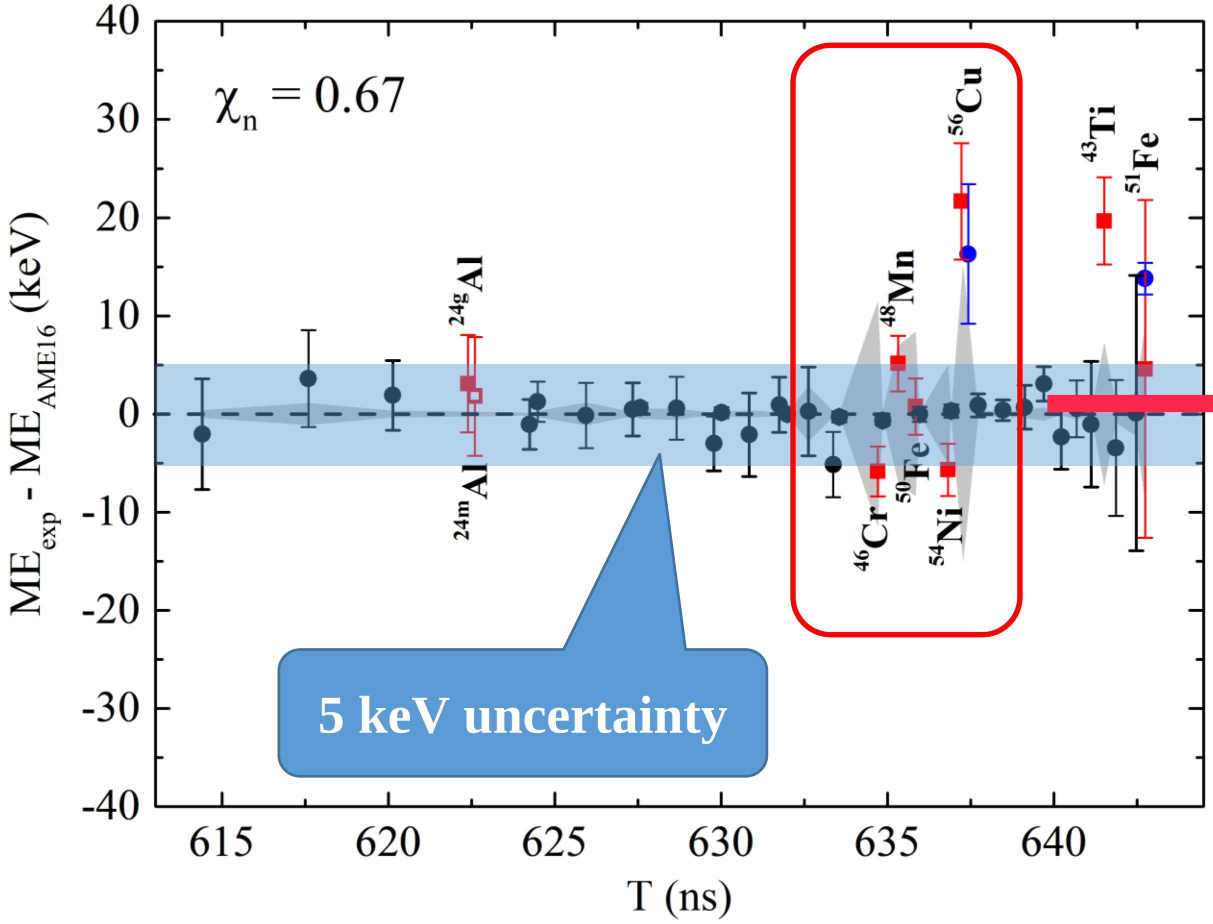

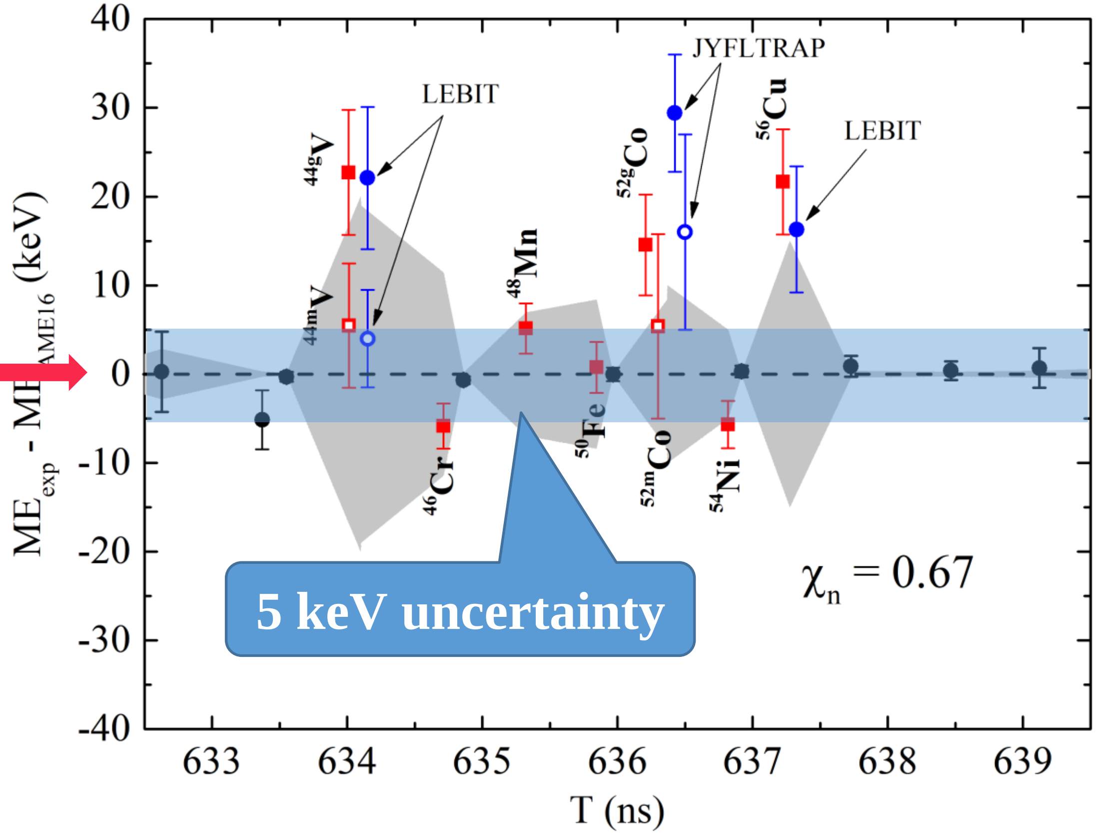

3. Realization of *B*ρ-defined IMS

Check the mass accuracy of the *B*ρ-defined IMS

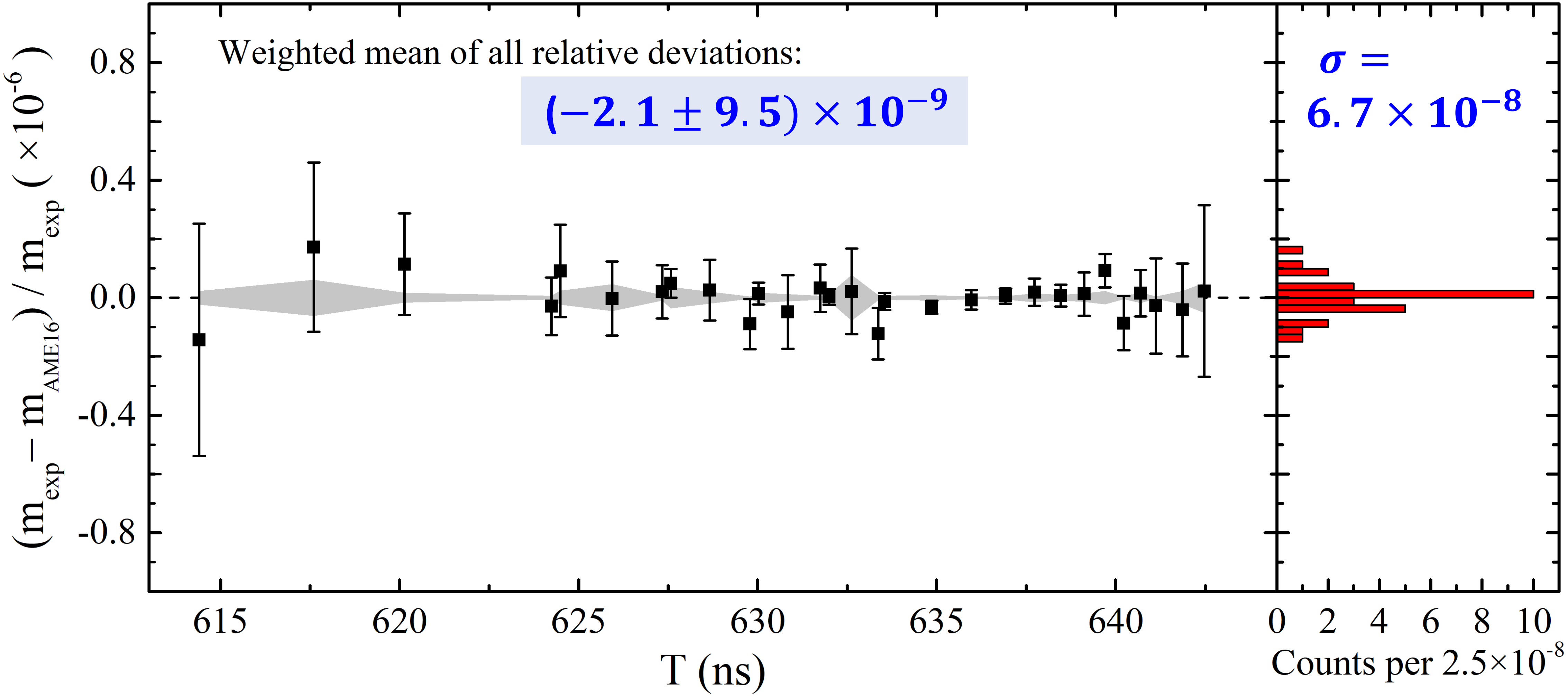

3. Realization of $B\rho$-defined IMS

Mass accuracy of the MR-TOF-MS at GSI

PHYSICAL REVIEW C 99, 064313 (2019)

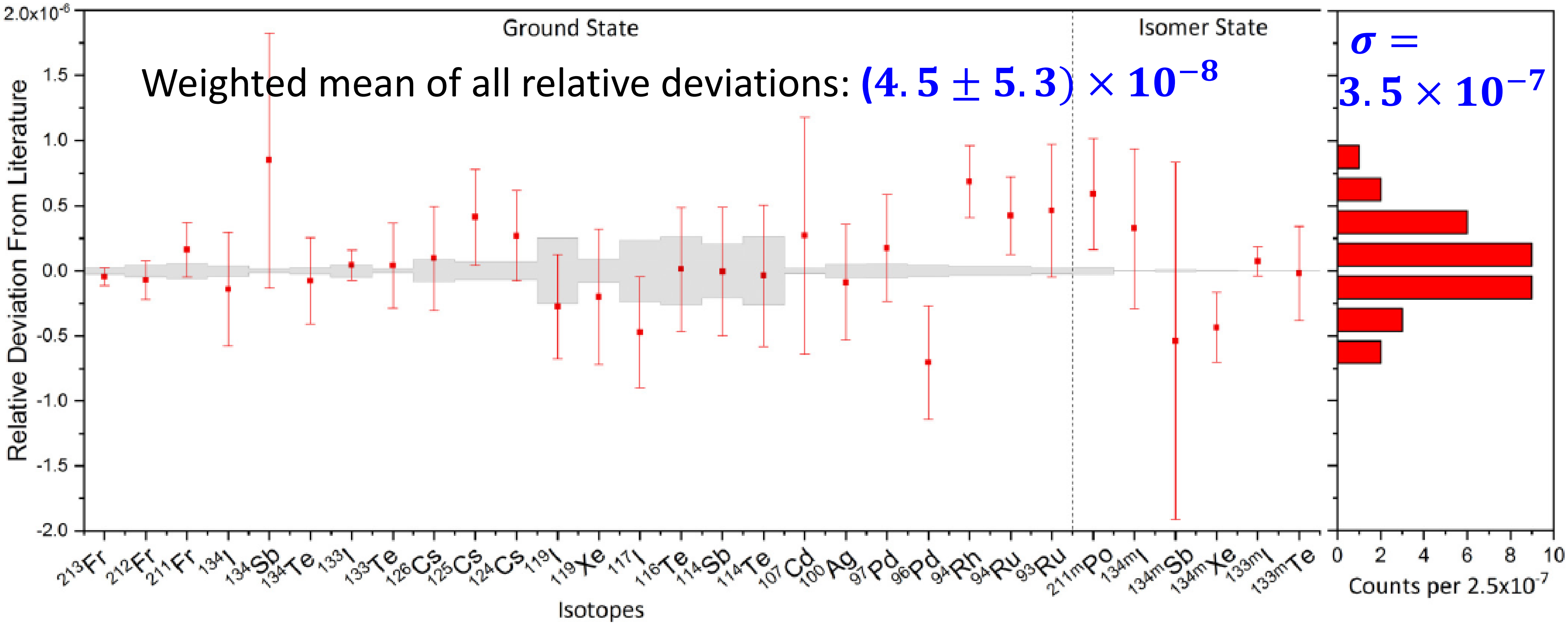

3. Realization of $B\rho$-defined IMS

Comparison with MR-TOF-MS@RIKEN

Mass accuracy using MR-TOF-MS at RIKEN

S. Kimura et al., IJMS 430, 134(2018)

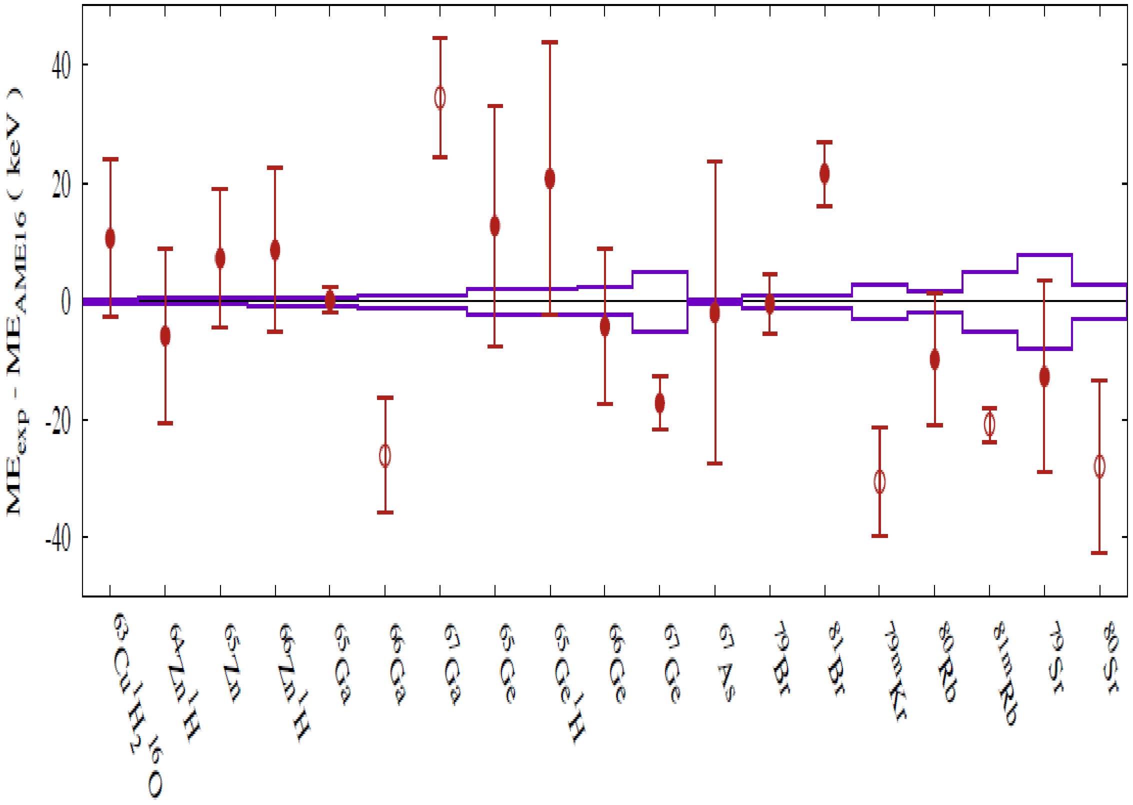

Mass accuracy using $B\rho$-IMS at IMP

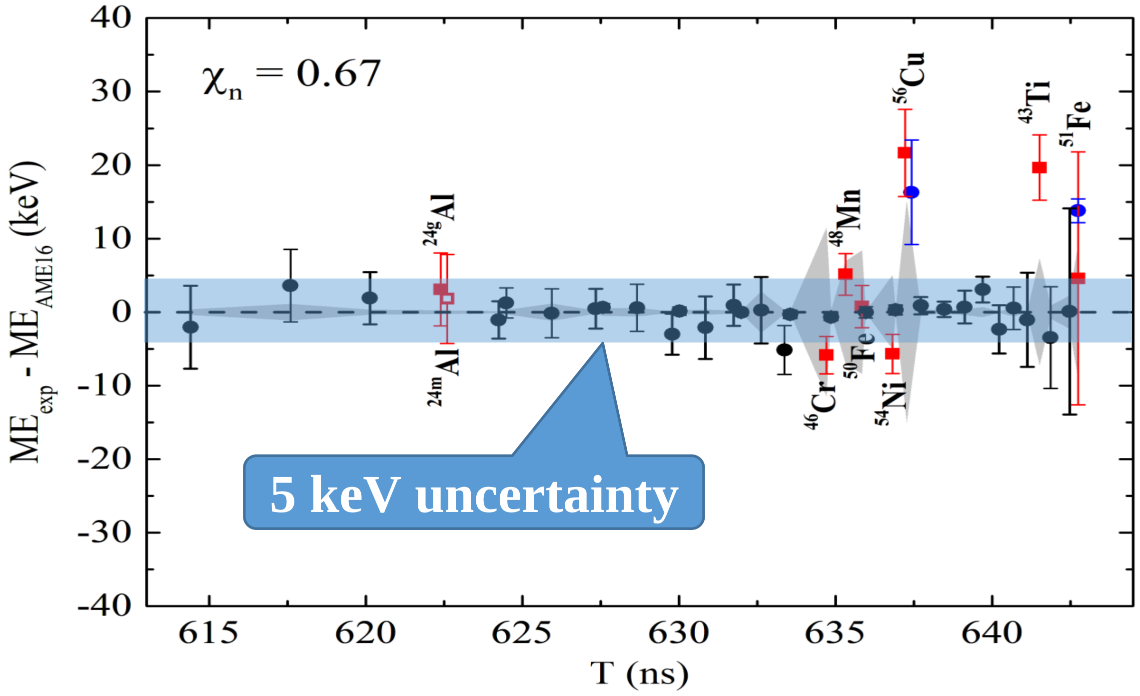

3. Realization of $B\rho$-defined IMS

Comparison with SMS @ GSI

SMS at GSI

Nucl. Phys. A 756, 3 (2005)

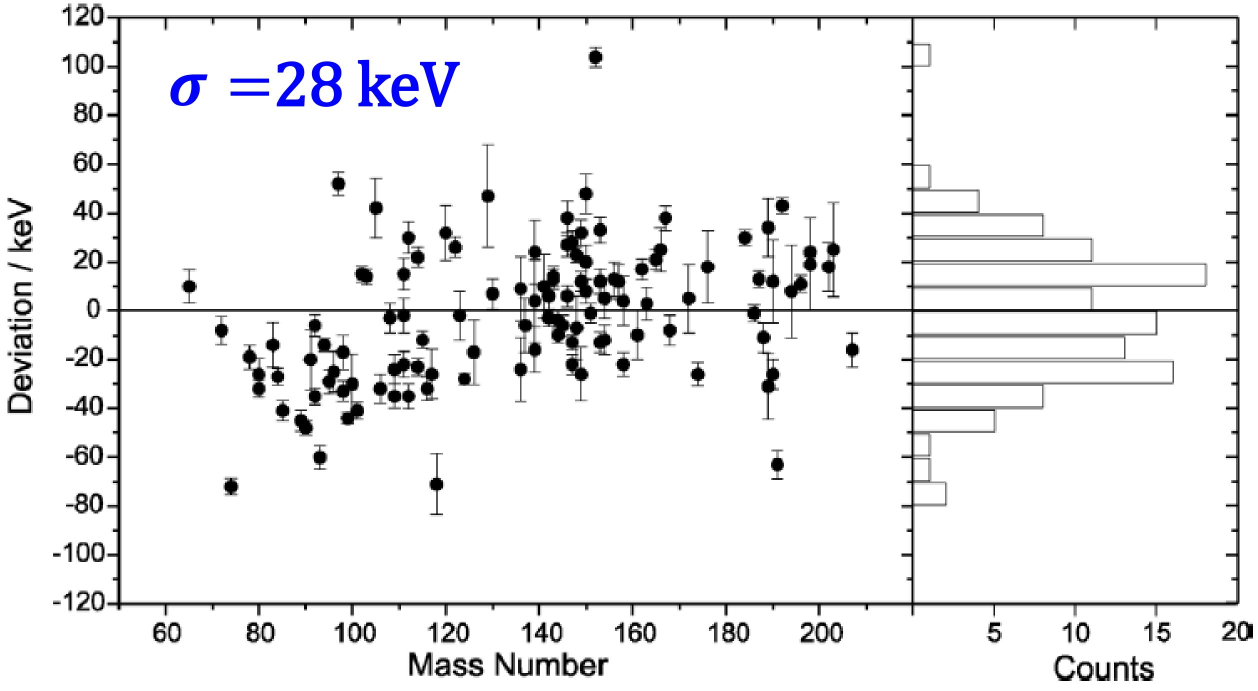

$B\rho$-IMS at IMP

PHYSICAL REVIEW C **106**, L051301 (2022)

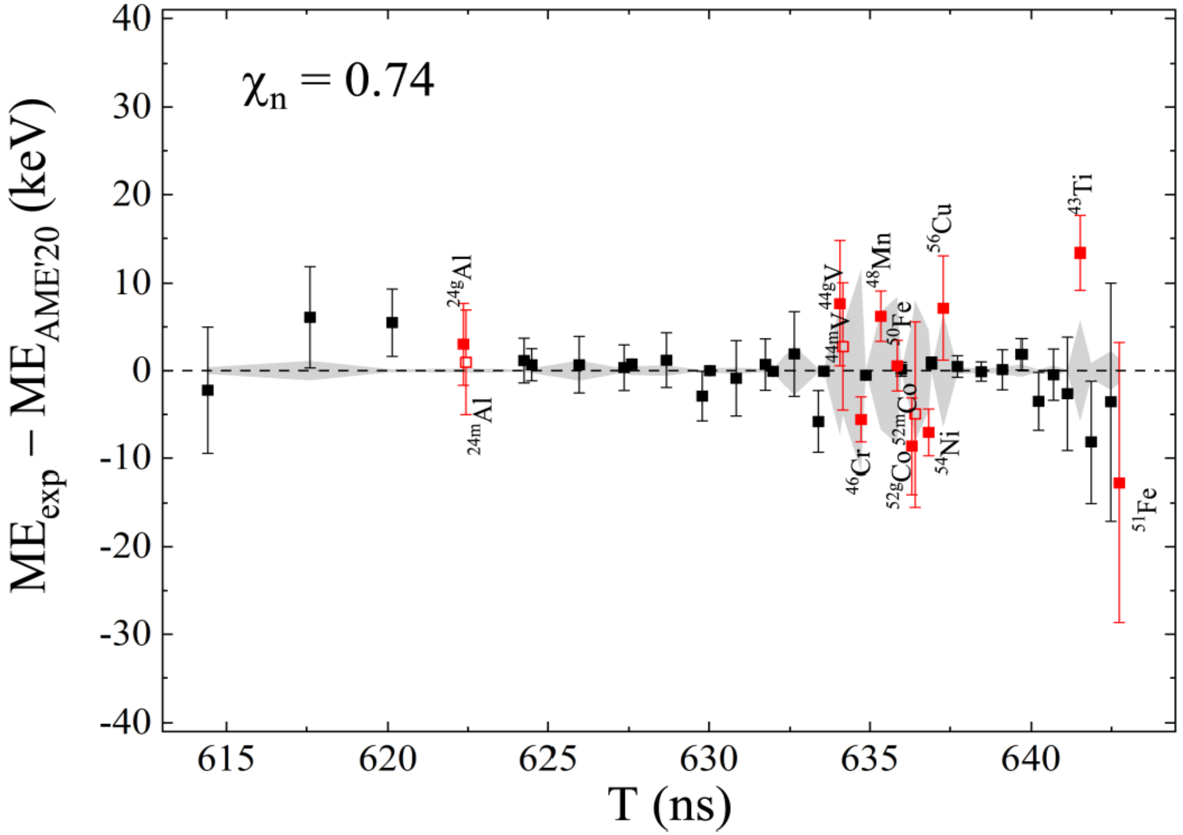

3. Realization of $B\rho$-defined IMS

Advantages of $B\rho$-defined IMS

1) Fast measurement: $t_{exp} \approx 0.1\ ms$

2) High sensitivity: $a\ single\ \ ion, \sigma_m \approx (3\sim5) \times q$ (keV)

3) High efficiency: $tens\ of\ ions\ in\ a\ single\ run$

4) High precision: *on par with PTMS for short-lived nuclei*

5) Zero background: *background-free measurements*

3. Realization of $B\rho$-defined IMS

PHYSICAL REVIEW C **106**, L051301 (2022)

Letter

$B\rho$-defined isochronous mass spectrometry: An approach for high-precision mass measurements of short-lived nuclei

M. Wang,[1,2,*] M. Zhang,[1,2] X. Zhou,[1,2] Y. H. Zhang,[1,2,†] Yu. A. Litvinov,[1,3,‡] H. S. Xu,[1,2] R. J. Chen,[1,3] H. Y. Deng,[1,2] C. Y. Fu,[1] W. W. Ge,[1] H. F. Li,[1,2] T. Liao,[1,2] S. A. Litvinov,[1,3] P. Shuai,[1] J. Y. Shi,[1,2] M. Si,[1,2] R. S. Sidhu,[3] Y. N. Song,[1,2] M. Z. Sun,[1] S. Suzuki,[1] Q. Wang,[1,2] Y. M. Xing,[1] X. Xu,[1] T. Yamaguchi,[4] X. L. Yan,[1] J. C. Yang,[1,2] Y. J. Yuan,[1,2] Q. Zeng,[5] and X. H. Zhou[1,2]

Eur. Phys. J. A (2023) 59:27
https://doi.org/10.1140/epja/s10050-023-00928-6

THE EUROPEAN PHYSICAL JOURNAL A

Check for updates

Regular Article - Experimental Physics

$B\rho$-defined isochronous mass spectrometry and mass measurements of ^{58}Ni fragments

M. Zhang[1,2], X. Zhou[1,2], M. Wang[1,2,a], Y. H. Zhang[1,2,b], Yu. A. Litvinov[1,3,c], H. S. Xu[1,2], R. J. Chen[1,3], H. Y. Deng[1,2], C. Y. Fu[1], W. W. Ge[1], H. F. Li[1,2], T. Liao[1,2], S. A. Litvinov[3,1], P. Shuai[1], J. Y. Shi[1,2], R. S. Sidhu[3], Y. N. Song[1,2], M. Z. Sun[1], S. Suzuki[1], Q. Wang[1,2], Y. M. Xing[1], X. Xu[1], T. Yamaguchi[4], X. L. Yan[1], J. C. Yang[1,2], Y. J. Yuan[1,2], Q. Zeng[5], X. H. Zhou[1,2]

4. New masses from the $B\rho$-defined IMS

^{78}Kr primary beam + $B\rho$-IMS

^{58}Ni primary beam + $B\rho$-IMS

^{36}Ar primary beam + $B\rho$-IMS

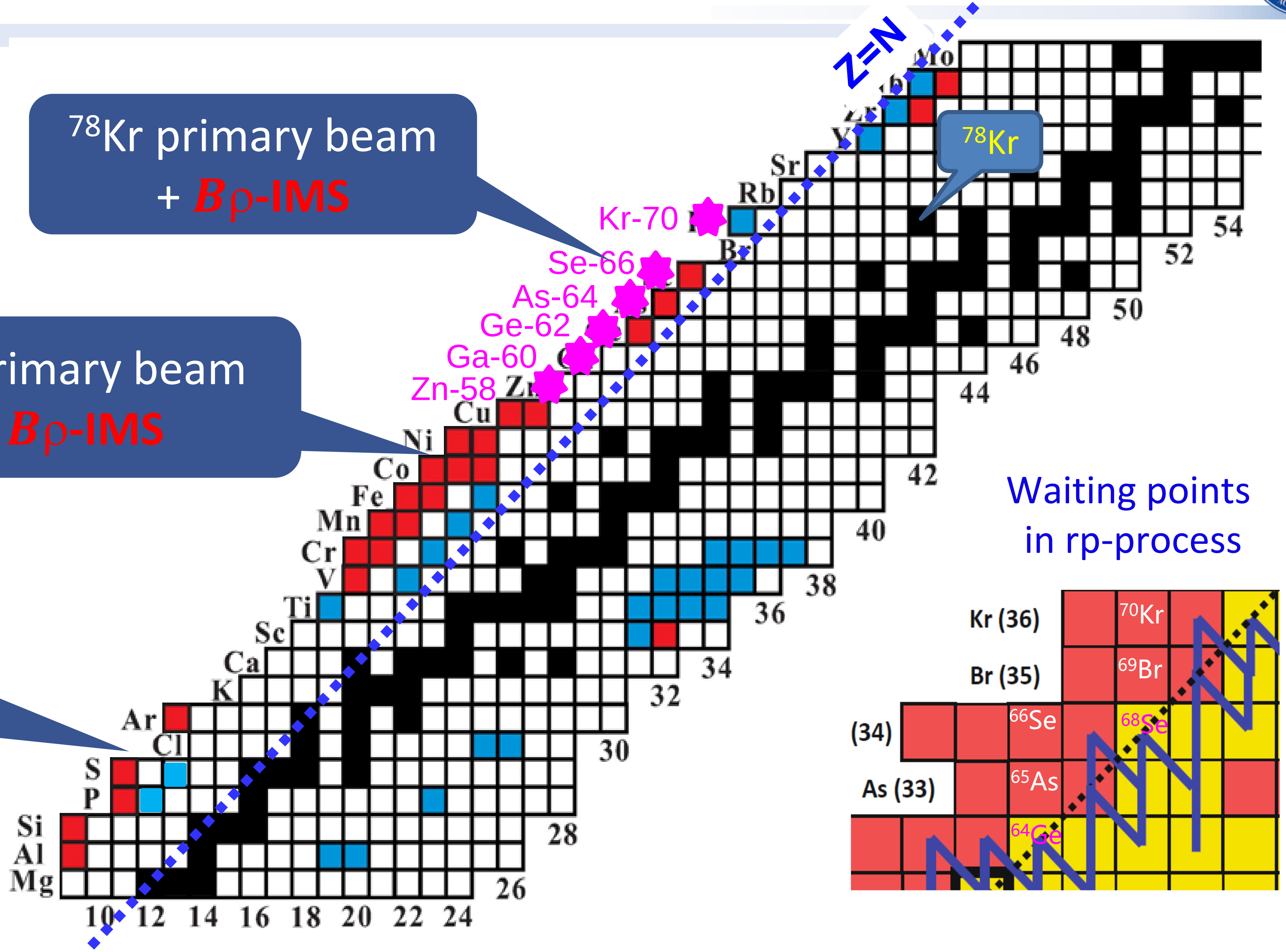

4. New masses from the $B\rho$-defined IMS

M. Zhang et al., Eur. Phys. J. A 59: 27(2023)

^{58}Ni beam

Table 1 Experimental mass excesses (MEs) obtained from this work (third column), from an earlier CSRe measurement (fourth column) [19,39–41] and from the literatures (sixth column). Also the recent Penning-trap measurements for ^{44g,44m}V [42], ^{52g,52m}Co [43], ^{56}Cu [44], ^{51}Fe [45] and AME2016 for ^{43}Ti [46] are included. All ME units are in keV

Atom	Number of events	ME This work	ME Earlier CSRe	ΔME_{CSRe}	ME Literature	$ME_{CSRe} - ME_{Lit}$
^{44g}V	334	−23800.4(71)	−23827(20)	−26(21)	−23804.9(80) [42]	−4.5(110)
^{44m}V	267	−23534.3(73)	−23541(19)	−6(20)	−23537.0(55) [42]	−2.7(91)
^{46}Cr	745	−29477.2(26)	−29471(11)	6(11)		
^{48}Mn	685	−29290.4(29)	−29299(7)	−9(8)		
^{50}Fe	782	−34475.8(29)	−34477(6)	−1(7)		
^{52g}Co	609	−34352.6(55)	−34361(8)	−8(10)	−34331.6(66) [43]	21(9)
^{52m}Co	236	−33973.0(106)	−33974(10)	−2(15)	−33958(11) [43]	15(15)
^{54}Ni	1254	−39285.4(27)	−39278.3(40)	7(5)		
^{56}Cu	294	−38622.6(60)	−38643(15)	−21(16)	−38626.7(71) [44]	−3.9(93)
^{41}Ti	25	−15724.3(187)	−15697.5(279)	27(37)		
^{43}V	9	−17899.3(316)	−17916.4(428)	−17(53)		
^{45}Cr	57	−19474.6(110)	−19514.8(354)	−40(37)		
^{47}Mn	18	−22560.8(192)	−22566.4(317)	−5.6(370)		
^{49}Fe	86	−24671.6(84)	−24750.7(242)	−79(27)		
^{51}Co	48	−27386.0(115)	−27342.1(484)	44(50)		
^{53}Ni	168	−29613.7(58)	−29630.8(252)	−17(26)		
^{55}Cu	11	−31807.0(248)	−31635(156)	172(158)		
^{43}Ti	757	−29302.2(42)	−29306(9)	−4(10)	−29321(7) [46]	19(8)
^{51}Fe	108	−40201.9(159)	−40198(14)	4(21)	−40189.2(14) [45]	13(16)

4. New masses from the $B\rho$-defined IMS

^{78}Kr beam

M. Wang et al., Phys. Rev. Lett. 130, 192501 (2023)

Atom	Counts	ME_{IMS} (keV)	$ME_{AME'20}$ (keV)	ΔME (keV)
^{58}Zn	51	−42 248(36)	−42 300(50)	51(62)
^{60}Ga	32	−40 034(46)	−39 590(200)[b]	−440(210)[b]
^{62}Ge	47	−42 289(37)	−42 140(140)[b]	−150(140)[b]
^{64}As[a]	6	−39 710(110)	−39 530(200)[b]	−170(230)[b]
^{66}Se[a]	20	−41 982(61)	−41 660(200)[b]	−320(210)[b]
^{70}Kr	4	−41 320(140)	−41 100(200)[b]	−220(250)[b]
^{61}Ga	124	−47 168(21)	−47 135(38)	−33(43)
^{63}Gs[a]	279	−46 978(15)	−46 921(37)	−57(40)
^{65}As[a]	33	−46 806(42)	−46 937(85)	131(95)
^{67}Se[a]	174	−46 549(20)	−46 580(67)	32(70)
^{71}Kr	148	−46 056(24)	−46 327(129)	270(130)
^{75}Sr	4	−46 200(150)	−46 620(220)	420(260)

4. New masses from the $B\rho$-defined IMS

^{58}Ni beam

M. Wang et al., PRC 106, L051301(2022)

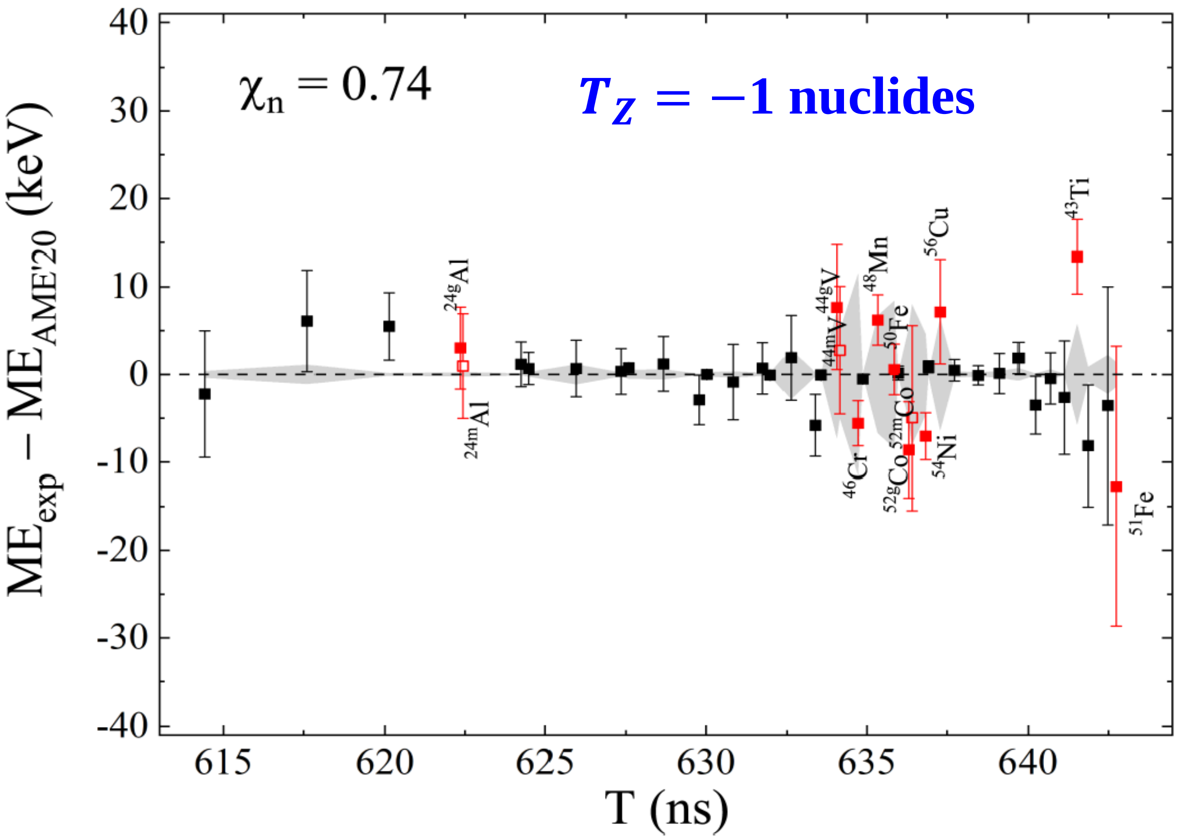

M. Zhang et al., Eur. Phys. J. A 59: 27(2023)

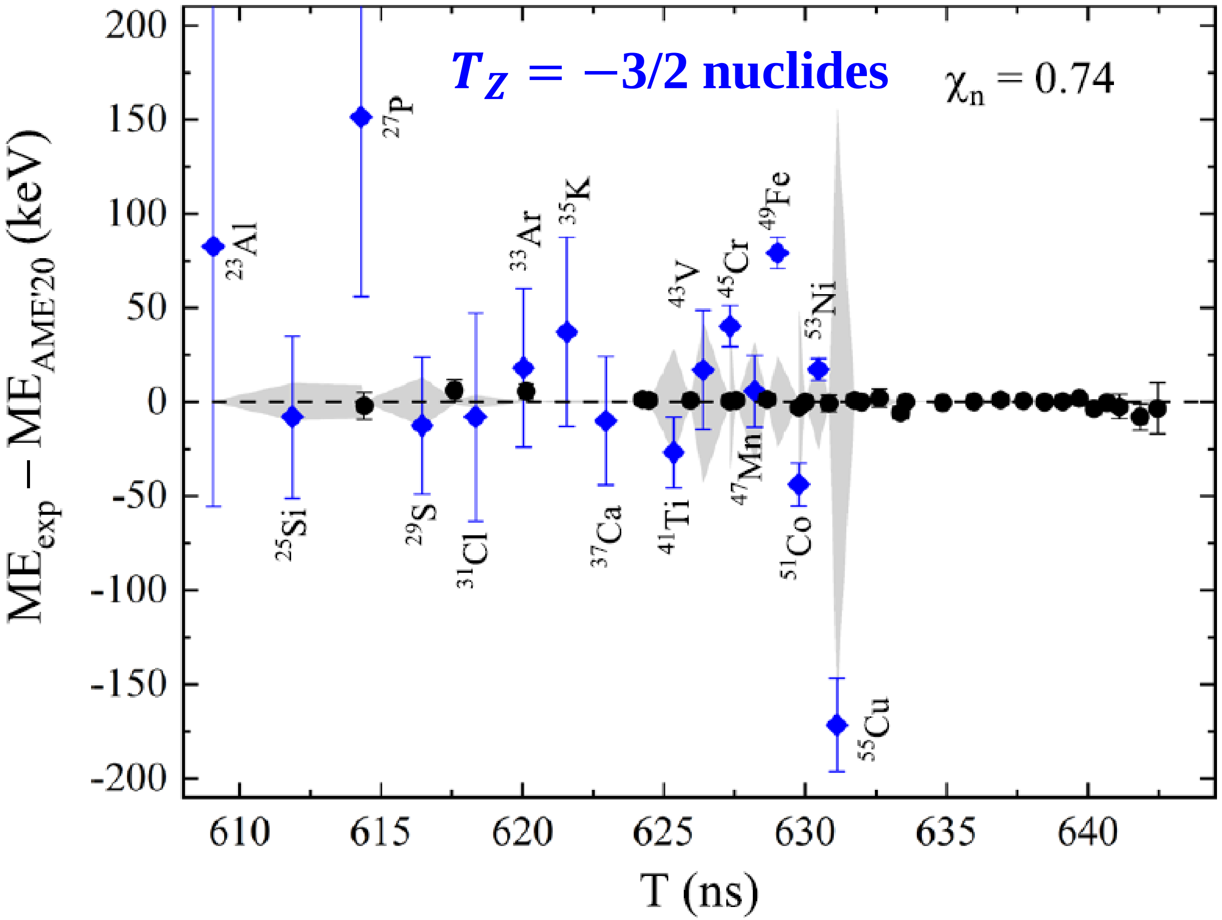

4. New masses from the $B\rho$-defined IMS

^{78}Kr beam

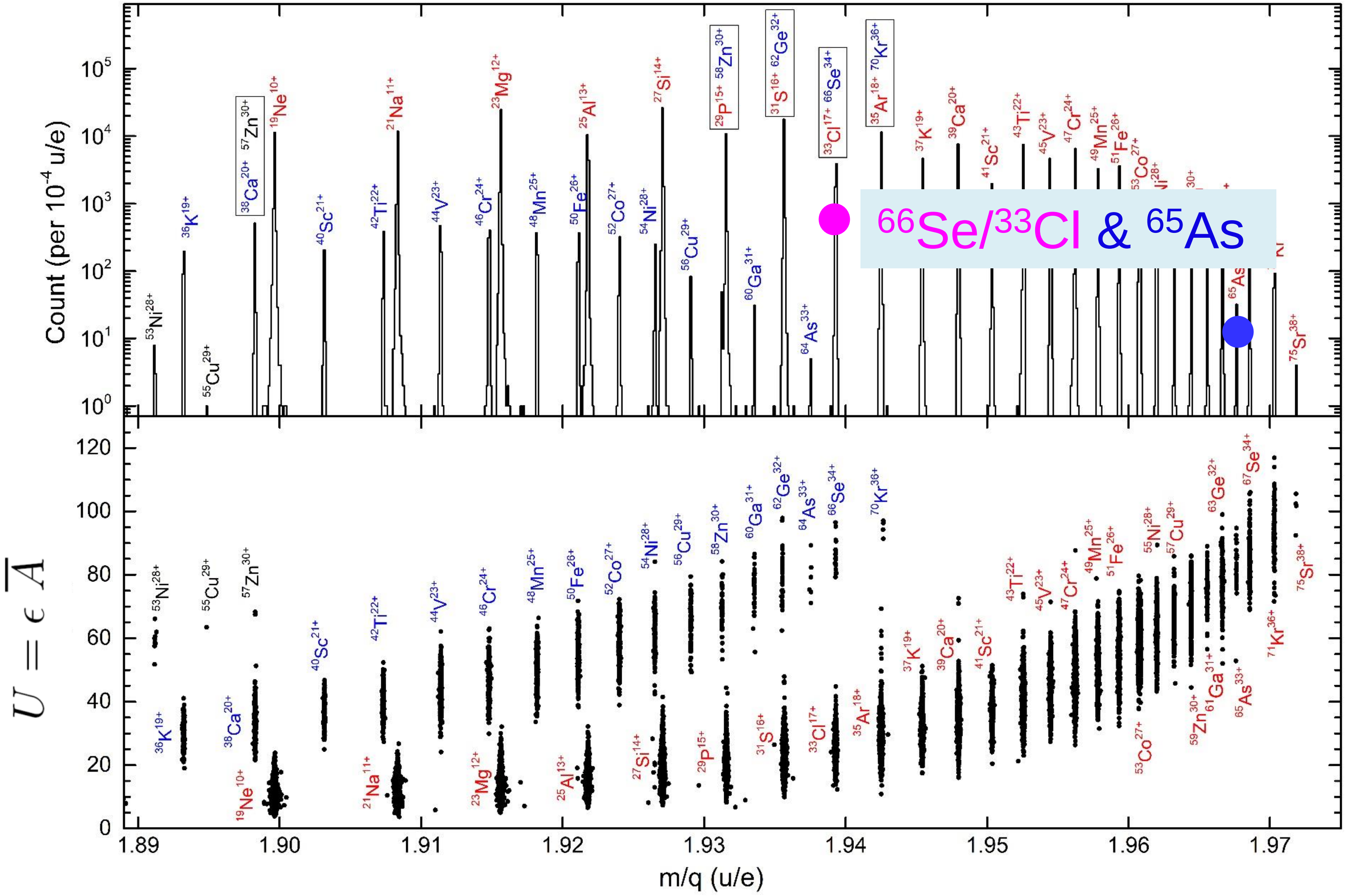

4. New masses from the $B\rho$-defined IMS

^{78}Kr beam

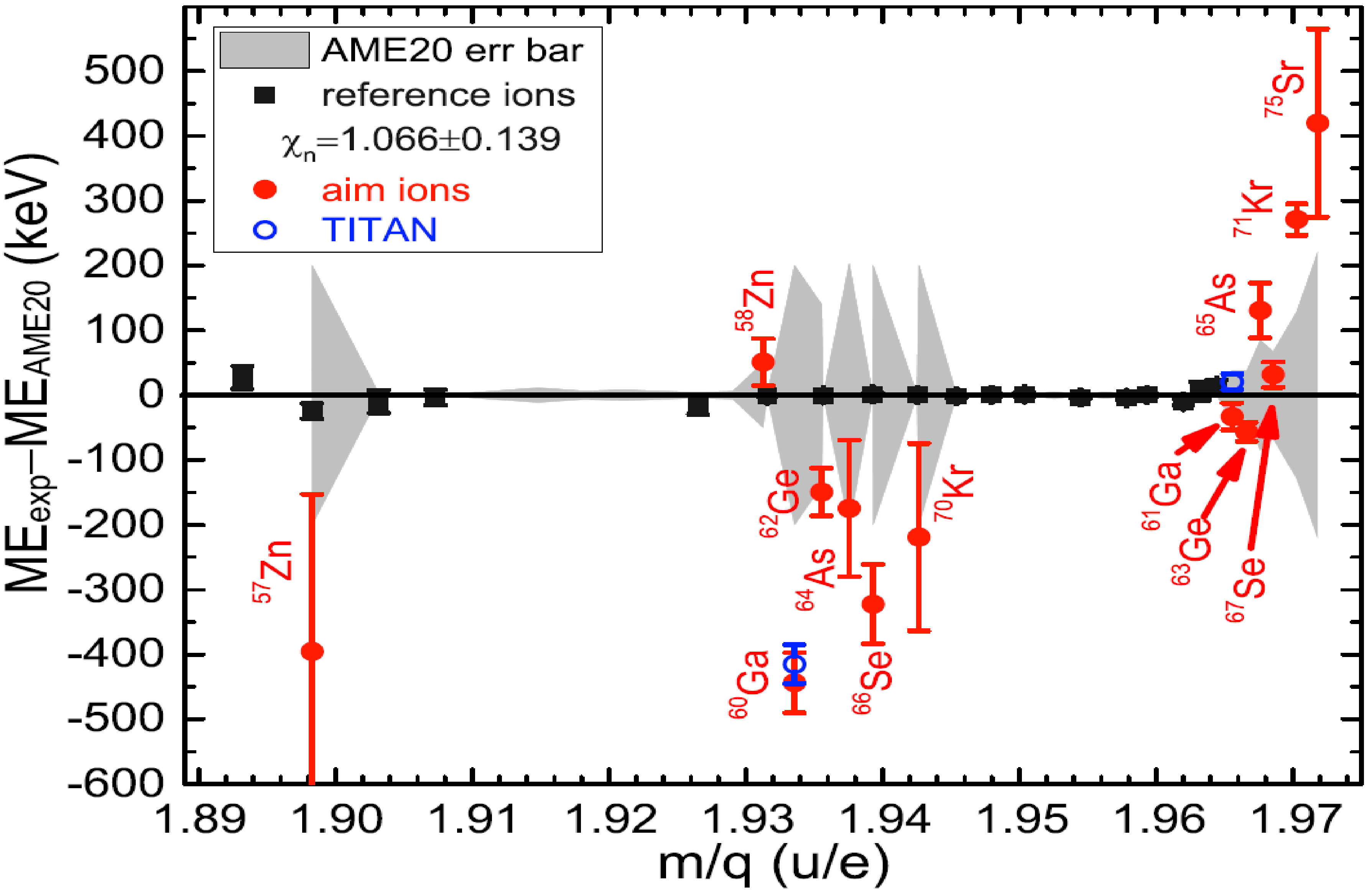

Validity of IMME for T=3/2 multiplet at A=55

$$M(A,T,T_z) = a(A,T) + b(A,T)T_z + c(A,T)T_z^2 + d(A,T)T_z^3$$

M. Zhang et al., Eur. Phys. J. A 59: 27(2023)

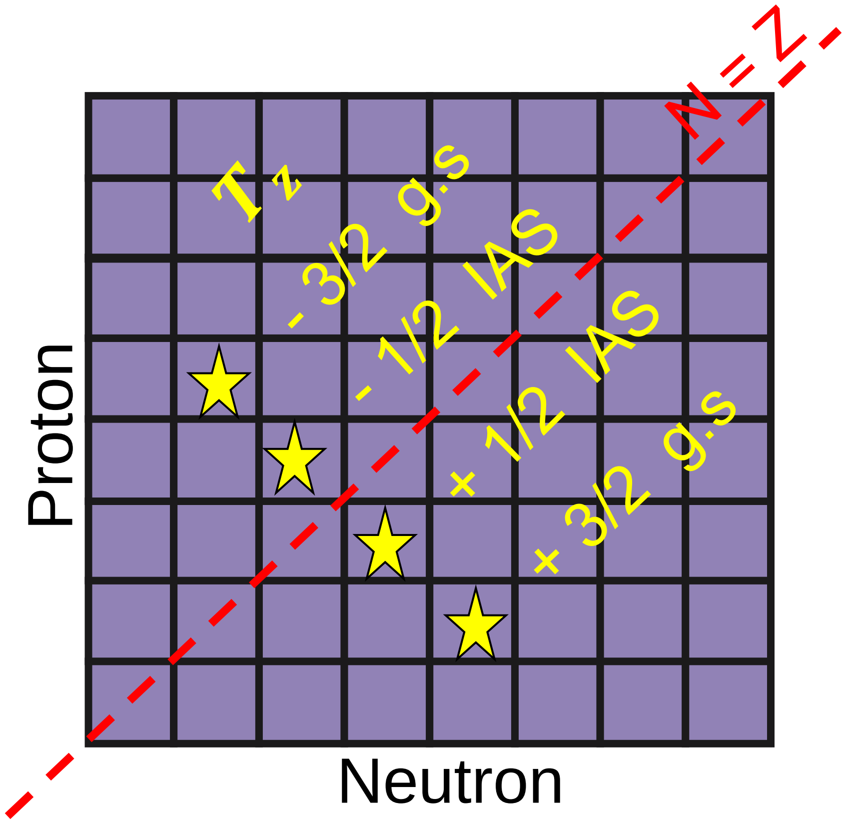

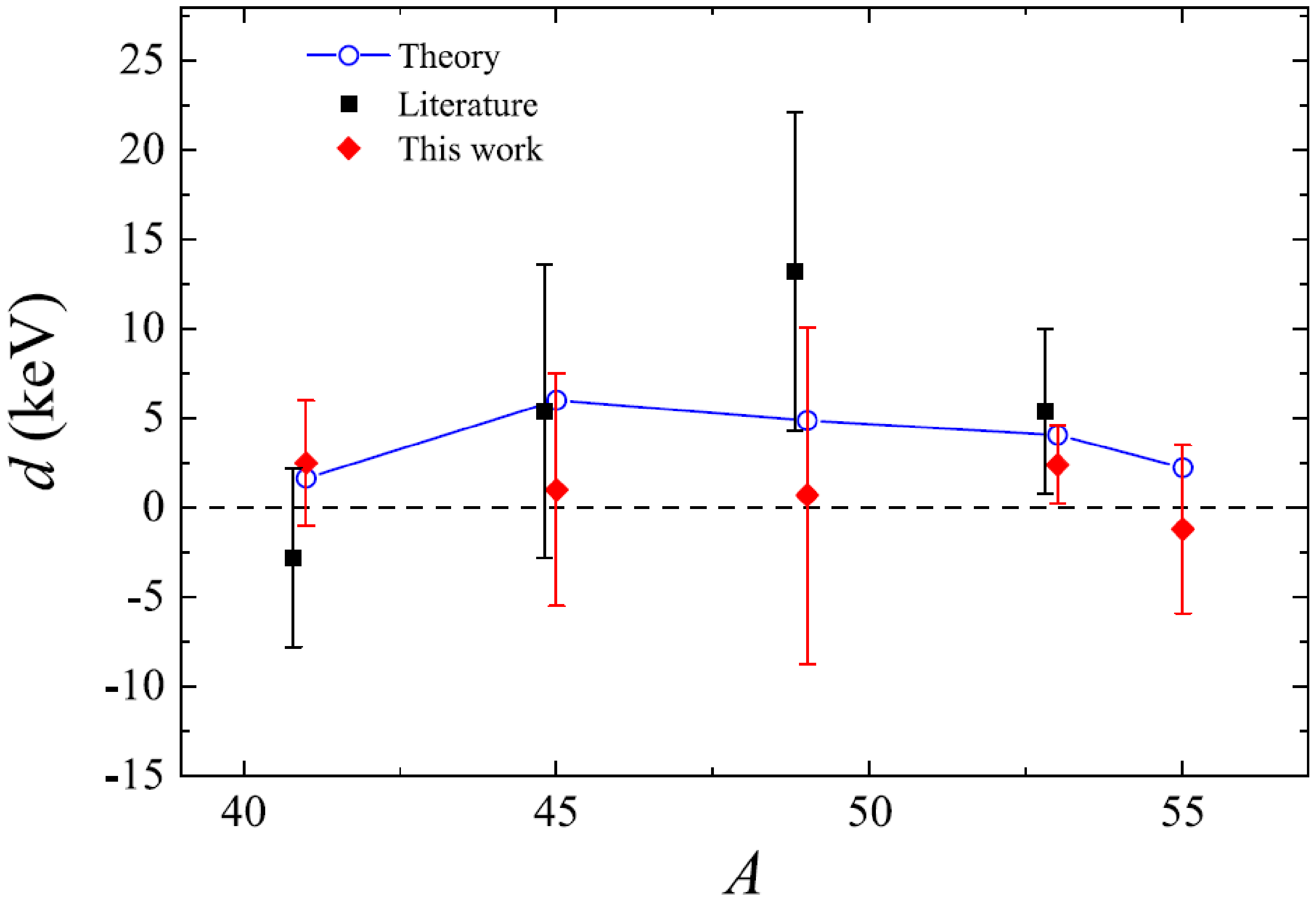

The ground state mass of ^{70}Br (W.J. Huang et al., PRC submitted)

IMME: $$M(A,T,T_z) = a(A,T) + b(A,T)T_z + c(A,T)T_z^2$$

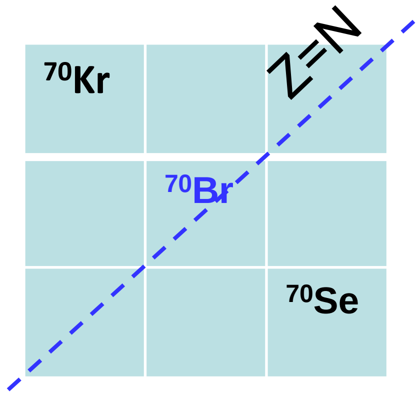

$$b = (M_1 - M_{-1})/2$$

Charge symmetry

$$c = \frac{M_1 + M_{-1}}{2} - M_0$$

Charge independence

Isovector component of NN interaction

Isotensor component of NN interaction

Coulomb interaction is the main contributor

Average properties like Coulomb radius or pairing

Sensitive to the WF of valence particles which contains particular nuclear structure information

The ground state mass of ^{70}Br (W.J. Huang et al., PRC submitted)

For T=1 multiplets $$c = \frac{M_1 + M_{-1}}{2} - M_0$$

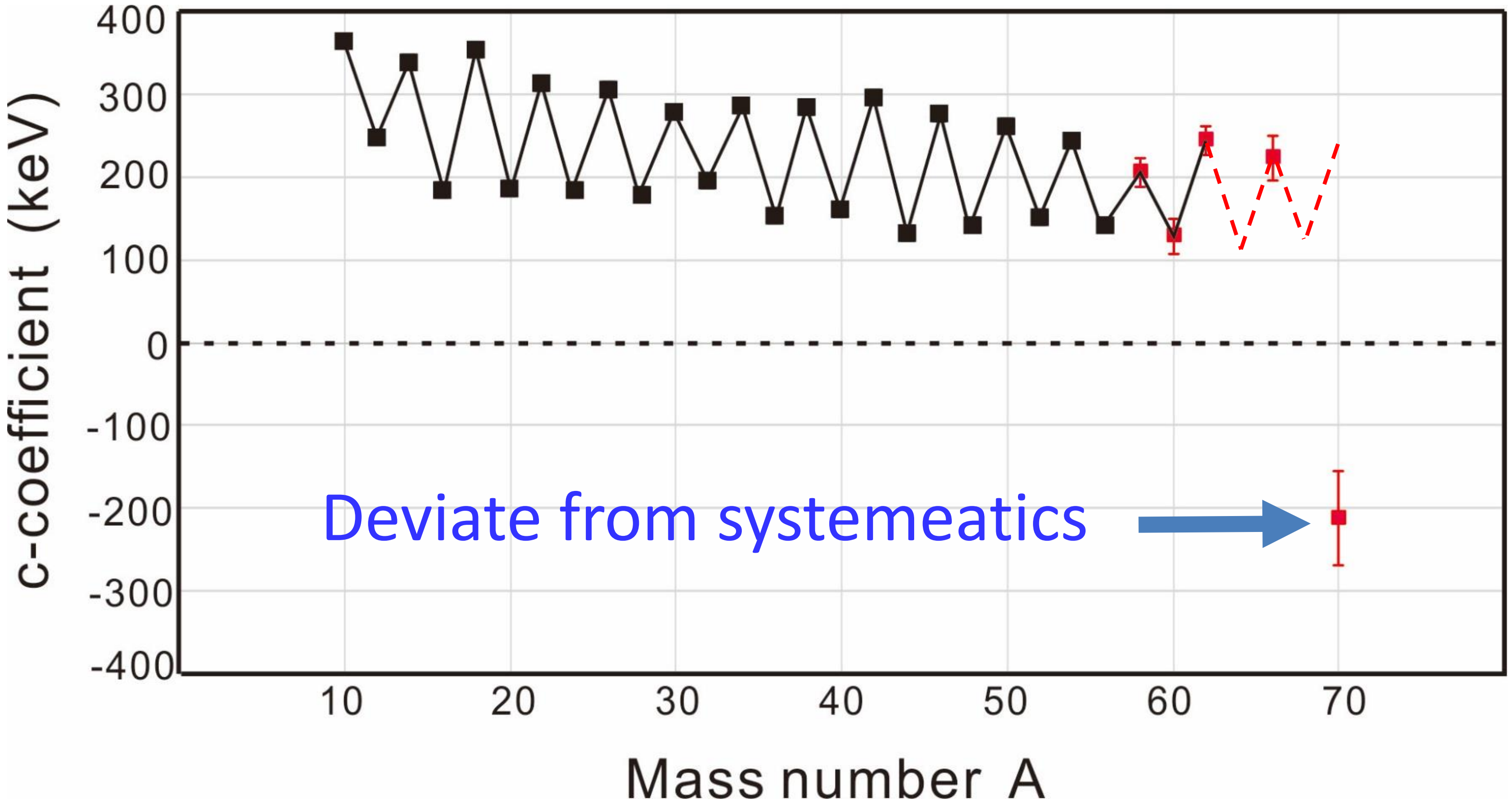

The ground state mass of ^{70}Br (W.J. Huang et al., PRC submitted)

For T=1 multiplets

$$b = (M_1 - M_{-1})/2$$

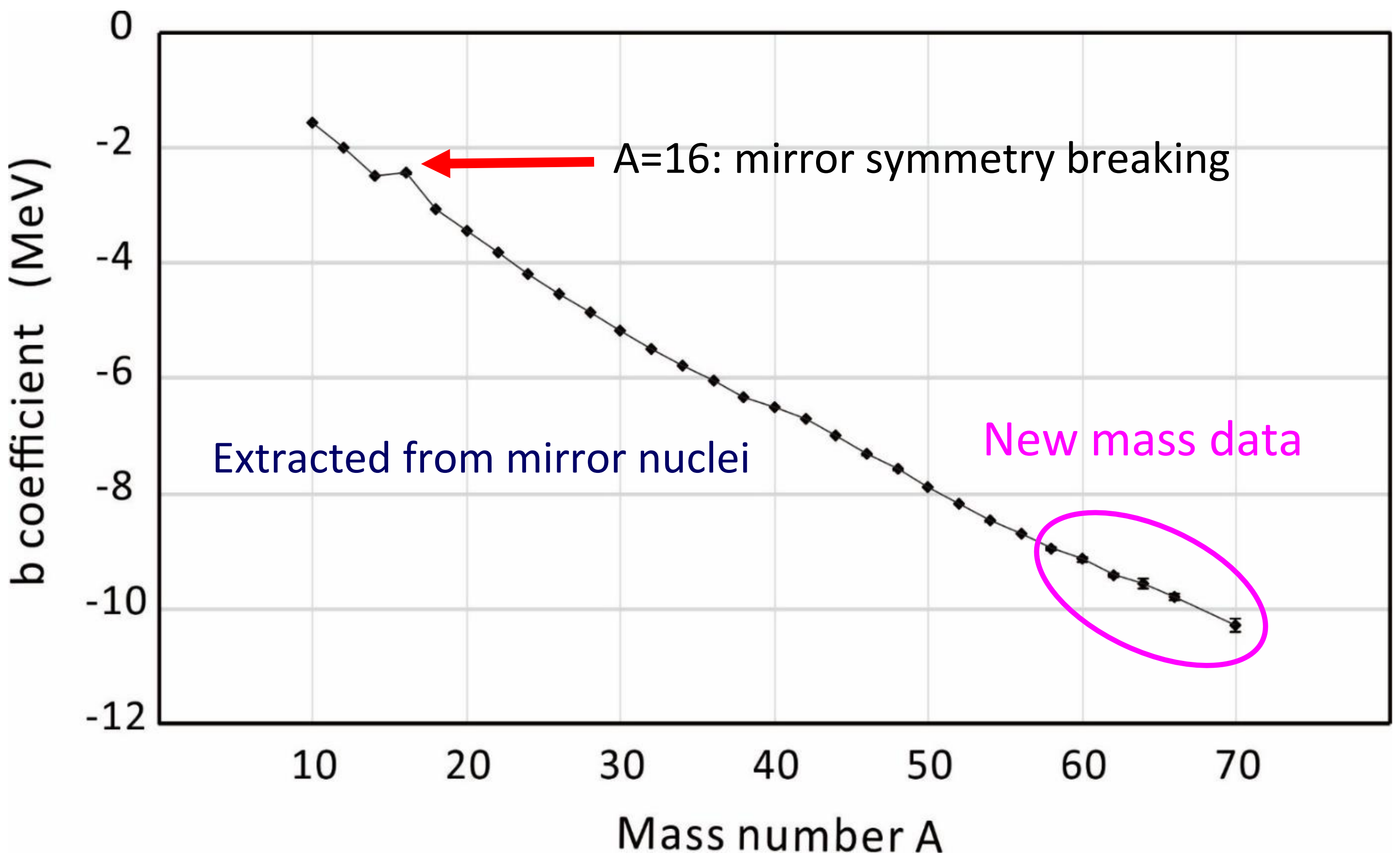

The ground state mass of ^{70}Br (W.J. Huang et al., PRC submitted)

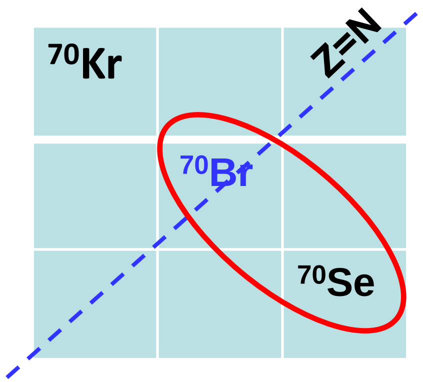

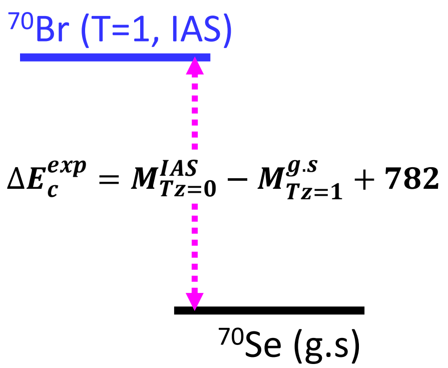

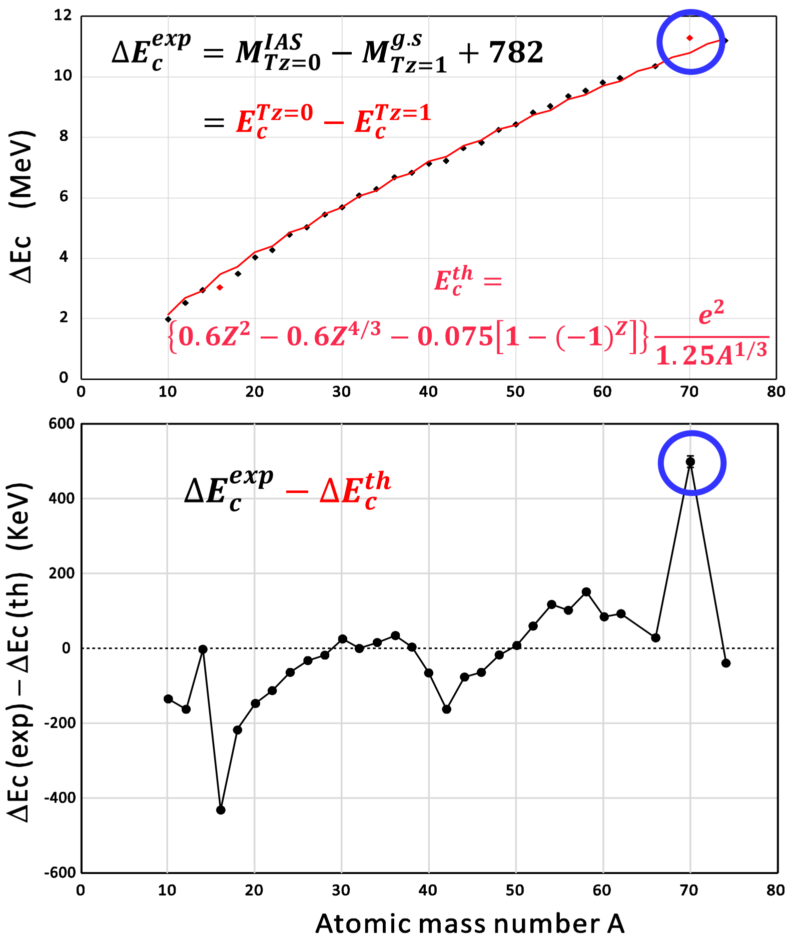

The ground state mass of ^{70}Br (W.J. Huang et al., PRC submitted)

J. Savory et al., PRL 102, 132501 (2009)

rp Process and Masses of N≈Z≈34 Nuclides

TABLE II. Mass excess values (ME) in keV obtained with LEBIT, from AME'03 [28] and the difference $\Delta ME = ME_{AME'03} - ME_{LEBIT}$. Also given are new mass predictions for ^{70}Kr and ^{71}Kr.

Species	ME_{LEBIT}	$ME_{AME'03}$	ΔME
^{68}Se	−54 189.3(5)	−54 210(30)	−21(30)
^{70}Se	−61 929.7(1.6)	−62 050(60)	−120(60)
^{70}Br	−51 425(15)	−51 430(310)	−5(310)
^{71}Br	−56 502.4(5.4)	−57 060(570)	−558(570)
	$ME_{LEBIT+CDE}$	$ME_{AME'03}$	ΔME
^{70}Kr	−41 304(100)	−41 680(390)	−376(403)
^{71}Kr	−46 025(100)	−46 920(650)	895(658)

PRC 70, 014310 (2004)
Q_{EC}(9+)=12.19 (±7±4) MeV
Q_{EC}(g.s.)=9.90(±7±4) MeV
ME(gs)= -52.03 (±7±4) MeV

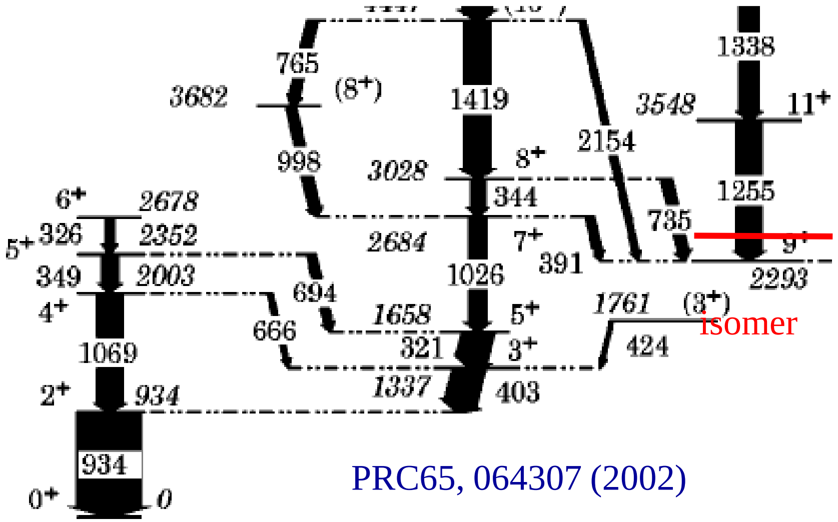

PRC65, 064307 (2002)

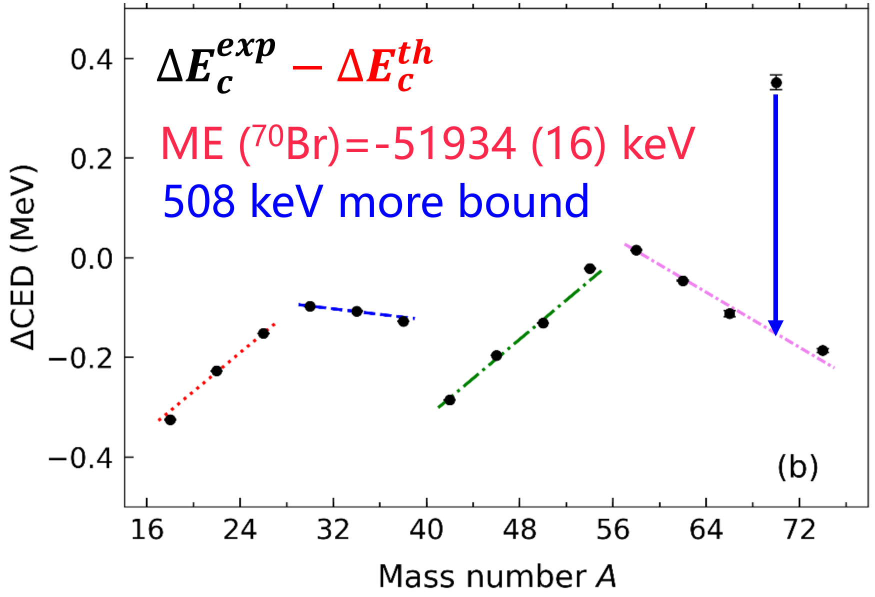

The ground state mass of ^{70}Br (W.J. Huang et al., PRC submitted)

$$M(A,T,T_z) = a(A,T) + b(A,T)T_z + c(A,T)T_z^2$$

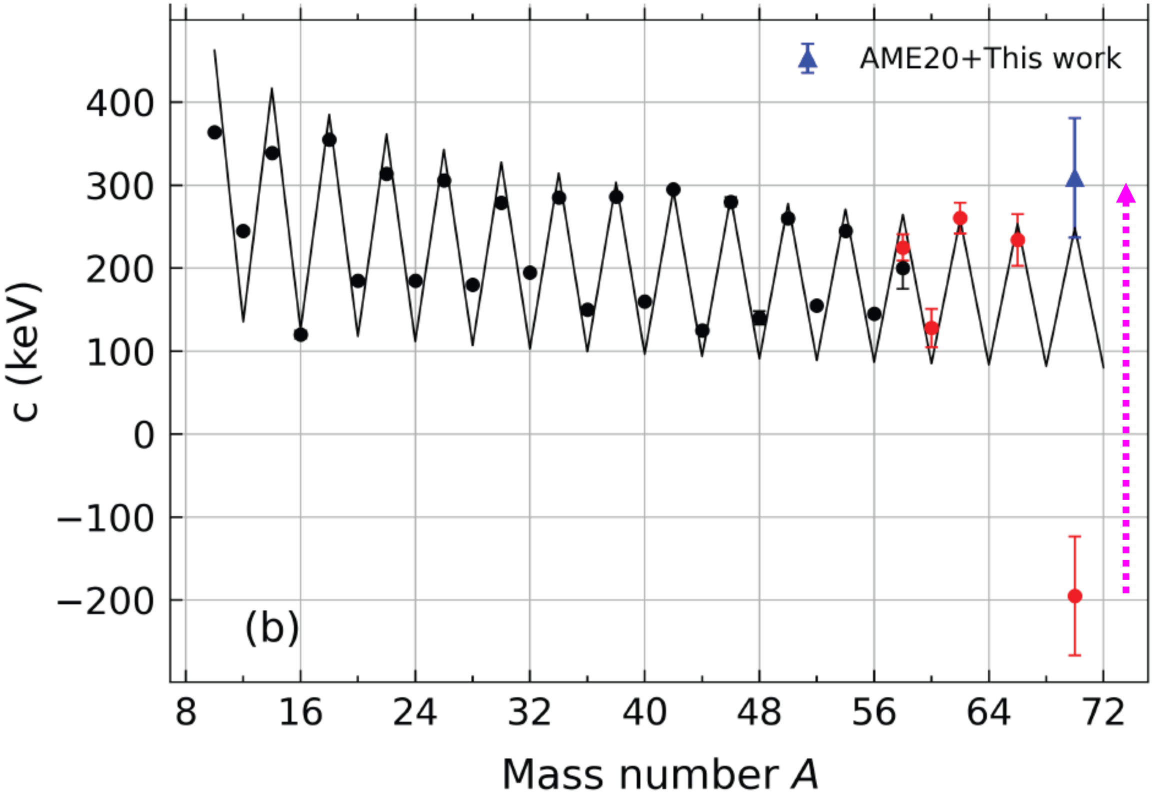

$$Ft \equiv ft(1+\delta'_R)(1+\delta_{NS}-\delta_C)$$

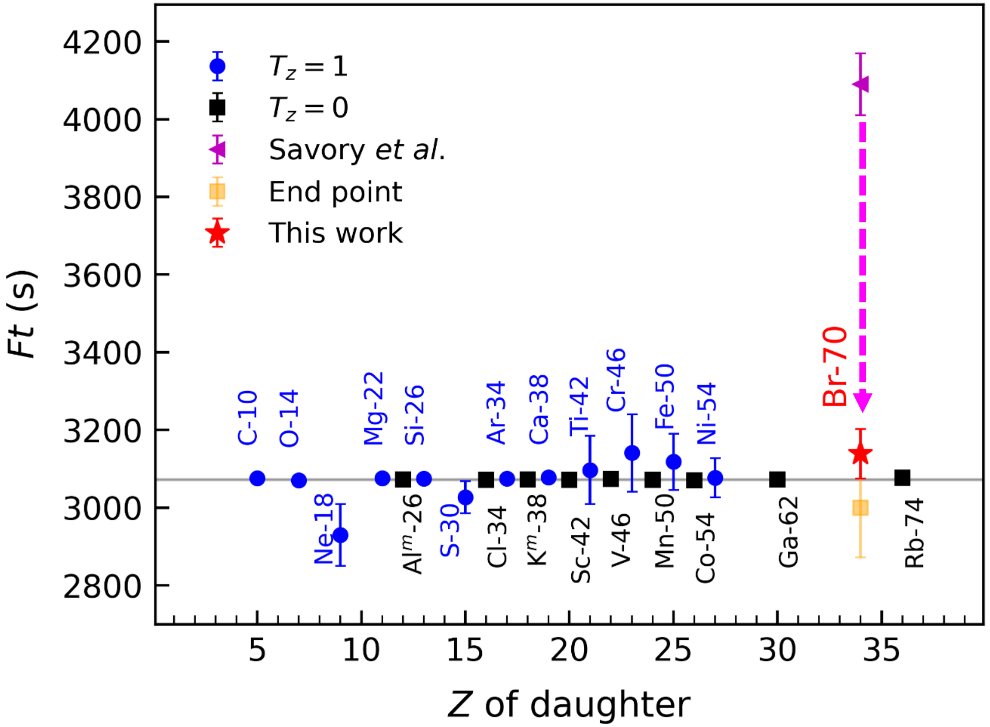

If CVC hypothesis is correct, the corrected Ft values should be same

Mirror symmetry of residual pn interaction

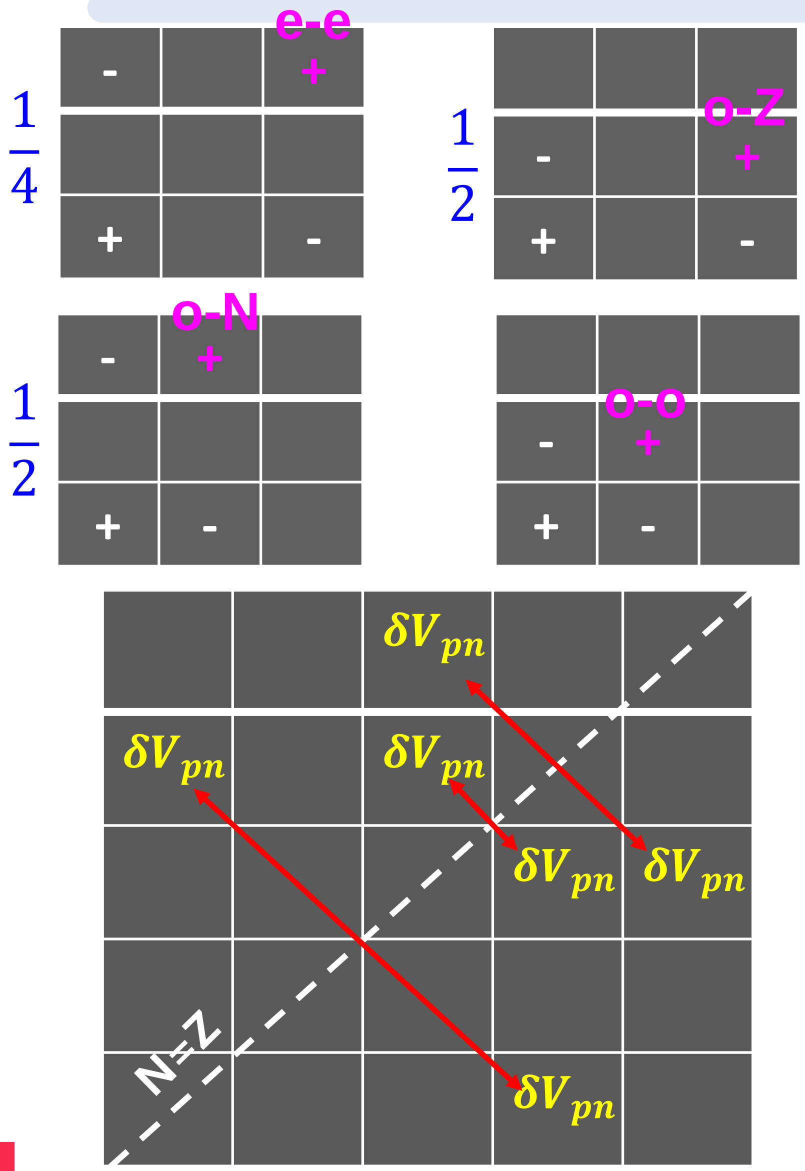

M. Zhang et al., Eur. Phys. J. A 59: 27(2023)

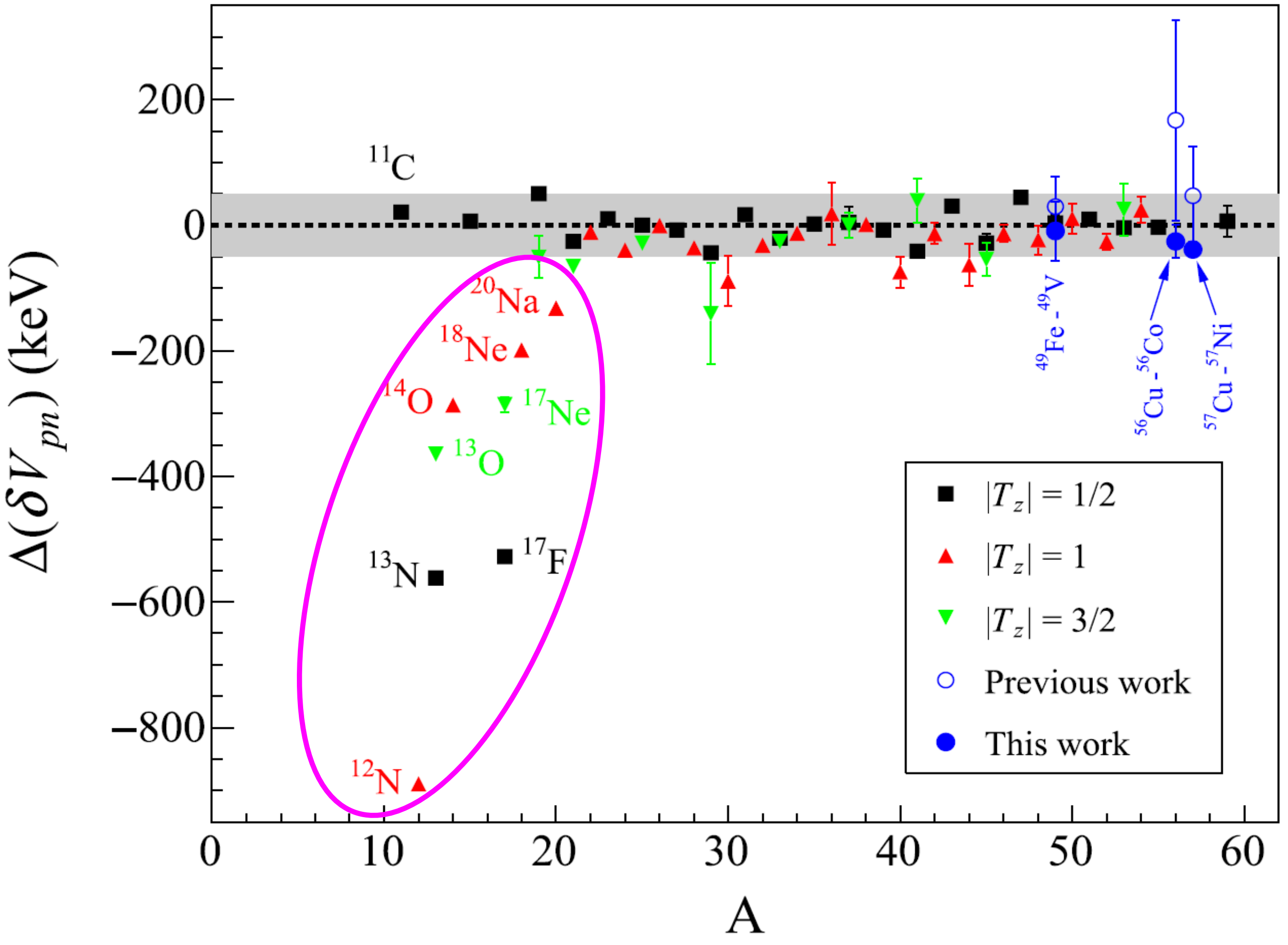

Mirror symmetry of residual pn interaction

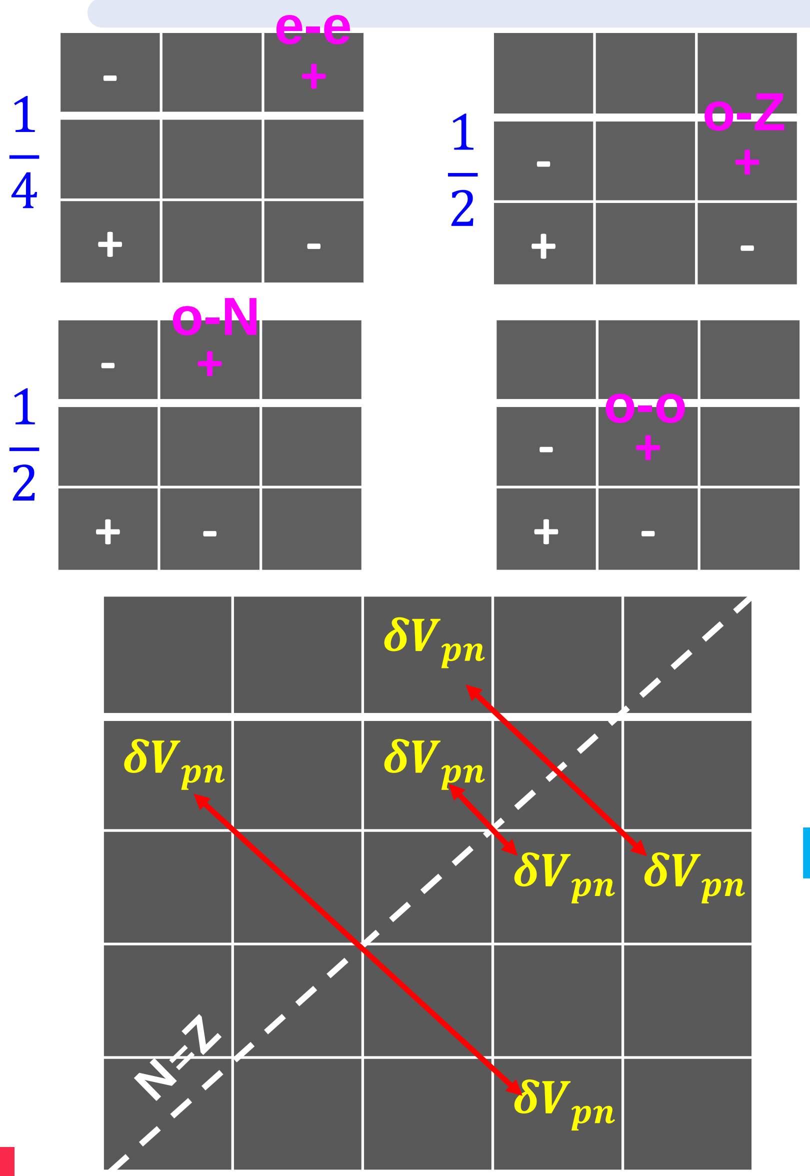

Local mass relationship

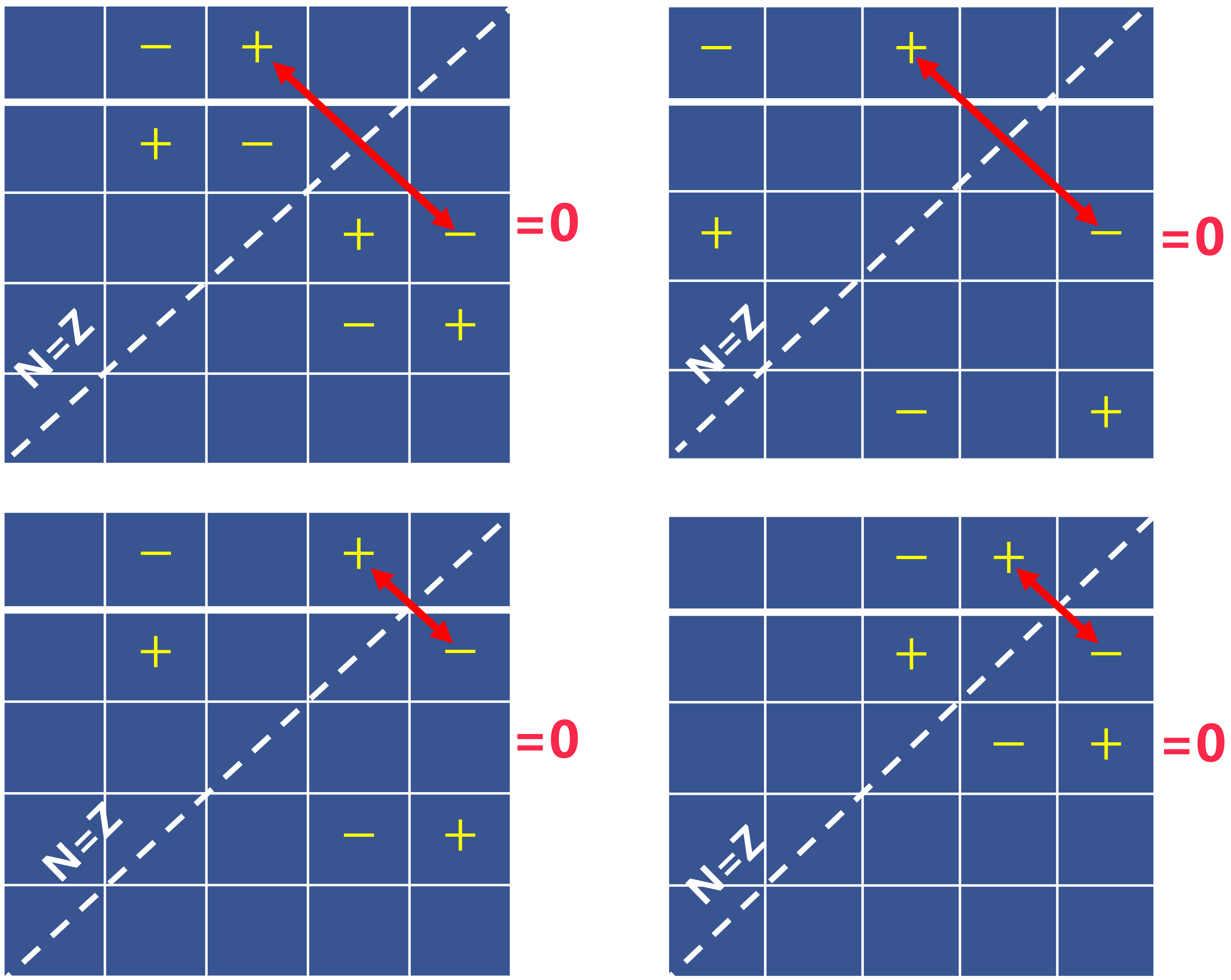

Bifurcation of residual pn interaction along the N=Z line

M. Wang et al., PRL 130, 192501 (2023)

Mass Measurement of Upper *fp*-Shell $N=Z-2$ and $N=Z-1$ Nuclei and the Importance of Three-Nucleon Force along the $N=Z$ Line

M. Wang,[1,2] Y. H. Zhang,[1,2,*] X. Zhou,[1,2] X. H. Zhou,[1,2,†] H. S. Xu,[1,2] M. L. Liu,[1] J. G. Li,[1] Y. F. Niu,[3,4] W. J. Huang,[1,5]
Q. Yuan,[6] S. Zhang,[6] F. R. X ... Yu. A. Litvinov,[1,7] K. Blaum,[8] Z. Meisel,[9] R. F. Casten,[10] R. B. Cakirli,[11]

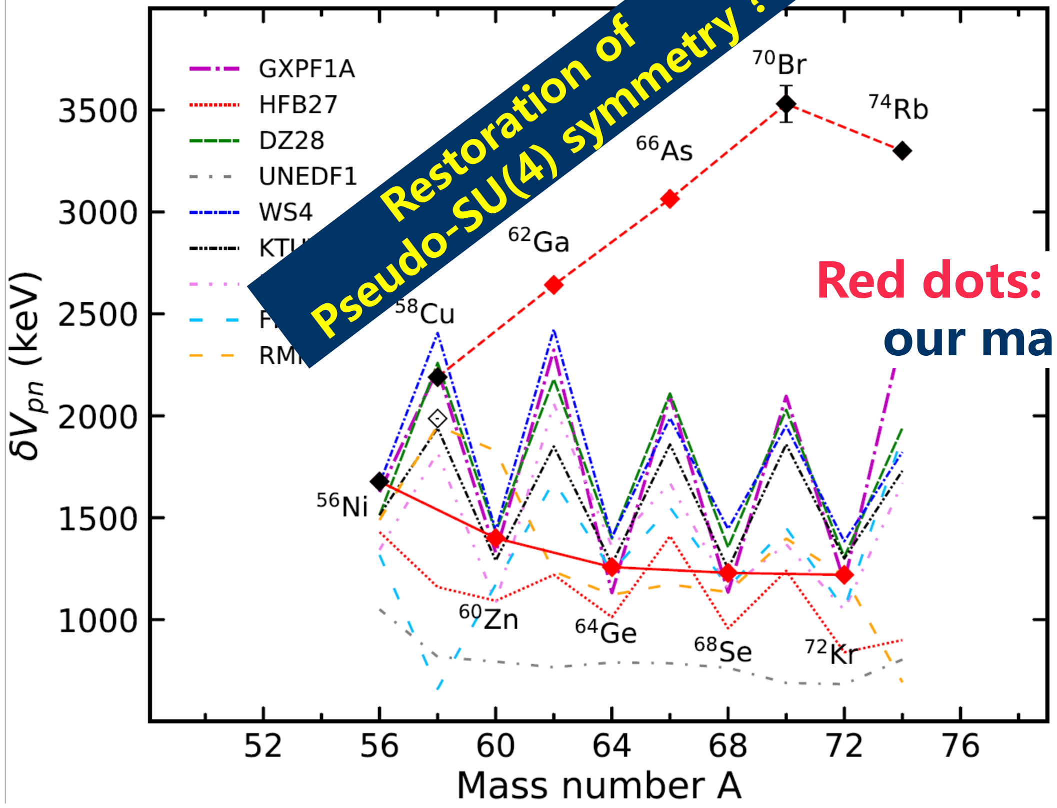

Red dots: at least one of our masses is used

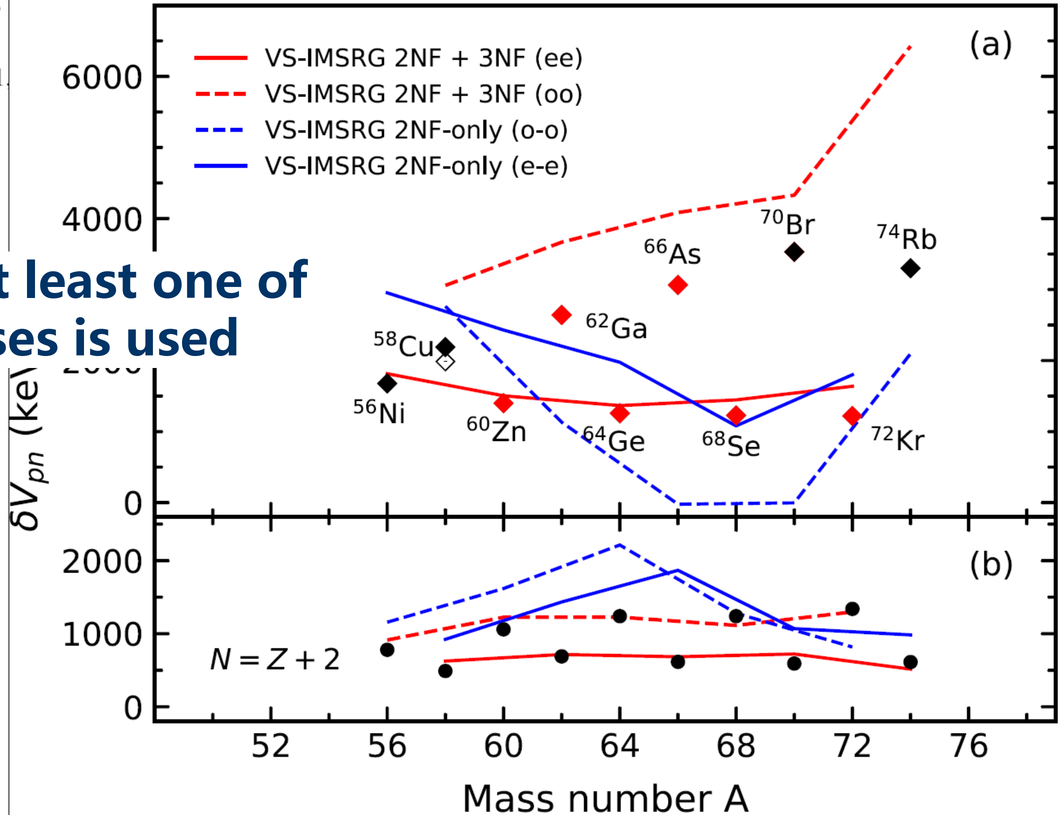

Waiting point ^{64}Ge in the rp-process of Type I X-ray bursts

Effective lifetimes of ^{64}Ge

T<1.5-2 GK，^{68}Se - ^{69}Br equilibrium

$$\lambda_{\text{total}} = \lambda_{\beta(Z,N)} + Y_p^2 \rho^2 N_A^2 \left(\frac{2\pi\hbar^2}{kT}\right)^{3/2} \frac{G_{(Z+1,N)}(T)}{2G_{(Z,N)}(T)} \exp\left(\frac{Q_{(Z,N)(p,\gamma)}}{kT}\right) \langle p\gamma \rangle_{(Z+1,N)}$$

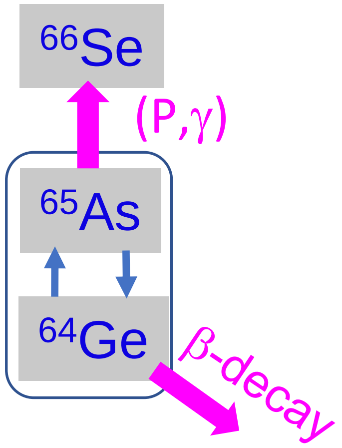

T ＞ 1.5-2 GK，^{68}Se - ^{70}Kr equilibrium

$$\lambda_{\text{total}} = \lambda_{\beta(Z,N)} + \left[Y_p \rho N_A \left(\frac{2\pi\hbar^2}{kT}\right)^{3/2}\right]^2 \left(\frac{1}{\mu_{(Z,N)}\mu_{(Z+1,N)}}\right)^{3/2} \frac{G_{(Z+2,N)}(T)}{4G_{(Z,N)}(T)} \times \exp\left(\frac{Q_{(Z,N)(p,\gamma)} + Q_{(Z+1,N)(p,\gamma)}}{kT}\right) \lambda_{\beta(Z+2,N)}$$

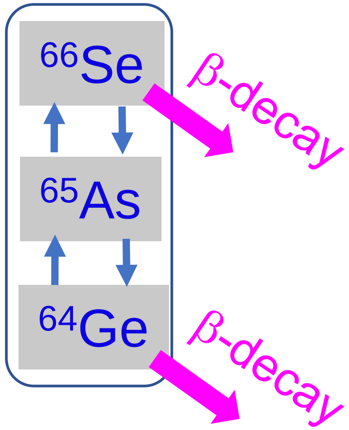

Effective lifetimes of ^{64}Ge

$T_{1/2}$ (^{64}Ge) = 63.7(2.5) (s)

^{64}Ge - ^{65}As equilibrium

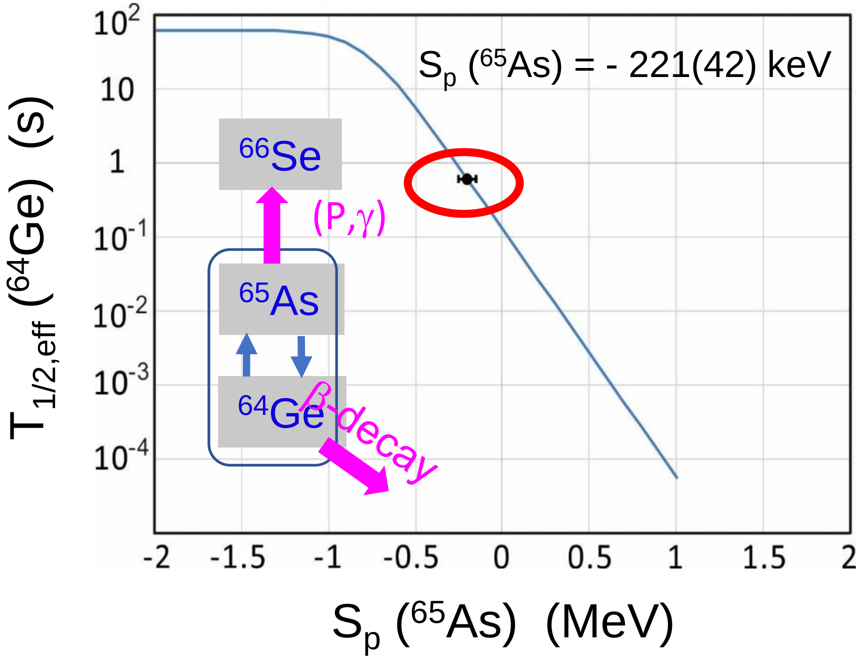

^{64}Ge - ^{66}Se equilibrium

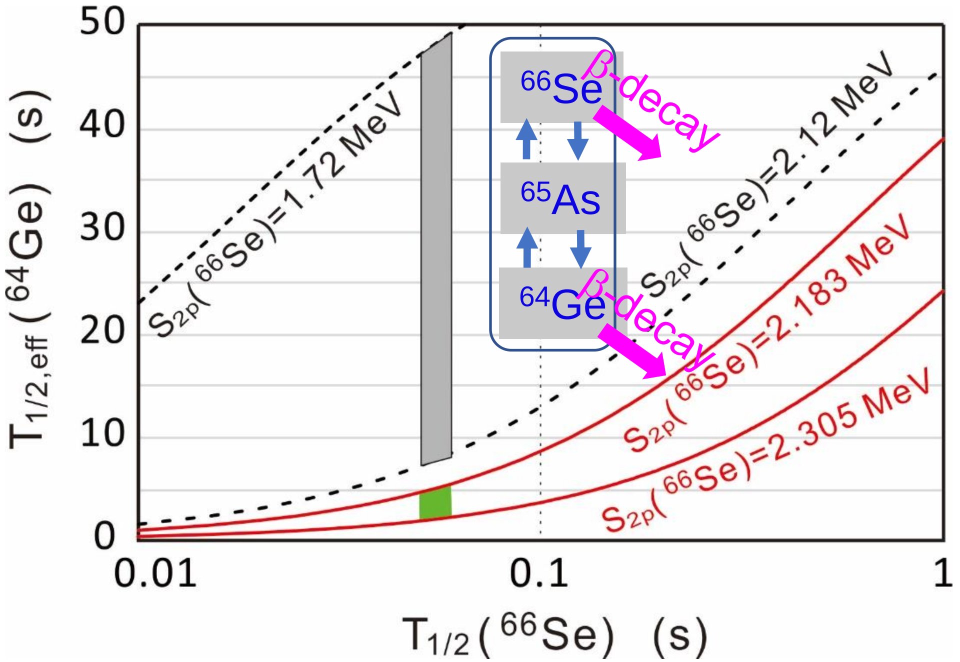

$S_p(^{65}As)$= - 221(42) keV

$T_{1/2}$ (^{66}Se) = 54(4) (ms)

$S_{2p}(^{66}Se)$=2.244(61) MeV

Waiting point ^{64}Ge in the rp-process of Type I X-ray bursts

All Q-values of (p,γ) reaction around ^{64}Ge obtained

less bound ^{65}As
more bound ^{66}Se,

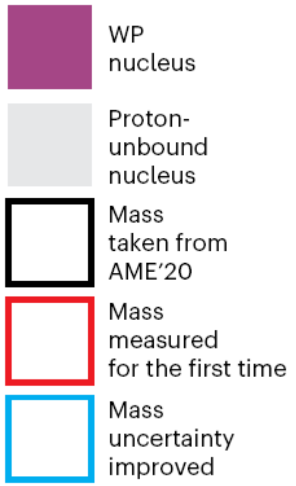

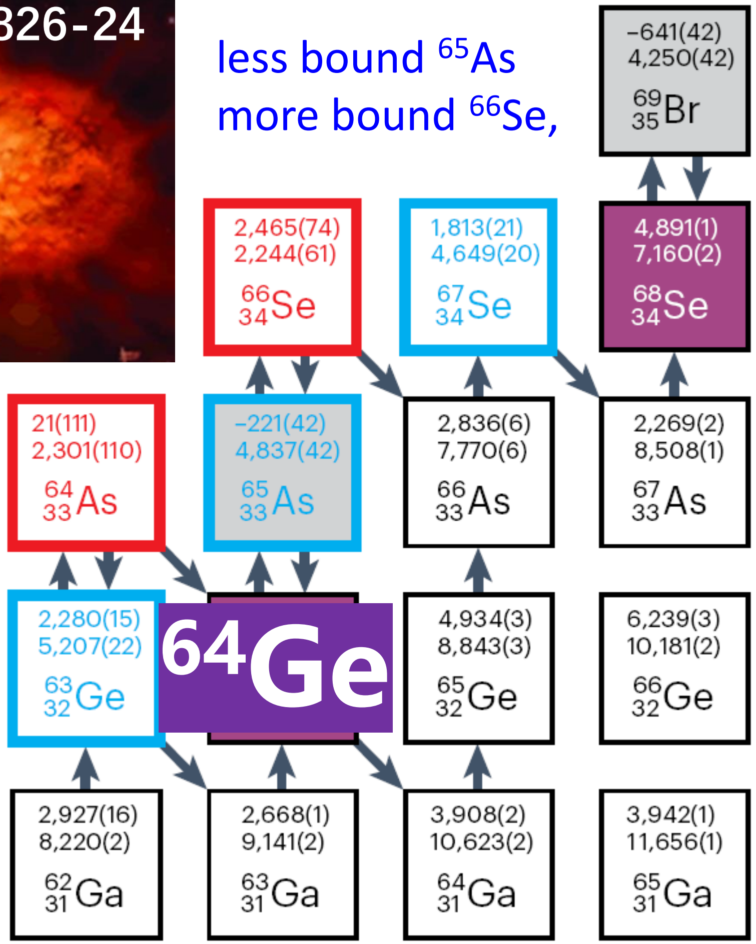

Multizone X-ray burst simulations

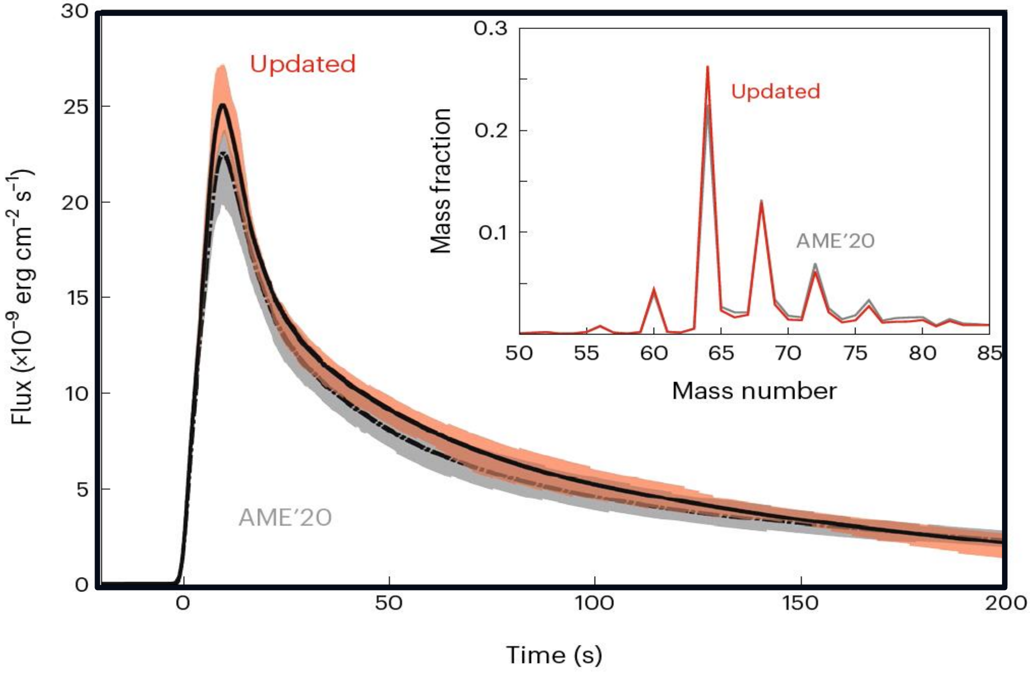

- peak luminosity (flux) increased
- A=64 mass fraction increased by 17%
- A=65 mass fraction decreased by 14%

Waiting point ^{64}Ge in the rp-process of Type I X-ray bursts

New light curve enables us to set new constraints on the optimal *d* and (1 + *z*) parameters

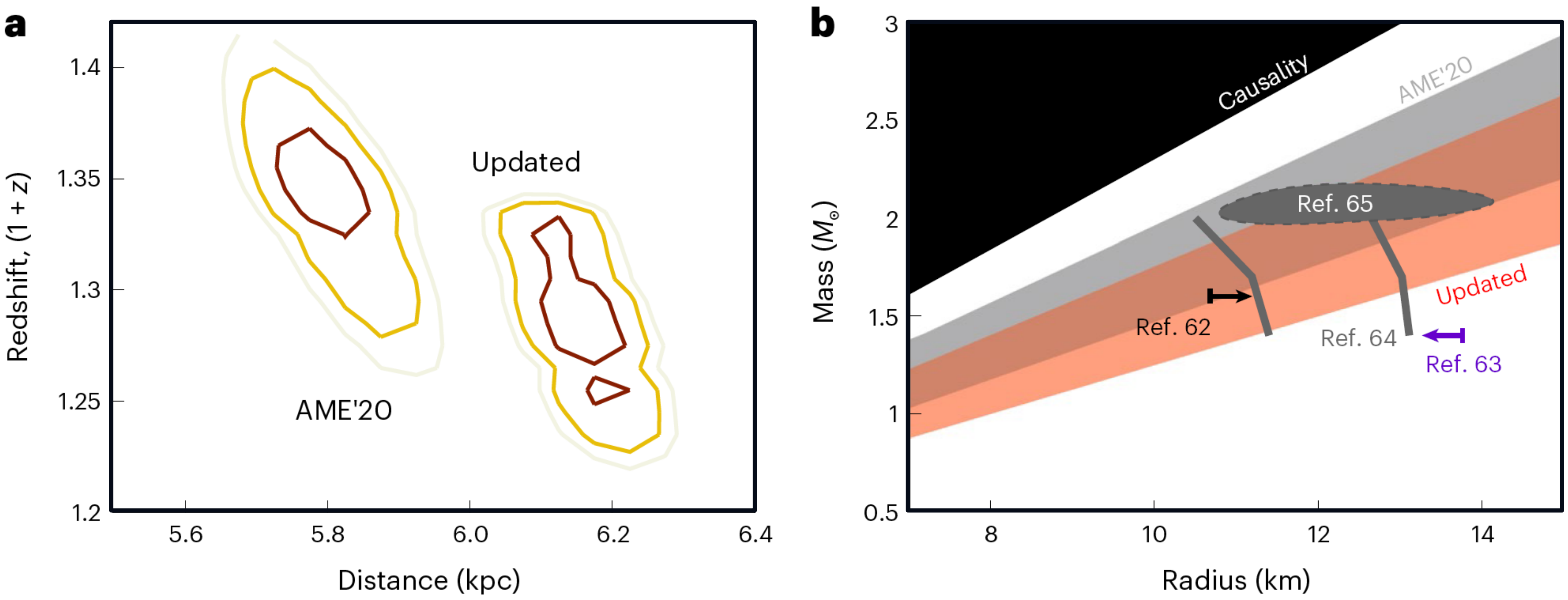

- **the neutron star in GS1826-24 is 6.5% farther away (0.4 kpc=1300 ly) from us !**
- **reduced 1+z value indicates weaker gravitation than believed !**

- **Mass and Radius are constrained**

Waiting point ^{64}Ge in the rp-process of Type I X-ray bursts

nature physics

Article https://doi.org/10.1038/s41567-023-02034-2

Mass measurements show slowdown of rapid proton capture process at waiting-point nucleus ^{64}Ge

Received: 14 June 2022

Accepted: 24 March 2023

Published online: 01 May 2023

Check for updates

X. Zhou[1,2], M. Wang[1,2], Y. H. Zhang[1,2], Yu. A. Litvinov[1,3], Z. Meisel[4], K. Blaum[5], X. H. Zhou[1,2], S. Q. Hou[1,2,6], K. A. Li[1], H. S. Xu[1,2], R. J. Chen[1,3], H. Y. Deng[1,2], C. Y. Fu[1], W. W. Ge[1], J. J. He[7], W. J. Huang[1,8], H. Y. Jiao[1,2], H. F. Li[1,2], J. G. Li[1], T. Liao[1,2], S. A. Litvinov[1,3], M. L. Liu[1], Y. F. Niu[9], P. Shuai[1], J. Y. Shi[1,2], Y. N. Song[1,2], M. Z. Sun[1], Q. Wang[1,2], Y. M. Xing[1], X. Xu[1], F. R. Xu[10], X. L. Yan[1], J. C. Yang[1,2], Y. Yu[1,2], Q. Yuan[10], Y. J. Yuan[1,2], Q. Zeng[11], M. Zhang[1,2] & S. Zhang[10]

5. Summary

1. $B\rho$-defined IMS has been established in CSRe which shows several advantages in mass measurement of short-lived nuclei
2. Masses of ^{78}Kr, ^{58}Ni, ^{36}Ar fragments have been measured, enabling to address several issues in nuclear structure and nuclear astrophysics
3. $B\rho$-defined IMS will be installed in the SRing of HIAF facility and the masses of heavy and n-rich exotic nuclei will be touched in the future
4. We need close collaborations both in experiment and in theory

Thanks for your attention

原子核质量与核天体物理

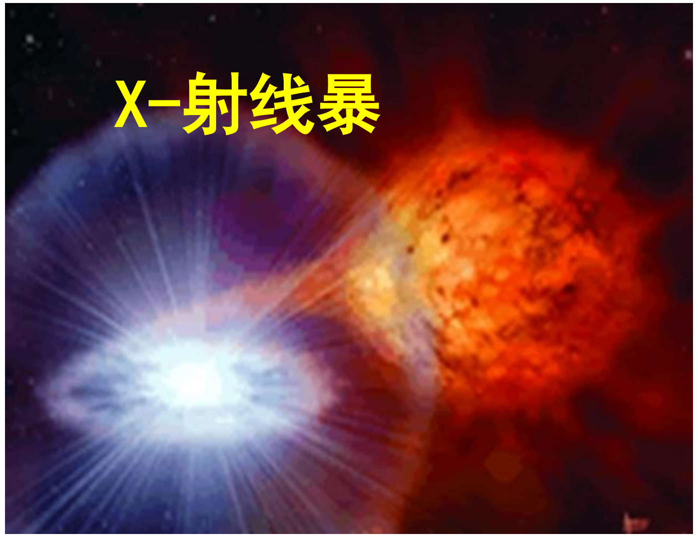

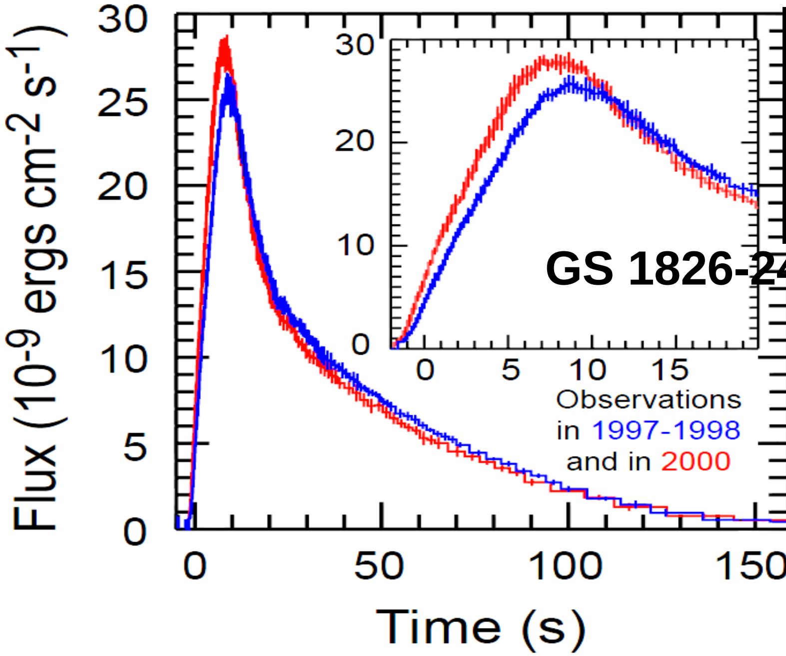

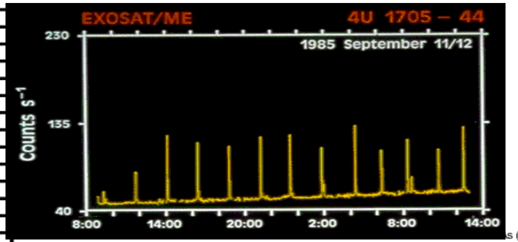

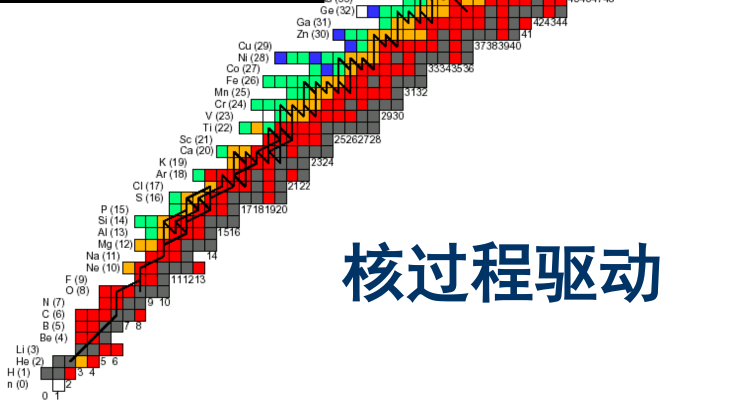

核过程驱动

X-射线暴模型
+核物理输入

灵敏度研究

光度曲线
元素丰度

模型预言与
天文观测比较

中子星性质